UNIVERSITEIT VAN PRETORIA
UNIVERSITY OF PRETORIA
YUNIBESITHI YA PRETORIA

A PREDICTIVE METHOD THAT ALLOWS A CONDITION-BASED MAINTENANCE IMPLEMENTATION BASED ON FAILURE STATISTICS AND PARTIAL KNOWLEDGE OF FAILURE MECHANISMS

by

JG van Zyl

Submitted in partial fulfilment of the requirements for the degree

Master of Engineering (Mechanical Engineering)

in the

Department of Mechanical and Aeronautical Engineering

Faculty of Engineering, Built Environment and Information Technology

University of Pretoria

February 2018

ABSTRACT

A PREDICTIVE METHOD THAT ALLOWS A CONDITION-BASED MAINTENANCE IMPLEMENTATION BASED ON FAILURE STATISTICS AND PARTIAL KNOWLEDGE OF FAILURE MECHANISMS

by

JG van Zyl

Supervisors	Prof. J Wannenburg and Prof. PS Heyns
Department	Mechanical and Aeronautical Engineering
University	University of Pretoria
Degree	Master of Engineering (Mechanical Engineering)
Keywords	Condition-Based Maintenance; Condition Monitoring; Remaining Useful Life; Reliability Theory; Proportional Hazards Model; PF Curve

Over the past decades, the progression from a reactive maintenance approach, to a time/use-based preventative approach, to a predictive approach, or Condition-Based Maintenance (CBM), for components subjected to ageing failure mechanisms such as fatigue, corrosion and wear, has led to significant savings on downtime and expenditures.

In this study, a spectrum of the level of insight and information available when embarking on this progression, is considered. On the one side of the spectrum is the case where a quantitative physical failure model is not available and/or the measurement of condition parameters is not feasible, but statistical failure data is available. This enables the use of Reliability Theory (RT) to implement a time/use-based Preventative Maintenance (PM) approach. On the other side is the ideal case for CBM, which entails feasible implementation of Condition Monitoring (CM) and where a physical failure model with all its parameters is known and the measured condition parameter enables the accurate calculation of the Remaining Useful Life (RUL). A bridge between CBM and time/use-based PM is represented by the Proportional Hazard Model (PHM) technique, which does not take a physical failure model into account, but where CM is feasible and relies on the fact that historic condition and failure data is available.

The main research question that is addressed during this study is the lack of an approach to implement CBM on equipment when historic condition monitoring data is not available, which may often be the case. On the spectrum, this would be placed between the ideal CBM case and the PHM technique. A new methodology is therefore developed that combines partial insight into the physical failure model with some form of measurable condition, as well as failure statistics, in order to develop degradation functions, or PF curves, to resemble component condition which may be used for CBM decisions. The newly developed method enables the implementation of CBM, which is initially based only on failure statistics and assumptions regarding the physical failure models, without the need for historic CM data. When the newly developed method is implemented, CM data is assembled, and this data may be used to continuously update the failure model assumptions, to progressively develop a full, economic CBM implementation.

The development of the new method is based on a numerical experiment, simulating components prone to fatigue failure, with various chosen initial conditions and operating conditions, to produce failure statistics. It is then assumed that, in practice, only these failure statistics would be known, as well as the form of the failure mechanism. The new method, to establish PF curves for a component with any given life based on this information, then entails arbitrarily choosing initial conditions, or defect sizes, and then calculating the operating condition parameter in the crack growth equation, to yield the required life. Using these arbitrarily chosen and calculated parameters, estimated PF curves may be derived, which would be used to base RUL and CBM decisions on.

With the "true" PF curve known from the numerically generated data, the accuracy of such decisions can be evaluated. This is done in the form of a sensitivity study, where the sensitivity of the accuracy of RUL decisions as a function of the arbitrary choice of initial conditions, can be tested for a wide range of component types. This sensitivity study yields promising results, as the error for all component types are low. The practical application of the new method is also demonstrated for bearings, where a fatigue related ageing mechanism is assumed and vibration CM provides indirect measurement of the condition. It is shown that the method provides sufficiently accurate predictions of RUL to enable implementation of CBM, without initial availability of historic CM data.

A further benefit of the new method is showcased, through its enablement of numerical simulation of the outcomes of the application of different maintenance tactics on a complex system. The simulated illustrative system consists of four component types, with

ten of each component type with randomised initial and operating conditions. A time-based simulation is made possible, since the estimated PF curves for each component is known, using the newly developed method. The model simulates a period of ten years and replacements are made according to the applied maintenance tactic. CBM, which forms part of a predictive approach and would be enabled by the method developed in this study, is compared to a reactive approach and a preventative approach. Compared to a reactive approach, the predictive approach resulted in 78% less downtime and 67% less expenditure. Compared to a preventative approach, the predictive approach resulted in 56% less downtime and 57% less expenditure. These promising results would assist in making a business case for the implementation of CBM in practical applications.

Acknowledgements

Acknowledgement and thanks goes out to the following people for their contribution to this work:

- Prof. J Wannenburg
- Prof. PS Heyns
- The Eskom Power Plant Engineering Institute (EPPEI) for its support of this research
- Anglo Platinum for access to failure data
- My friends and family for their continuous support throughout this study

Contents

List of Abbreviations

AM	Asset Management
CBM	Condition-Based Maintenance
CM	Condition Monitoring
CO	Corrective Operations
CV	Coefficient of Variance
IMF	Intrinsic Mode Function
KPI	Key Perfomance Indicators
LEFM	Linear Elastic Fracture Mechanics
MDT	Mean Downime
MLE	Maximum Likelihood Estimator
MTBF	Mean Time Between Failure
MTTF	Mean Time To Failure
MTTR	Mean Time To Repair
PdM	Predictive Maintenance
PEPD	Plant Engineering Performance Daily
PEPDC	Plant Engineering Performance Daily Cost
PHM	Proportional Hazards Model
PM	Preventative Maintenance
RCM	Reliability-Centered Maintenance
RM	Reactive Maintenance
RMS	Root Mean Square
RT	Reliability Theory
RUL	Remaining Useful Life

List of Symbols

a	Defect size
a_1	Reliability factor
a_2	Special bearing property factor
a_3	Special operating condition factor
a_{cr}	Critical defect size
a_i	Initial defect size
a_{i_μ}	Initial defect mean
a_{i_σ}	Initial defect standard deviation
$a_{i_{true}}$	True initial defect size
$a_{i_{pred}}$	Predicted initial defect size
β	Shape parameter
C	Operating condition parameter
C'	Modified operating condition parameter
C_μ	Operating condition parameter mean
C_σ	Operating condition parameter standard deviation
$C(tp)$	Replacement cost per unit time
C_f	Cost of a failure cycle
C_p	Cost of a preventative cycle
C_r	Basic dynamic load
C_t	Total cost per cycle
$cond$	Condition variable
$cond_i$	Initial condition
$cond_{cr}$	Critical condition
$cond_{i_{true}}$	True initial condition
$cond_{i_{pred}}$	Predicted initial condition
$E(t)$	Expected component life
η	Scale Parameter

$f(t)$	Probability density function
$F(t)$	Failure distribution function
$h_0(t)$	Baseline hazard
$\lambda(yz(t))$	Adjusting functional term
y	Vector of regression coefficient
K	Stress intensity factor
ΔK	Range of stress intensity factor
ΔK_{th}	Threshold alternating stress intensity factor
L_{10}	Bearing basic life rating
L_e	Expected cycle length
L_{na}	Adjusted life rating
M	Prior mean
m	Material property constant
m'	Modified material property constant
μ_0	Mean of historic means
μ_1	Posterior mean
μ	Prior mean
μ'	Sample mean
μ''	Posterior mean
N	Time taken to reach a certain crack/defect size
N_f	Time to failure/Component lifetime
n	Sample dataset size
P_r	Dynamic equivalent load
$R(t)$	Reliability function
$\Delta\sigma$	Paris law stress factor
σ	Prior standard deviation
σ'	Sample standard deviation
σ''	Posterior standard deviation
t	Time
t_p	Length of a preventative cycle
t_f	Length of a failure cycle
τ	Historic data standard deviation
τ^2	Prior standard deviation
T_f	Time needed to make a failure replacement
T_p	Time needed to make a preventative cycle

V	Vibration measurement
V_i	Initial vibration measurement
$V_{cr_{predicted}}$	Predicted critical vibration measurement
$V_{cr_{true}}$	True critical vibration measurement
V_{cr}	Critical vibration measurement
X	Sample dataset
X_{rand}	Random variable
$\bar{x}$	Sample data mean
Y	Paris law geometry factor
$z(t)$	Hazard function
$z_1(t)$	Vector of time dependent covariates

Chapter 1

Introduction

1.1 Background

Effective Asset Management (AM) is a key business objective for engineering industries. The backdrop to this requirement is ever increasing financial constraints married to reductions in manpower and expertise [Judd et al., 2002]. Failure is detrimental to the objectives of the organisation, thus the process of failure needs to be managed properly and for this reason various maintenance strategies have been developed to know what to do when and how [Coetzee, 1997]. Up to the Second World War the mechanical sophistication of industry was quite low, that is, most of the equipment was over-designed and simple. The consequences of failure did not have a strong influence and the effect was neglected [Fredriksson and Larsson, 2012].

Traditionally there was the notion that all equipment wears out and inevitably becomes less reliable with increasing operating age. This led to the incorrect conclusion that the overall rate of failure of the system will always be reduced by introducing a limit on the operating life of critical components. Some component failures can best be handled by measuring certain technical and operational parameters associated with them, so as to determine when they are on the verge of failure, thus being able to take preventative action before the failure occurs (condition-based prevention). Whatever techniques and management methods we use to manage the maintenance function, it is of critical importance that we understand the failure process well, both from a physical and a statistical perspective [Coetzee, 2015].

There are great incentives to maintain plant equipment more efficiently, and it is unequivocal that careful thought should be given to the most appropriate form of maintenance planning. Breakdown maintenance, or a so-called run-to-failure maintenance tactic, can be applicable in cases where a non-critical component is employed, the breakdown of the component does not cost enough time and money, or if a significant amount of redundancy is available. Many sectors of industry have adopted maintenance planning based on replacement and overhaul at fixed time periods, so that outage work can be scheduled, and diversions and loads can be planned. According to Hameed et al., fault detection systems and Condition Monitoring (CM) may lead to a number of benefits such as avoidance of premature breakdown, reduction of maintenance costs, remote diagnosis and support for further component development [Hameed et al., 2009]. Statistical Reliability Theory (RT) may be used to make optimum time/use-based preventative replacement decisions, but the remaining lives of many components are wasted. Alternatively, Condition-Based

Maintenance (CBM) may be used, but an ideal implementation of CBM relies on the fact that a physical failure model, CM, historic failure data and historic CM data are available. Degradation modelling essentially attempts to characterize the evolution of degradation signals [Zhou et al., 2011].

The following definitions for an asset management/maintenance strategy, maintenance approach and maintenance tactic are used throughout this dissertation:

- Asset management/maintenance strategy: An overall intent (targets) with regard to reaching asset management improved maturity levels on each pillar and a high level plan (timelines and resources) to reach these targets, for the operation.
- Maintenance approach: The mix of maintenance tactics employed for a system/-plant/equipment, implying that a reactive approach may be employed for systems of low criticality and a pro-active approach for systems with high criticality.
- Maintenance tactic: A specific type of maintenance activity (eg. servicing) employed on a specific maintenance significant item (eg. a pump)

1.2 Maintenance Approaches

In a study done in the United States, it was noticed that traditional maintenance costs (i.e. labour and material) have escalated at an astonishing rate over 10 years from 1981 to 1991 [Mobley, 2004]. Implementation of optimised maintenance approaches are in some instances omitted, resulting in over - or under maintenance being conducted. This can lead to large losses and unnecessary money spent and can be catastrophic to some organisations. In order to keep the maintenance cost as low as possible, optimised maintenance approaches need to be implemented. This can mean large initial costs, but exceptional savings over a longer period - that is the direction in which most organisations strive to move. Efficient operation of machinery not only means a maximum possible profit for the organisation, but can lead to environmental protection and a more satisfying work environment.

The structure shown in table 1.1 is the view on maintenance approaches and its correlating maintenance tactics that is followed in this dissertation. Maintenance approaches are separated into two sections: reactive maintenance and pro-active maintenance, where pro-active maintenance is separated into preventative maintenance and predictive maintenance. A reactive maintenance approach includes run to failure - and corrective maintenance tactics, where both tactics allow a component to fail before replacement. The difference between a run to failure tactic and a corrective tactic is that the former does not allow detection of imminent component failure, where the latter allows for detection of imminent component failure, although action is only taken once the component has failed in both cases. A preventative maintenance approach includes time/use-based -, servicing -, and design-out maintenance tactics. A time/use-based maintenance tactic is used to maintain components based on an optimised maintenance interval, calculated using failure data. Servicing occurs on a fixed-interval routine basis. Design-out maintenance involves redesigning components in order to remove characteristics that cause unnecessary maintenance. The redesigned component needs to consist of a decreased need for maintenance, and that is achieved by removing unwanted failure modes [Coetzee, 1997]. A predictive maintenance approach is based on a CBM tactic, where component condition is known throughout the life of the component. With knowledge of the condition of a component, it is possible to predict when the component will fail using a physical failure model. The focus of this study is that of pro-active maintenance, particularly predictive maintenance. The literature shown in this section focuses on the working of a time/use-based preventative maintenance tactic and a condition-based predictive maintenance tactic.

Table 1.1: Maintenance Approaches and Correlating Maintenance Tactics

Maintenance Approach	**Reactive**	**Pro-Active**	
		Preventative	Predictive
Maintenance Tactic	Run to Failure	Time/Use-Based	Condition-Based
	Corrective	Servicing	
		Design-Out	

1.2.1 Preventative Maintenance Tactic: Time/Use-Based Maintenance

In order to apply a time/use-based preventative maintenance tactic, failure statistics are required. Various functions that characterize component life, such as a survival or hazard function, can then be developed using historic failure data and optimal replacement time can be calculated. Using these functions and their theories, certain verdicts can be made with regards to maintenance decisions.

1.2.1.1 Quantitative Description of Failure and Reliability Theory

Renewal theory is the theory that explains failure situations where preventative actions lead to complete restoration. This theory is often approached with use of statistical distributions and the four functions that are of primary importance in renewal theory, often called the 'reliability functions', are [Coetzee, 2015]:

- **Probability density function**
  Consider a random variable X_{rand}. The probability density function is defined as,
  $$f(t) = \lim_{\Delta t \to 0} \frac{P(t < X_{rand} < t + \Delta t)}{\Delta t} \tag{1.1}$$
  where $f(t)$ is the limit of the probability that X_{rand} lies in the interval $(t, t + \Delta t]$ divided by the length of the interval as the length of the interval approaches 0.

- **Failure distribution function**
  The failure distribution function is defined as the probability that failure will occur before or at time t, therefore within the interval $[0, t]$. It is calculated by cumulatively summing the area under the probability density function. The failure distribution function is represented by
  $$F(t) = \int_0^t f(t)dt \tag{1.2}$$

- **Survival (or reliability) function**

  The survival (reliability) function is defined as the probability that failure will occur after time t, which is thus the complement of the failure distribution function.

$$R(t) = 1 - F(t) \tag{1.3}$$

- **Hazard function**

  To a large extent does this function determine which maintenance tactic will be used to maintain a specific component. It is defined as the probability that the time of failure will fall in the next instant $(t, t+\Delta t)$, given that it has not yet failed at point t. It is the conditional probability of failure at a specific time, given that failure has not occurred before then.

$$z(t) = \frac{f(t)}{R(t)} \tag{1.4}$$

1.2.1.2 Weibull Data Representation

The Weibull distribution is a very versatile distribution that can simulate most failure situations found in the maintenance practice. Most important is the fact that it can handle many shapes of the hazard rate function, including those of the exponential and normal distributions. It is therefore possible to use this one distribution for most practical failure analysis applications [Ondrasovic and Ondrasovicova, 2009]. The four functions stated in renewal theory can be represented within a Weibull distribution with the following relations, where β and η represent the shape parameter and scale parameter respectively.

- **Weibull density function**

$$f(t) = \frac{\beta}{\eta}\left(\frac{t}{\eta}\right)^{\beta-1} \exp\left[-\left(\frac{t}{\eta}\right)^{\beta}\right] \tag{1.5}$$

- **Cumulative distribution function**

$$F(t) = 1 - e^{-\left(\frac{t}{\eta}\right)^{\beta}} \tag{1.6}$$

- **Survival function**

$$R(t) = 1 - F(t) = e^{-\left(\frac{t}{\eta}\right)^{\beta}} \tag{1.7}$$

- **Hazard rate function**

$$z(t) = \frac{f(t)}{R(t)} = \frac{\beta}{\eta}\left(\frac{t}{\eta}\right)^{\beta-1} \tag{1.8}$$

The four renewal theory functions are shown in figure 1.1 for various values of the shape and scale parameters. It can be seen that with a certain combination of parameters, the Weibull distribution approximates other known distributions.

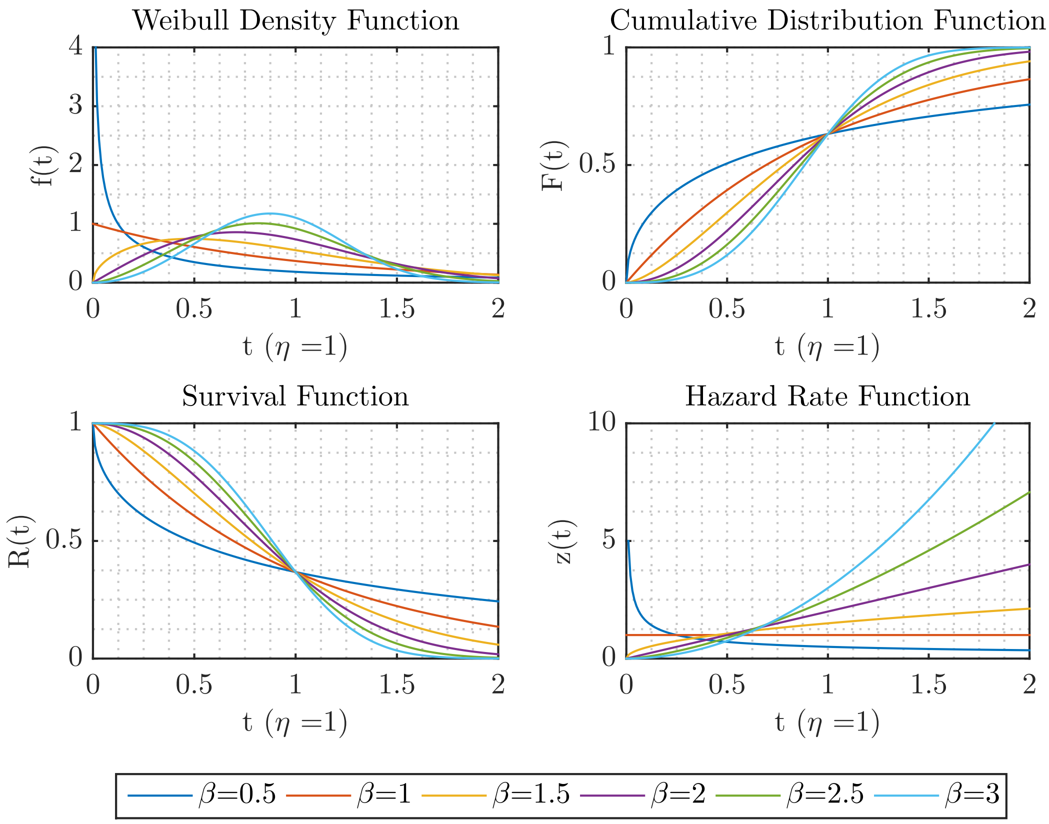

Figure 1.1: Renewal Theory Weibull Functions

The bath tub curve is a special case of the hazard rate function and indicates the risk of failure of a typical component or system. The early failure phase of the bath tub curve is commonly referred to as infant mortality and is a fairly short period during the life of the component with relatively high risk. The second region normally spans much longer in comparison to the other two regions. During this time the risk of failure is relatively low, random and constant. The third region is known as the wearout phase and sets in when the component structural integrity due to wear and tear changes. This results in a speedy degradation and is commonly due to fatigue [Coetzee, 1997]. Common problems with the bath tub curve are:

- Not all components and systems have early failure and wearout regions.
- Not all components and systems have constant risk to fail over its operating life.
- Drenick's limit theorem states that a constant failure will result from a system consisting of many components [Drenick, 2012].

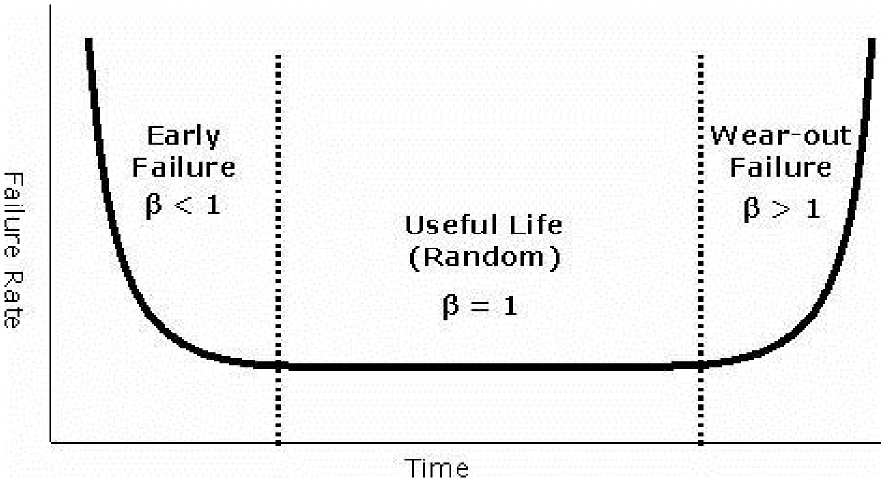

Figure 1.2: Bath Tub Curve Parameters [Lasky, 2012]

Most failure data sets encountered in the maintenance environment can be fitted with one of the Weibull family of distributions. The scale parameter and shape parameter of the distribution that fit the data need to be estimated. The process of estimating the parameters is fairly complicated, but is simplified when done automatically. Using the Maximum Likelihood Estimator (MLE) method, the following two equations that can be solved simultaneously are derived [Coetzee, 1997].

$$\frac{1}{n_i}\sum_{i=1}^{n}\ln t_i = \frac{\sum_{i=1}^{n}\left(t_i^{\beta}\ln t_i\right)}{\sum_{i=1}^{n} t_i^{\beta}} - \frac{1}{\beta} \tag{1.9}$$

$$\eta = \left[\frac{\sum_{i=1}^{n} t_i^{\beta}}{n}\right]^{1/\beta} \tag{1.10}$$

η is determined using equation 1.10, and equation 1.9 is used to determine β via an iterative process.

1.2.1.3 Mathematical Modelling

Coetzee has derived a method for determining the optimal preventative replacement age of equipment taking replacement times into account. This is indeed an optimisation of profit/cost [Coetzee, 1997]. The total cost per cycle is given by,

$$C_t = C_p R(t_p) + C_f\left[1 - R(t_p)\right]$$

where C_t is the total cost per cycle, C_p is the cost of a preventative cycle and C_f is the cost of a failure cycle. In the case of the expected cycle length, the effect of the replacement times is evident,

$$L_e = (t_p + T_p)R(t_p) + (t_f + T_f)\left[1 - R(t_p)\right]$$

where T_p is the time required to make a preventative replacement and T_f is the time required to make a failure replacement. The expected life of a component is given by

$$E(t) = \frac{\int_{-\infty}^{t_p} tf(t)dt}{1 - R(t_p)} \tag{1.11}$$

and the replacement cost per unit time in this case is

$$C(t_p) = \frac{C_t}{L_e} = \frac{C_p R(t_p) + C_f \left[1 - R(t_p)\right]}{(t_p + T_p)R(t_p) + \int_{-\infty}^{t_p} tf(t)dt + T_f \left[1 - R(t_p)\right]} \tag{1.12}$$

1.2.1.4 Bayes' Theorem

The setting for Bayesian statistics is a family of distributions parametrized by one or more parameters along with a prior distribution for those parameters [Joyce, 2009]. The prior distribution is developed for the sole purpose of expressing the uncertainty of a parameter, such as the mean or standard deviation of a dataset. One key to understanding the essence of Bayes' theorem is to recognize that there is dealt with sequential events, whereby new additional information is obtained for a subsequent event, and that new information is used to revise the probability of the initial event. In this context, the terms prior probability and posterior probability are commonly used [Bayes et al., 2015]. The posterior probability is obtained by combining the prior and sample data. That is, the sample data obtained is adjusted with knowledge from the prior distribution. In order to achieve this, the predictive process is split into five components, as derived by Nederlof [Nederlof, 2010]:

1. **Process Distribution**
   This is an initial distribution based on a data generating process. This might be a completely subjective guess [Nederlof, 2010], or it can be based on historic data. The process distribution consists of a mean of past data means, μ_0, and a standard deviation of past data means, τ. When new data is obtained, the sample size is n and the new dataset, X, has a mean of $\bar{x}$ and standard deviation of σ.

2. **Prior Distribution**
   This is a key part of the Bayesian inference and the critical element in developing predictive distributions [Gelman, 2002]. It represents information about an uncertain paramenter and is combined with sample data in order to develop a posterior distribution. This distribution is obtained from the data in the process distribution [Nederlof, 2010]. According to Nederlof, the mean of the prior would be the same as that of the process, or a mean of means and the variance would equal the process

variance divided by the sample size [Nederlof, 2010]. Using Bayes' rule:

$$p(\mu_0|X) \propto p(X|\mu_0)p(\mu_0) \tag{1.13}$$

Where $p(X|\mu_0)$ is the likelihood function for the current data and $p(\mu_0)$ is the prior for the past data mean. Assuming the current data is normally distributed with a mean of μ_0 and a variance of σ^2, then the likelihood function for X is

$$p(X|\mu_0) = \prod_{i=1}^{n} \frac{1}{\sqrt{2\pi\sigma^2}} \exp\left\{-\frac{(x_i-\mu_0)^2}{2\sigma^2}\right\} \tag{1.14}$$

According to Jacobs, the prior distribution can be obtained using the following relation [Jacobs, 2008],

$$p(\mu_0) = \frac{1}{\sqrt{2\pi\tau^2}} \exp\left\{-\frac{(\mu_0-M)^2}{2\tau^2}\right\} \tag{1.15}$$

where M is the prior mean and τ^2 reflects the variation of μ_0 around M.

3. **Sample Distribution**
This distribution is developed from the data obtained through monitoring or logging of physical components. Upon observing the sample data, the likelihood function needs to be constructed [Glickman and van Dyk, 2007]

$$L(\mu_0|X) = p(X_1, ..., X_n|\mu_0) = \prod_{i=1}^{n} p(X_i|\mu_0) = \prod_{i=1}^{n} \frac{1}{\sqrt{2\pi\sigma^2}} \exp\left\{-\frac{(x_i-\mu_0)^2}{2\sigma^2}\right\} \tag{1.16}$$

4. **Posterior Distribution**
This is often referred to as the updated or revised prior, based on new information from the sample data. Upon observation of the sample data, the likelihood function is developed. The likelihood is then combined with the prior distribution to determine the posterior distribution, which is the probability distribution of the parameters once the data has been observed [Glickman and van Dyk, 2007]. This indicates that by simply multiplying the prior distribution by the likelihood and determining the constant that forces the expression to integrate to 1, the posterior distribution can operationally be obtained [Glickman and van Dyk, 2007]. According to Jacobs, the posterior mean (μ") and variance ($\sigma"^2$) can be obtained to be used in a normal distribution function by combining the likelihood and prior into Bayes' theorem [Jacobs, 2008].

$$p(\mu_1|X) \propto \frac{1}{\sqrt{\tau^2\sigma^2}} \exp\left\{\frac{-(\mu_0-M)^2}{2\tau^2} + \frac{-\sum_{i=1}^{n}(x_i-\mu_0)^2}{2\sigma^2}\right\} \tag{1.17}$$

Since the terms outside the exponential are normalizing constants with respect to μ_0, it can be dropped. The terms inside the exponential can therefore be re-written, following some algebra [Jacobs, 2008].

$$p(\mu_1|X) \propto -\frac{1}{2}\left[\frac{\mu_0^2 - 2\mu_0 M^2}{\tau^2} + \frac{\sum x^2 - 2n\bar{x}\mu_0 + n\mu_0^2}{\sigma^2}\right] \tag{1.18}$$

Any term that does not include μ can be viewed as a proportionality constant, can be factored out of the exponent and can then be dropped (recall that $e^{a+b} = e^a e^b$) [Jacobs, 2008]. The following is then obtained.

$$p(\mu_1|X) = -\frac{1}{2}\left[\frac{\sigma^2\mu_0^2 - 2\sigma^2\mu_0 M - 2\tau^2 n\bar{x}\mu_0 + \tau^2 n\mu_0^2}{\sigma^2\tau^2}\right]$$

$$p(\mu_1|X) = -\frac{1}{2}\left[\frac{(n\tau^2+\sigma^2)\mu_0^2 - (\sigma^2 M + \tau^2 n\bar{x})\mu_0}{\sigma^2\tau^2}\right]$$

$$p(\mu_1|X) = -\frac{1}{2}\left[\frac{\left(\mu_0 - \frac{\sigma^2 M + n\tau^2\bar{x}}{(n\tau^2+\sigma^2)}\right)^2}{\frac{\sigma^2\tau^2}{(n\tau^2+\sigma^2)}}\right]$$

$$p(\mu_1|X) = -\frac{1}{2}\left[\frac{\mu_0^2 - 2\mu_0\frac{(\sigma^2 M + n\tau^2\bar{x})}{(n\tau^2+\sigma^2}) }{\frac{\sigma^2\tau^2}{(n\tau^2+\sigma^2)}}\right]$$

In other words, $\mu_1|X$ is normally distributed with mean

$$\frac{\sigma^2 M + n\tau^2\bar{x}}{n\tau^2+\sigma^2}$$

and variance

$$\frac{\sigma^2\tau^2}{n\tau^2+\sigma^2}$$

For the sake of simplicity, the following is used,

$$\mu'' = \frac{\sigma^2\mu' + n\sigma'^2\mu}{n\sigma'^2+\sigma^2} \tag{1.19}$$

$$\sigma''^2 = \frac{\sigma^2\sigma'^2}{n\sigma'^2+\sigma^2} \tag{1.20}$$

where μ'' is the posterior mean, σ''^2 is the posterior variance, μ' is the prior mean, σ'^2 is the prior variance, μ is the sample mean, σ^2 is the sample variance and n is the sample size.

5. **Predictive Distribution** This is the distribution of future observations. The mean of this distribution is the same as the posterior mean, but the variance is a weighted combination of the process and posterior variance [Nederlof, 2010].

1.2.2 Predictive Maintenance Tactic: Condition-Based Maintenance

Within the framework of maintenance tactics, CBM plays an important role that forms part of a predictive approach. CBM is applicable to any failure mode where it is found to be technically feasible and worth doing. CBM can generally be separated into two subgroups: inspection and CM. The former includes inspection via human senses and the latter involves parameter monitoring such as vibration analysis, oil analysis, thermography etc [Coetzee, 1997].

CBM dictates that maintenance should only be performed when certain indicators show signs of decreasing performance or upcoming failure. Checking a machine for these indicators may include non-invasive measurements, visual inspection, performance data and scheduled tests. Condition data can then be gathered at certain intervals, or continuously, and CBM can be applied to mission critical and non-mission critical assets. CBM allows preventative and corrective actions to be scheduled at the optimal time, thus reducing the total cost of ownership [Budynas and Nisbett, 2011][Fiix, 2016].

1.2.2.1 Condition Monitoring (CM)

Predictive maintenance consists of physical parameter analyzing, such as vibration monitoring, thermography and oil analysis. CM is a tool commonly employed for the early detection of faults/failures so as to minimise downtime and maximize productivity [García Márquez et al., 2012]. Carnero proposed a method for determining the optimal CM technique based on discrete probability distriburions [Carnero, 2009]. CM architecture normally supports the capture and interpretation of diagnostic data, and provides engineers with meaningful diagnostic advice using intelligent system technologies [Judd et al., 2002].

Technology is seen as a means of solving the asset management problem, driving the research and development of advanced monitoring systems with a view to implementing CBM. As a result, an increasing volume of CM data is captured and presented to engineers. This leads to a number of problems [Judd et al., 2002]:

- The data volume is onerous for engineers to deal with.
- The relationship between the plant item, its health and the CM data generated is not always well understood. Therefore, the extraction of meaningful information from the CM data is difficult.

- The translation of the health of the plant item into an estimate of its lifetime expectation is not always apparent.

According to Tchakoua et al., the application of reliable and cost effective CM techniques offers an efficient approach to achieving the goal of improving reliability, specifically in the development of more highly evolved wind turbine designs [Tchakoua et al., 2014]. With CM, the regular monitoring of deterioration results in a function similar to that in figure 1.3 to give advanced warning of failure.

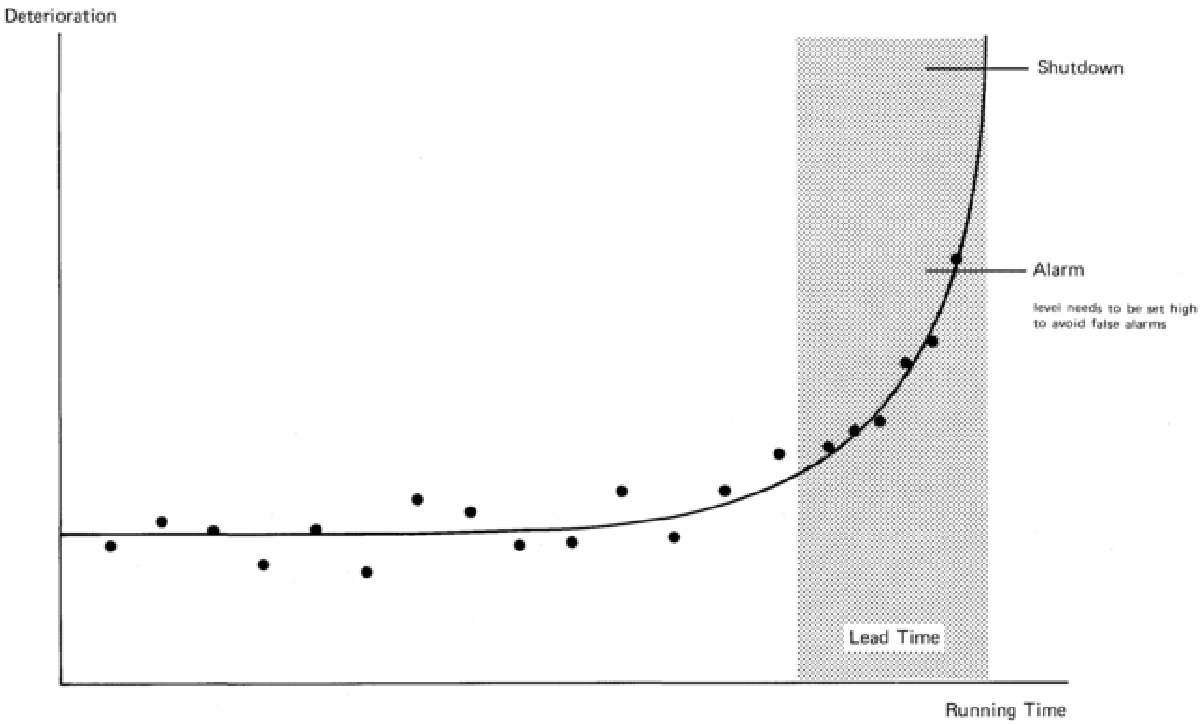

Figure 1.3: The Regular Monitoring of Deterioration to Give Advanced Warning of Failure [Neale and Woodley, 1975]

1.2.2.2 PF-Curve

A common curve that illustrates the behaviour of equipment as it approaches failure is the PF-curve, which normally obtains its data from CM. Figure 1.4 shows that as failure starts manifesting, the equipment deteriorates to the point at which it can possibly be detected (P). If the failure is not detected and mitigated, it continues until a "hard" failure occurs (F). The time ranges between P and F, commonly called the PF interval, is the window of opportunity during which an inspection can possibly detect the imminent failure and address it. PF intervals can be measured in any unit associated with the exposure to the stress (running time, cycles, miles, etc). For different failure modes, the PF interval can vary from fractions of a second to several decades. For example, if the PF interval is 200 days and the item will fail at 1000 days, the approaching failure begins to be detectable at 800 days. Hence the frequency of inspection is determined wholly and solely based on the PF interval [Saravanan et al., 2014].

By extending the PF interval, CBM methods provide the earliest possible prediction of equipment failure, with maximum benefit: minimum production loss, reduced maintenance labour and materials costs, extended equipment life and reduced capital expenditures [Blann, 2013]. The periodicity at which inspections takes place is often ill-determined and appropriate quantitative analysis seldom takes place. Such an approach often leads to excessive direct costs and can result in significant indirect costs if asset failure is considered [Arthur, 2005].

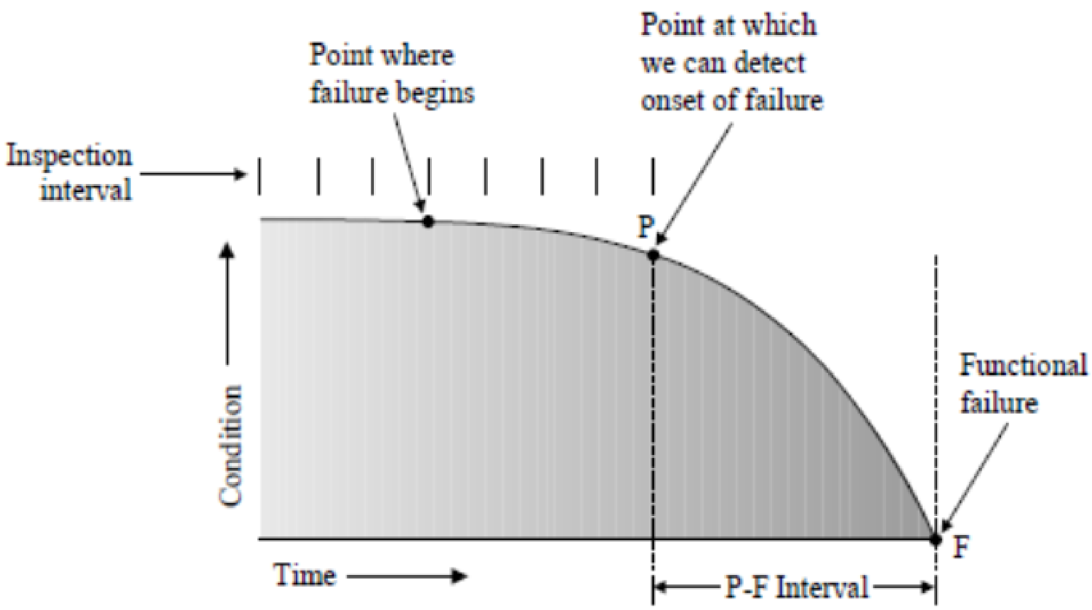

Figure 1.4: PF Curve [ReliaSoft, 2016]

1.2.2.3 Proportional Hazards Models (PHM)

PHM was originally proposed by Cox [Cox, 1992] in 1972. It was primarily applied in the biomedical field and only later introduced in reliability modelling. The PHM assumes that the total hazard rate of a unit is the product of a baseline hazard rate and a functional term,

$$h(t, z_1(t)) = h_0(t)\lambda(yz(t)) \tag{1.21}$$

where $h_0(t)$ is the baseline hazard rate depending on time only and $\lambda(yz(t))$ is an adjusting functional term that models the effect of the particular system characteristics, with y a vector of regression coefficients and $z_1(t)$ a vector of time dependent covariates [Vlok et al., 2002]. The optimal preventative replacement time is usually selected to minimize the long run replacement cost per unit time, assuming fixed costs of preventative and failure replacements. To calculate the optimal replacement policy, it is necessary to describe behaviour of the covariates. Makis and Jardine have combined the Weibull PHM with a non-homogeneous discrete Markov process to predict the future development of covariates and failure times [Makis and Jardine, 1991]. The complexity of modelling Preventative Maintenance (PM) stems from the difficulty of quantifying the effect of performing PM at different intervals [Kobbacy et al., 1997].

Samrout et al. used PHM as a modelling tool to expound a new method to integrate the effect of CM while planning for the PM policy, based on component age [Samrout et al., 2009]. Tian and Liao have shown that PHM can be used to optimize a maintenance policy [Tian and Liao, 2011]. Ghasemi et al. motivates that CBM is based on collecting observations over time in order to assess equipment state. Their work has shown that it is possible to derive an optimal CBM replacement policy when the state of equipment is unknown but can be estimated based on observed condition. PHM is used to represent component degradation [Ghasemi et al., 2007].

In the literature, numerous work have been done to show the effectiveness of using PHM to optimize a maintenance policy or to estimate component Remaining Useful Life (RUL). The means of estimating component degradation is based on component age and PHM does not take a physical failure model into account.

1.3 Prognostics Based on Physical Failure Models and Historic Failure Data

Various degradation models have been proposed to predict fatigue life of structures, which relate to the degradation rate $\frac{da}{dN}$, where a is a defect size and N the time taken to reach the said defect, to load amplitude or maximum load, which can be expressed in the stress intensity factor K, in the case of Paris' law. Phenomenological models are formulated and fitted by close inspection of statistical failure growth data. All these relations describe $\frac{da}{dN}$ to be a function of the stress σ and the condition a, or in the case of Paris' law of crack growth, the crack size. However, in Linear Elastic Fracture Mechanics (LEFM), $\frac{da}{dN}$ is mostly related to ΔK by Paris' law, using two parameters: a coefficient (operating condition parameter) and an exponent (material constant) [Schreurs, 2012],

$$\frac{da}{dN} = C\left(\Delta K\right)^m \qquad (1.22) \qquad\qquad \Delta K = f(\sigma, \sqrt{a}) = \Delta\sigma Y\sqrt{\pi a} \qquad (1.23)$$

where a is the crack size, N is the time taken to reach the said crack size, $\frac{da}{dN}$ is the crack growth rate, C and m are operating condition and material dependent parameters respectively and ΔK is the range of the stress intensity factor during fatigue cycles. Paris and Erdogan published the crack grow law, which has become known as the Paris law in 1963 and it is still widely used. On a double-logarithmic axes, the Paris law is represented by a straight line. The two parameters C and m can be fitted easily when two data points are known. These values depend on material, geometry, load and loading frequency [Budynas and Nisbett, 2011].

C and m are material and test condition-dependent parameters. The Paris law, or sometimes, as the Paris-Erdogan law, is most universally applied to Stage 2 fatigue crack growth, that is, crack growth at alternating stress intensity values somewhat larger than the threshold alternating stress intensity factor, ΔK_{th}, but below the value ΔK at which unstable crack propagation begins to occur. Paris' law is applicable where crack lengths in components are monitored, as it is used to show the degradation of a component using a PF curve.

In many cases the physical failure mechanism is not known and therefore a physical failure model cannot be used to represent the component degradation. When this is the case, a time/use-based maintenance tactic is applied and all components are replaced based on an optimal replacement time, as discussed in section 1.2. Prognostics focuses on predicting the future performance of a system, specifically the time at which the system no longer performs its desired functionality, its time to failure. Due to system complexity, data availability and application constraints, there is no universally accepted best model to estimate RUL and therefore hybrid prognostics approaches have been developed, which attempts to leverage the advantages of combining various methods to estimate RUL [Liao and Köttig, 2014].

The full strength of prognostics can be unveiled when incorporating the strengths of different prognostics models such as experience-based, data-driven and physics-based models. The advantage lies in the fact that shortcomings of one prognostics model are filled by strengths from other models. For instance, physics-based models characterize a degrading system using analytical descriptions of the underlying physical principals, and hence provide precise predictions. This is rarely the case in industrial applications. Data-driven prognostics models can mitigate this problem due to their capability to model only from historic data without sufficient knowledge about the underlying physics of degradation. Experience and expert knowledge is highly valuable and can enhance the prognostics capabilities of both physics-based and data-driven models, which eventually motivates the application of using all three prognostics models in a hybrid approach. The hybrid approach mentioned may be difficult to implement due to the difficulty that might be encountered by each type of model. However, it is potentially beneficial to leverage the strengths of all types of models and fuse the information [Liao and Köttig, 2014].

1.4 Scope and Research Objectives

Table 1.2 summarises the methods used for the implementation of a pro-active (preventative/predictive) maintenance approach within a spectrum. On the one side of the spectrum is the case where a quantitative physical failure model is not available and/or the measurement of condition parameters is not feasible, but statistical failure data is available. This enables the use of RT to implement a time/use-based PM approach. On the other side is the ideal case for CBM, which entails feasible implementation of CM and where a physical failure model with all its parameters is known and the measured condition parameter enables the accurate calculation of the RUL. A bridge between CBM and time/use-based PM is represented by the PHM techniques, which does not take a physical failure model into account, but where CM is feasible and relying on the fact that historic condition and failure data is available.

Table 1.2: Proactive Maintenance Spectrum

	Ideal CBM	**This Study**	**PHM**	**Reliability Theory**
Failure Statistics	Yes	Yes	Yes	Yes
Failure Mechanism	Yes	Yes	No	No
Condition Monitoring Possible	Yes	Yes	Partially	N.A
Condition Monitoring History	Yes	No	Yes	No
Mainte-nance Approach	Predictive Maintenance	Predictive Maintenance	Predictive Maintenance	Preventative Maintenance
Method	Physical Failure Model	Unknown	PHM	Time/Use-Based

The first part of this study addresses the main problem, which is the lack of a method, hereinafter referred to interchangeably as the "newly developed method/new method-/method", to implement a CBM tactic on equipment when historic CM data is not available. This case would be placed between the ideal case for CBM and PHM on the spectrum shown in table 1.2. Therefore, the question is asked: can a method that allows the implementation of CBM without knowledge of historic CM data, but with knowledge of failure data, be developed?

The second part of this study entails the discussion of a maintenance approach simulation, which is a techno-economic simulation of an engineering system. Current models are not great at simulating Predictive Maintenance (PdM) and successful CM can only be assumed. The first step to a new method is a theoretical model which is time-based and includes actual causes of simulation and variability, as well as degradation.

The two parts (maintenance approach simulation and development of a new method) intertwine in a special way that enables the maintenance approach simulation to benefit from the newly developed method. In this way, the maintenance approach simulation forms a foundation for the development of the new method and its findings are implemented in the maintenance approach simulation.

1.5 Report Layout

Chapter 1 entails background and research with regards to the maintenance industry, in particular common proactive maintenance approaches. The opportunity to combine different maintenance tactics is also identified and this forms part of the problem that is addressed throughout this study.

Chapter 2 discusses a time-based maintenance strategy simulation. The arguments and methods described in chapter 2 are employed throughout the study. Complications are identified and the remainder of this study aims to address it.

Chapter 3 addresses the complications identified in chapter 2 and discusses the numerical experiment procedure, its preparation and its configuration.

Chapter 4 discusses the application of the newly developed method for CBM on bearings and motivates that the newly developed method is applicable to components whose condition degrades according to a specific physical failure model.

Chapter 5 discusses a simulated case study that compares the implementation of CBM using the newly developed method to a reactive and preventative approach in terms of maintenance time and cost.

Chapter 6 implements the findings from the numerical experiment, chapter 3, to the model in chapter 2 in order to run the simulation based on real statistical failure data.

Chapter 7 concludes this study and provides recommendations for future work in this field.

Figure 1.5 below shows a graphical breakdown of the structure of this dissertation. The reader must keep this structure in mind while reading through the document, as it is crucial to know how each chapter flows into the next in order to understand the argument that is made in this dissertation. In figure 1.5, each chapter is depicted by a large block (excluding the introduction and conclusion) that feeds from a certain input (IN) and returns an output (OUT). The output forms a result (small block) from the findings in its preceding chapter that is used as an input in the following chapter.

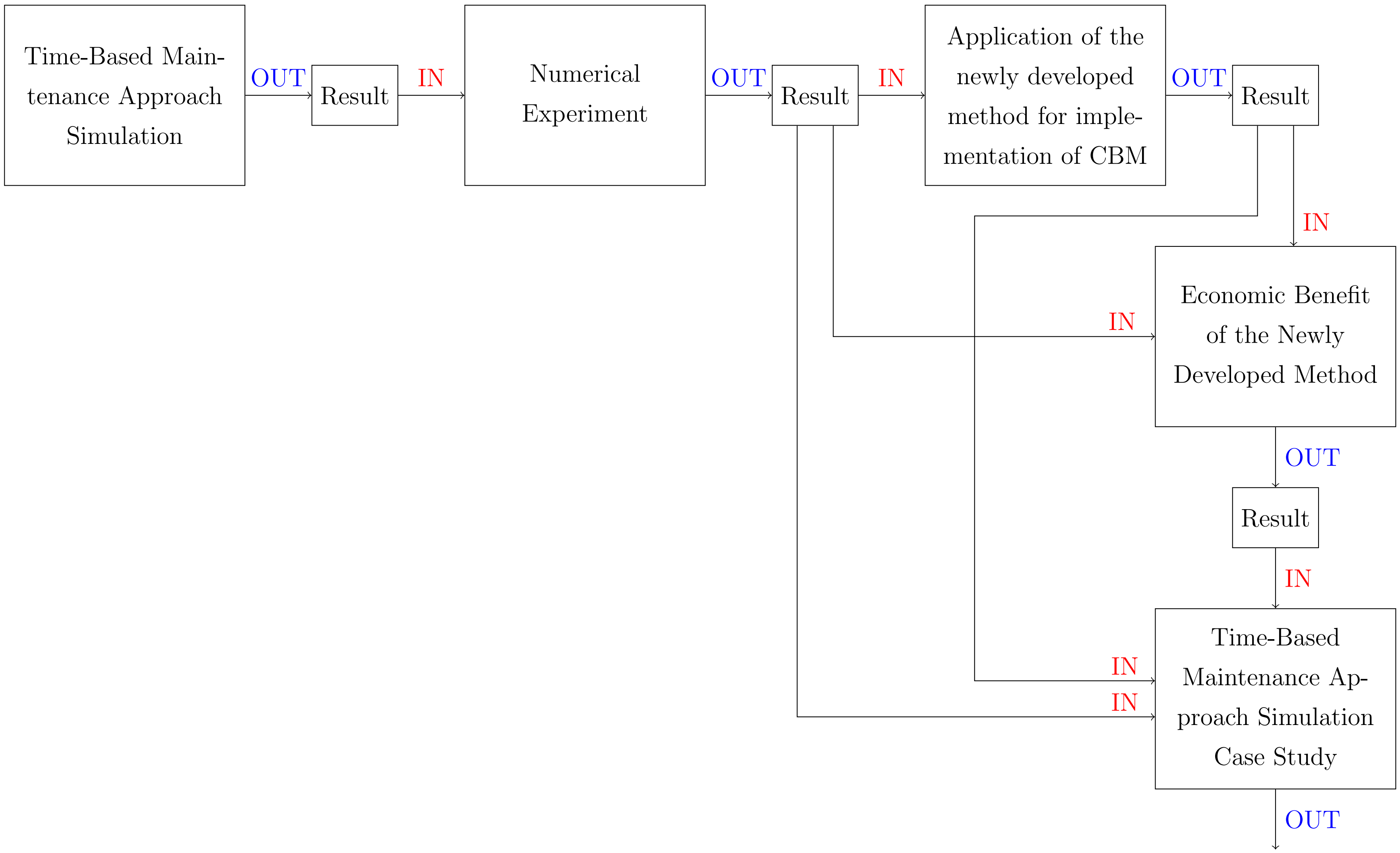

Figure 1.5: Dissertation Flowchart

Chapter 2

Time-Based Maintenance Approach Simulation

2.1 Introduction

The time-based maintenance approach simulation is a model developed by J Wannenburg, privately shared August 2016, to demonstrate the effect of various maintenance tactics on an arbitrary system built up out of various component types. Reference is made throughout this study to concepts and methods that were obtained from the prior work done on the time-based maintenance approach simulation, in order to differentiate between it and the subsequent work done by the present author. It is recognised that the time-based maintenance approach simulation work has been done for illustrative and explorative purposes and has not been peer-reviewed. The work building on such concepts or using such methods is therefore presented in this dissertation in sufficient detail, so as to allow the reader to understand and evaluate it from first principles.

The model derives an analytical expression for PF curves, based on a Paris power law, in order to simulate the effect of CBM on Key Performance Indicators (KPIs). Component types along with their initial condition and operating condition parameters are specified. Over time the components degrade based on a Paris power law and the components are replaced based on a chosen maintenance approach, which is a mix of maintenance tactics. It is important to realise that the power law, initially based on the Paris crack propagation equation, but later generalised for other failure modes, is used as a form of a physical failure model throughout this dissertation, not a power law statistical distribution (zeta distribution).

The model's outputs include KPIs in the form of maintenance cost, downtime due to maintenance and overall production rate, given that the component forms a crucial part in some production line or operating chain. The model demonstrates the influence that a mix of various maintenance tactics can have on a system. At the commencement of the current study, an attempt was made to model a real-life system by using real failure data in the model, but complications were encountered due to too many unknown parameters such as initial condition and operating condition of various components, making it impossible to model component life degradation. This forms a firm foundation for chapter 3 where a numerical experiment is conducted which aims to solve this problem.

2.2 Model Overview

The model comprises of various interdependent modules that each play a significant role in developing a result. The different modules and how they are interconnected are shown in figure 2.1. The modules act in series, as the logic in each module is based on the result of its predecessor. This chapter explains the various modules and how they operate and interconnect. It is fundamental to keep in mind that the model was initially developed to simulate an arbitrarily composed non-genuine system and that the data used in the model is not real, but dummy data is used. That makes the system simulated by the model entirely arbitrary, this is the case due the initial outcome of the model being to function as a prototype to show the significant effect that different maintenance tactics can have on a system.

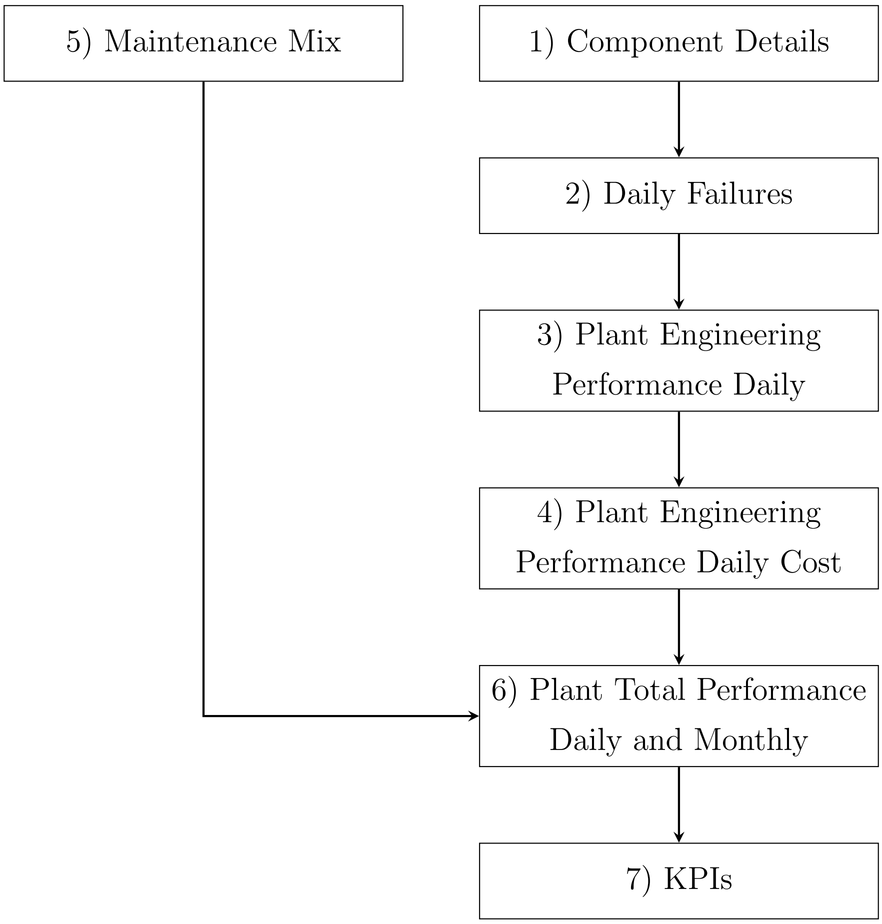

Figure 2.1: Time-Based Maintenance Approach Simulation Modules

2.2.1 Component Details

PF curves form an integral part of the model due to the fact that it is used to simulate the effect of maintenance tactics on KPIs. The model derives an analytical expression $\frac{da}{dN}$, where a is the defect size and N is time to reach defect size, a, for PF curves from a Paris power law. The details for all component types' initial conditions, operating parameters and material properties are specified in this module to develop PF curves to represent respective components' degradation over time. These parameters include initial condition distribution properties such as mean and standard deviation and the failure characteristic parameters used to represent the respective components' condition degradation within a Paris power law. This holds an advantage in the fact that nearly any type of component behaviour can be replicated through statistical modelling. The component life degradation is represented by Paris's power law, which is shown in equation 2.1 and is obtained by combining equation 1.22 and 1.23.

$$\frac{da}{dN} = C\left(\Delta\sigma Y\sqrt{\pi a}\right)^m \tag{2.1}$$

All parameters not relating to defect size, a, such as stress -, geometry -, and material property constants in equation 2.1 are grouped to form a modified operating condition parameter, C'. This makes working with Paris' power law less complicated.

$$\begin{aligned} \frac{da}{dN} &= C\Delta\sigma^m Y^m \pi^{\frac{m}{2}} a^{\frac{m}{2}} \\ Let \quad C' &= C\Delta\sigma^m Y^m \pi^{\frac{m}{2}} \\ \frac{da}{dN} &= C' a^{\frac{m}{2}} \end{aligned}$$

Rearranging yields the following equation,

$$dN = \frac{da}{C' a^{m/2}} \tag{2.2}$$

where N is the time/amount of cycles to reach the specified defect size, a, C' is the modified operating condition parameter and m is the material property constant. Equation 2.2 is integrated over a specific period of time/cycles in order to determine the time/cycles to failure, N_f, given the initial defect size, a_i, critical defect size (defect size at failure), a_{cr}, modified operating condition parameter, C', and material property constant, m.

$$\begin{aligned}
\int_0^{N_f} dN &= \int_{a_i}^{a_{cr}} \frac{da}{C' a^{m/2}} \\
&= \frac{1}{C'} \int_{a_i}^{a_{cr}} \frac{da}{a^{m/2}} \\
&= \frac{1}{C'} \left[\frac{a^{-\frac{m}{2}+1}}{-\frac{m}{2}+1} \right]_{a_i}^{a_{cr}} \\
&= \frac{1}{C'} \left[\frac{a^{\frac{2-m}{2}}}{\frac{2-m}{2}} \right]_{a_i}^{a_{cr}}
\end{aligned}$$

The material property constant is altered to be represented by m', a modified material property constant, instead of m, in order to avoid confusion and difficult algebra. Therefore, let $m' = \frac{2-m}{2}$. For the sake of simplicity, the critical defect size, a_{cr}, is normalised to be 1, therefore $a_{cr} = 1$.

$$\begin{aligned}
\int_0^{N_f} dN &= \frac{1}{C'm'} \left[a^{m'} \right]_{a_i}^{a_{cr}} \\
N_f &= \frac{1}{C'm'} \left[a_{cr}^{m'} - a_i^{m'} \right] \\
N_f &= \frac{a_{cr}^{m'} - a_i^{m'}}{C'm'} \\
\therefore N_f &= \frac{1 - a_i^{m'}}{C'm'} \qquad (2.3)
\end{aligned}$$

A per time unit/per cycle degradation function is also derived from equation 2.2, which is shown below. In the following derivation, one time unit/one cycle is taken as 1.

$$\begin{aligned}
\int_{N_k}^{N_{k+1}} dN &= \frac{1}{C'} \int_{a_k}^{a_{k+1}} \frac{da}{a^{m/2}} \\
1 &= \frac{1}{C'} \left[\frac{a^{\frac{2-m}{2}}}{\frac{2-m}{2}} \right]_{a_k}^{a_{k+1}} \\
&= \frac{1}{C'} \left[\frac{a_{k+1}^{\frac{2-m}{2}}}{\frac{2-m}{2}} - \frac{a_k^{\frac{2-m}{2}}}{\frac{2-m}{2}} \right] \\
&= \frac{1}{C'} \left[\frac{a_{k+1}^{m'}}{m'} - \frac{a_k^{m'}}{m'} \right] \\
\frac{a_{k+1}^{m'}}{C'm'} &= 1 + \frac{a_k^{m'}}{m'C'} \\
\therefore a_{k+1} &= \left[C'm' + a_k^{m'} \right]^{\frac{1}{m'}} \qquad (2.4)
\end{aligned}$$

For the remainder of this study and for the sake of simplicity, the modified operating condition, C', will be referred to as C and the modified material property constant, m', will be referred to as m. Therefore, equation 2.3 and 2.4 becomes:

$$N_f = \frac{1 - a_i^m}{Cm} \tag{2.5}$$

$$a_{k+1} = [Cm + a_k^m]^{\frac{1}{m}} \tag{2.6}$$

Throughout the remainder of this dissertation, the form of the Paris power law used, or referred to, is that shown in equation 2.5 and 2.6. Component degradation according to equation 2.6 is shown in figure 2.2 on the left-hand side. In order to transform this into a PF curve it is flipped over a center horizontal axis and to achieve this the defect size variable, a, is replaced by a condition variable, $cond$, resulting in the following.

$$\begin{aligned} cond &= \frac{a_{cr} - a}{a_{cr}} = 1 - a \\ cond_i &= \frac{a_{cr} - a_i}{a_{cr}} = 1 - a_i \\ cond_{cr} &= \frac{a_{cr} - a_{cr}}{a_{cr}} = 1 - 1 = 0 \end{aligned}$$

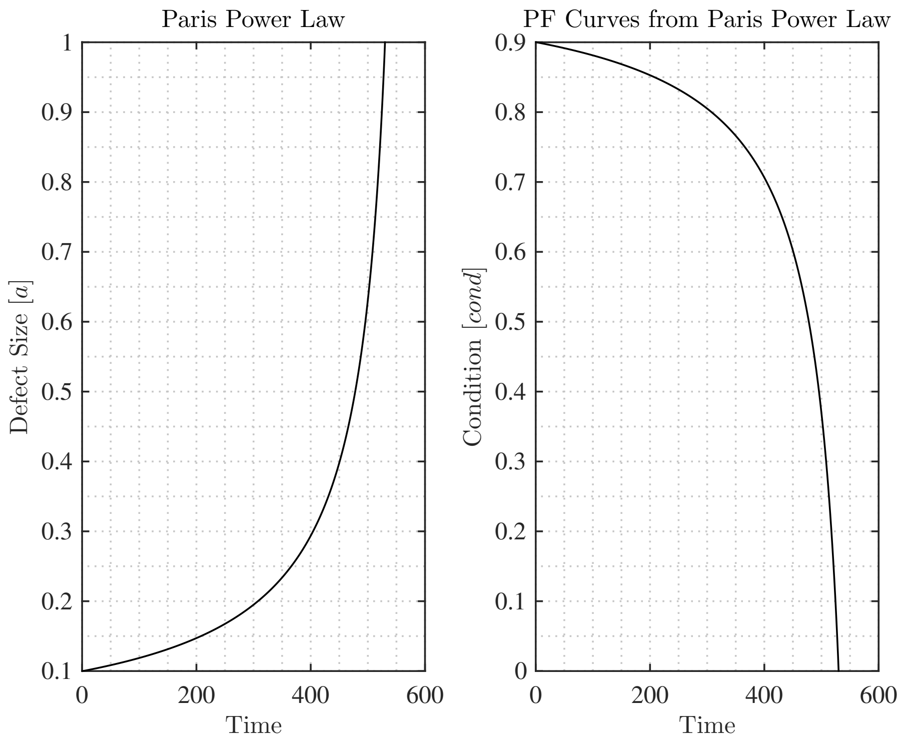

Figure 2.2: Paris Power Law PF Curve Representation

In the model randomness of failure events is introduced by randomising either initial defect size, a_i, or the operating condition parameter, C. Using equation 2.5, component lifetimes can be calculated and a failure distribution can be developed. Figure 2.3 shows the result of randomising a_i and keeping C and m constant. The respective component lifetimes from 50 randomly generated a_i values are calculated using equation 2.5 and the PF curves are developed using equation 2.6. The a_i and N_f distributions are shown in red. In all three instances the initial defect size mean $a_{i_\mu} = 0.1$ and initial defect size standard deviation are varied according to $a_{i_\sigma} = \{0.005; 0.03; 0.07\}$.

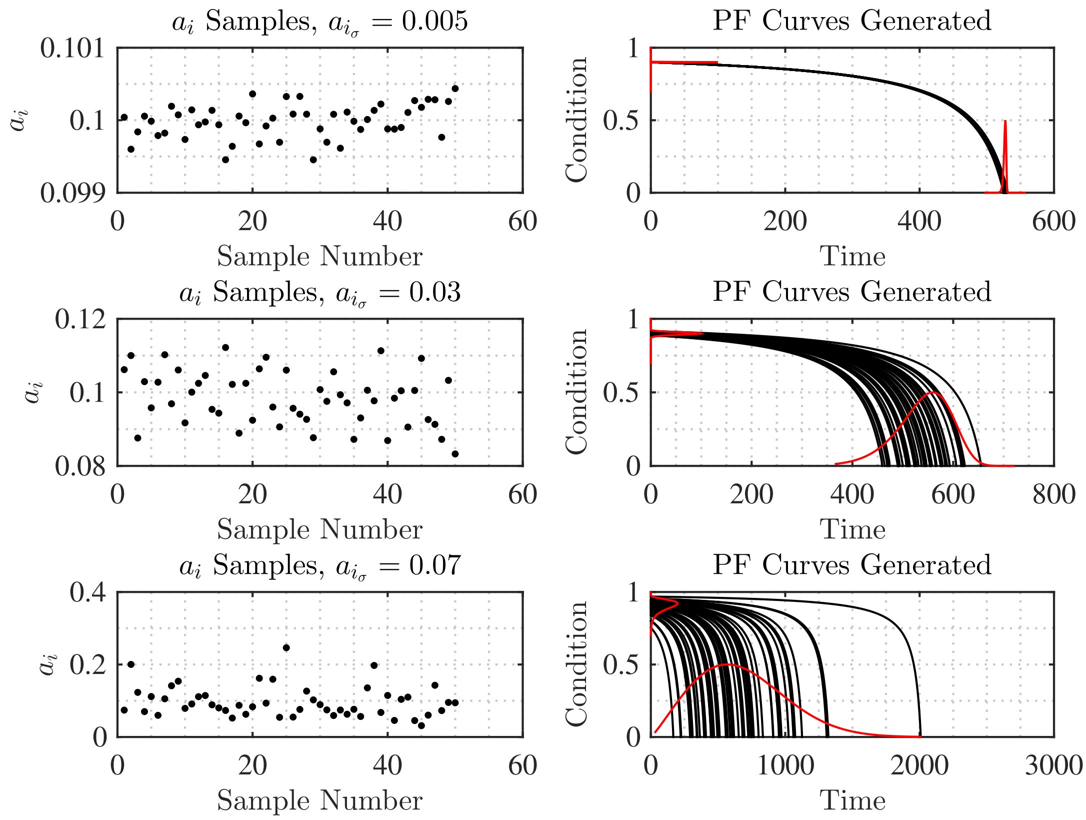

Figure 2.3: PF Curves Generated by Alternating a_i

Figure 2.4 shows the result of randomising C and keeping a_i and m constant. The respective component lifetimes from 50 randomly generated C values are calculated using equation 2.5 and the PF curves are developed using equation 2.6. The N_f distributions are shown in red. In all three instances the operating condition parameter mean $C_\mu = 0.02$ and operating condition parameter standard deviation is varied according to $C_\sigma = \{0.0009; 0.007; 0.009\}$.

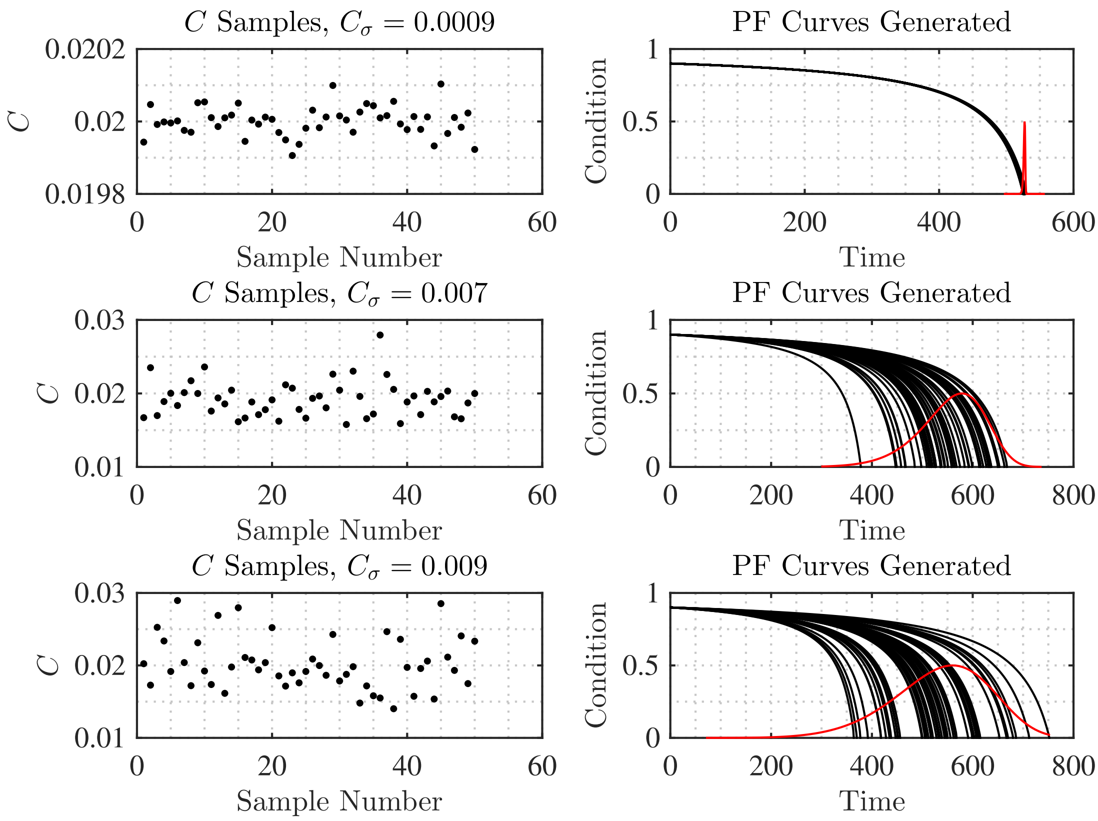

Figure 2.4: PF Curves Generated by Alternating C

It can be seen that by randomising a_i and keeping C constant, equation 2.5 forces the shape of the a_i distribution to determine the shape of the N_f distribution, provided that m remains constant, which is examined in more depth in section 3.1. By, for example, having a narrowly distributed a_i distribution, the N_f distribution would be distributed narrowly as well, but the wider the a_i distribution becomes, the closer the N_f distribution approaches an exponential distribution. The same applies by randomising C and keeping a_i constant. This is shown in figure 2.5 and 2.6 where the a_i and C distribution shapes are respectively compared to the shape of the N_f distribution.

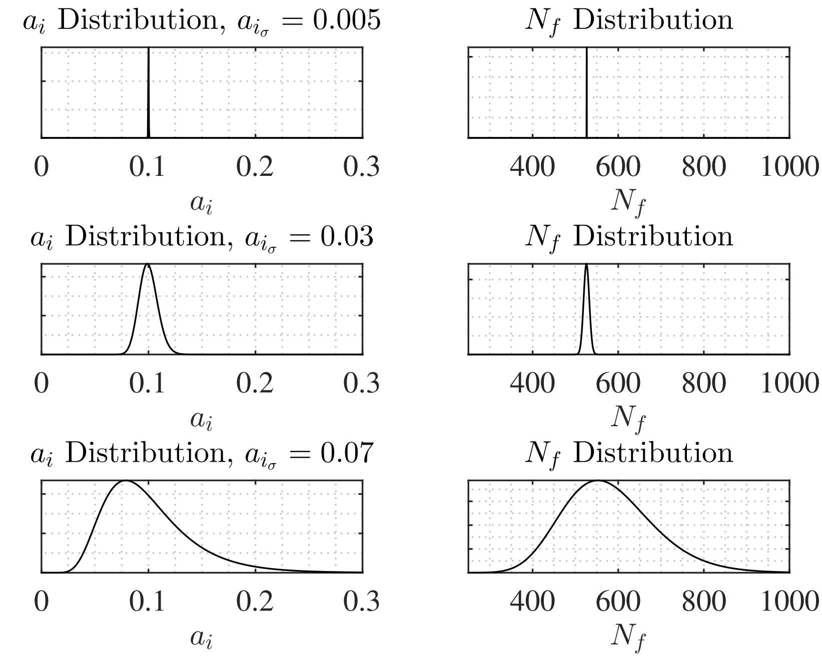

Figure 2.5: N_f Distribution Resulting from a_i Distribution

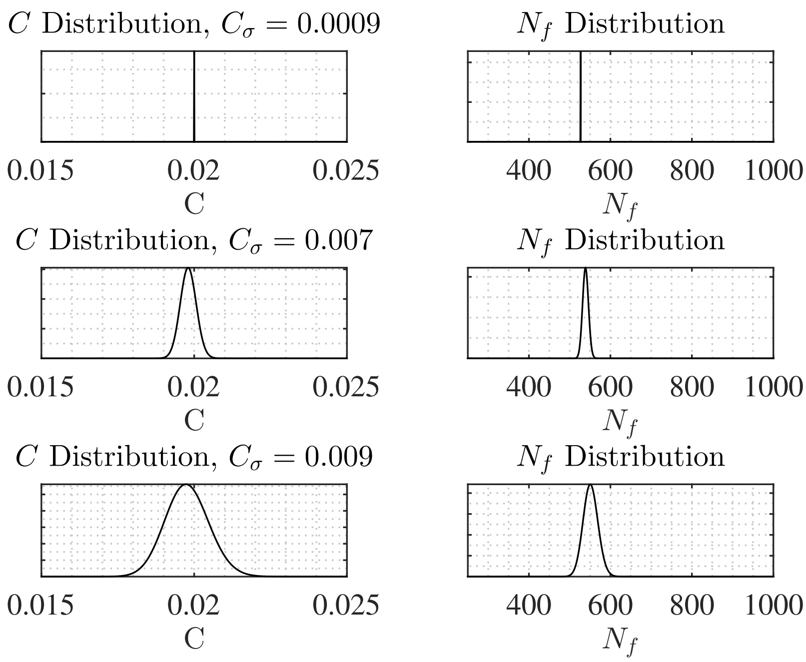

Figure 2.6: N_f Distribution Resulting from C Distribution

2.2.2 Daily Failures

The degradation according to the Paris power law is simulated for a fixed period of time. This module accounts for six maintenance tactics and components are replaced according to the respective chosen maintenance tactic. The six maintenance tactics are

- Run to failure, where no attempt is made to detect imminent failure and components are replaced based on a reactive approach.
- Corrective maintenance, where imminent failure can be detected, but components are still replaced on failure. This means that reactive replacements can be scheduled.
- Time-based maintenance, where preventative replacements are based on optimum replacement times calculated from statistical failure data.
- Servicing, where components are serviced at fixed intervals to an as-new condition.
- Condition-based maintenance, where components are monitored and preventative replacements are based on physical failure models.
- Design-out maintenance, where preventative replacements are made by redesigning a component.

The replacements are based on two *smart* parameters that are employed to replicate each respective maintenance tactic. The two parameters are the minimum crack length that can be detected and the probability of detecting the flaw. Each component has a different flaw size at which detection becomes possible and each maintenance tactic has a different probability of detection. The distinction between a run to failure and condition-based tactic, for instance, is that the run to failure tactic's probability of detection is 0% where a condition-based tactic's probability of detection is, say, 50%. This section of the model accounts for all possible replacement outcomes for all maintenance tactics and once a maintenance tactic is applied for a certain period, or a maintenance approach that consists of a combination of maintenance tactics is applied, can the degradation and replacement consequences of the applied maintenance tactic be extracted from this module.

2.2.3 Plant Engineering Performance Daily (PEPD)

After obtaining all possible daily failures with regards to all maintenance tactics, the maintenance tactics must be applied over time according to the chosen maintenance approach for the entire period that the model will simulate. The applied maintenance approach result in maintenance consequences that can be of a different nature than that of the selected maintenance tactics. For instance a time-based tactic will result in mostly time-based replacements, but some components might fail before replacement, resulting in a combination of scheduled and unscheduled, replacements. This is reasonable due to the fact some components' degradation rates would be more drastic compared others, depending on the distributed initial condition parameter. The output of this module is a combination of maintenance consequences, or events, for each respective maintenance tactic. All possible maintenance consequences for this model are shown for each respective maintenance tactic in table 2.1.

Table 2.1: Time-Based Maintenance Approach Simulation: Maintenance Tactics and Replacement Consequences

		Maintenance Tactic					
		Run to Failure	Corrective Maintenance	Time-Based Maintenance	Servicing	Condition-Based Maintenance	Design-Out Maintenance
Replacement Consequence	Failure						
	Unscheduled Replacement						
	Scheduled Replacement						
	Time Replacement						
	Servicing Replacement						
	Condition Replacement						
	Design-Out Maintenance						

2.2.4 Plant Engineering Performance Daily Cost (PEPDC)

This section is a basic derivation from PEPD, as the replacement events are multiplied by the respective cost.

2.2.5 Maintenance Mix

Up to this point, the model has considered all possible outcomes by applying all maintenance tactics. This module takes a combination of maintenance tactics, called the *maintenance mix*, and applies each respective maintenance tactic over a certain period. As mentioned previously, this module extracts the specific component degradation functions and replacement consequences from its predecessors based on the periods that respective maintenance tactics are applied. Future work on the model involves developing a maintenance mix optimiser, which weighs the cost of maintenance, downtime and production losses to find the optimal maintenance mix over the simulation time.

2.2.6 Plant Total Performance Daily and Monthly

The maintenance mix, PEPD and PEPDC merges to form the plant total performance on a daily basis, which is then summarised into a monthly performance. The output of this module is total maintenance consequence in the form of replacement events and replacement cost. This module can be used to compare the monthly performance of the system on a monthly basis.

2.2.7 Key Performance Indicators (KPIs)

If the system is of a production nature, an expected production rate for a running system can be specified statistically in this module. The daily production depends on the applied maintenance tactic and hence to the downtime of the system. While the system is running, the daily production will vary according to the certain specified production distribution. The outputs of this module include daily production, a total production histogram and maintenance mix with respect to downtime and monetary expense.

2.3 Simulating a Real-Life System

At the commencement of the current study it was intended to develop the time-based maintenance approach simulation further to accommodate real components and it was hypothesised that the PF curve generating mathematics may be reversed so that real-life failure data is the input and PF curves are the output (in the case where full knowledge of the failure mechanism is not known). Failure data from a ball mill operating at an Anglo Platinum mine in Mogalakwena, Limpopo (South Africa) over the past two years is accessible and no history of CM is available, which means that the only knowledge that is present with regards to the Paris power law as a failure mechanism is that of times to failure, or component lifetimes, meaning that component life, N_f, can be estimated, although not necessarily accurately. The material type is also known and therefore the material property constant, m, is also known. Testing of the hypothesis stated above is a challenging task due to the fact that full knowledge of the failure mechanism is not known, initial defect sizes, a_i, and the operating condition parameter, C, are unknown. Figure 2.7 shows the variables from the Paris power law failure mechanism, equation 2.5, that are known and unknown.

$$N_f = \frac{1 - {a_i}^m}{Cm}$$

Figure 2.7: Known and Unknown Variables in the Paris Power Law for Real Failure Data

Using equation 2.5, it would be impossible to reverse the mathematics as hypothesised in this section due to the fact that knowledge of the failure mechanism is not sufficient. Attempting to develop the model further to accommodate real components is impossible with access to failure data alone. A second hypothesis is made, which states that a reasonable estimate of a PF curve may be derived from failure data + partial knowledge of the failure mechanism. This could solve the fact that there is no method present to solve the second column shown in figure 2.2. This hypothesis is elaborated on and tested in chapter 3.

Table 2.2: Proactive Maintenance Spectrum

	Ideal CBM	**This Study**	**PHM**	**Reliability Theory**
Failure Statistics	Yes	Yes	Yes	Yes
Failure Mechanism	Yes	Yes	No	No
Condition Monitoring Possible	Yes	Yes	Partially	N.A
Condition Monitoring History	Yes	No	Yes	No
Mainte-nance Approach	Predictive Maintenance	Predictive Maintenance	Predictive Maintenance	Preventative Maintenance
Method	Physical Failure Model	**Unknown**	PHM	Time/Use-Based

2.4 Conclusion

The time-based maintenance approach simulation is a model that is used to show the influence of various maintenance tactics on the production and monetary expense, such as maintenance cost and profit lost due to downtime, on an arbitrary system using dummy data. The model includes specifying different component types with parameters used in a Paris power law failure mechanism. In an attempt to model a real-life system using obtained failure data, a problem is encountered that obstructs this goal. The lack of CM data results in a roadblock on the path to modelling a real-life system using the model described in this chapter. It is found that full knowledge of the failure mechanism must be available in order to accommodate a real-life system in the model. Section 2.3 sets the hypothesis to be tested in chapter 3 and states that it might be possible to derive a reasonable estimate of a PF curve from failure data + partial knowledge of the failure mechanism.

Chapter 3

Numerical Experiment

3.1 Introduction

The hypothesis from chapter 2 states that a reasonable estimate of a PF curve may be derived from failure date + partial knowledge of the failure mechanism. The goal is to develop PF curves to represent component degradation with access to only failure data and no CM history. In the context of the Paris power law, equation 2.5, this means that knowledge regarding component lifetimes, N_f, is present, but no knowledge regarding initial defect size, a_i, or initial condition, $cond_i$, and the operating condition parameter, C, is present. The material property constant, m, is known from the material type of the component used.

In order to develop an estimated PF curve, failure data + full knowledge of the failure mechanism is needed. The data used in the experiment can be obtained either by laboratory tests, gathered field data or numerically generated data. The time-based maintenance approach simulation's process of generating PF curves, which is of a numerical nature, perfectly fits this purpose.

3.2 PF Curve Generation

As previously mentioned, the failure data that is used in the numerical experiment is generated numerically. Within this chapter, reference is made to "true" and "predicted" PF curves, which differs from each other accordingly:

- True PF curve
  - A true PF curve is generated with knowledge of all parameters in the Paris power law, equation 2.5. This means that the PF curve is generated by numerically calculating the degradation per time to condition $cond = 0$, using equation 2.6, and the component's real condition is known for every instance. The condition parameter, $cond$, is normalised to ensure prime condition is $cond = 1$ and failure is $cond = 0$.
- Predicted PF curve
  - A predicted PF curve is generated by assuming that we only have knowledge regarding the time to failure, N_f, and the material constant, m. Therefore two parameters, the initial condition $cond_i$ and operating condition parameter C, are unknown. It would be impossible to calculate these values, as the

assumption is made that no CM history is available, which could be used to estimate an initial condition, $cond_i$. By bringing CM history into play, the problem that the work in this dissertation is trying to solve does not exist, because a PF curve can then be calculated based on pre-existing CM data and CBM can simply be implemented (in practice new implementation of CBM on equipment would often imply that CM data had not been gathered historically). The solution is to estimate a value for the initial condition, $cond_i$, and calculate the value of the operating condition parameter, C, using the Paris power law equation 2.5. It would then be possible to generate a PF curve due to the fact that all parameters would be available, but the accuracy of the thus generated predicted PF curve needs to be validated against the true PF curve to validate the method. The solution can also be obtained by estimating a value for the operating condition, C, and calculating the value of the initial condition, $cond_i$, using the Paris power law equation 2.5.

The difference between the true and predicted PF curves are shown in figure 3.1, where the true PF curve is developed with full knowledge of the failure mechanism and the predicted PF curve is developed with failure data and an estimate with regards to the initial condition, $cond_i$, or the operating condition parameter, C.

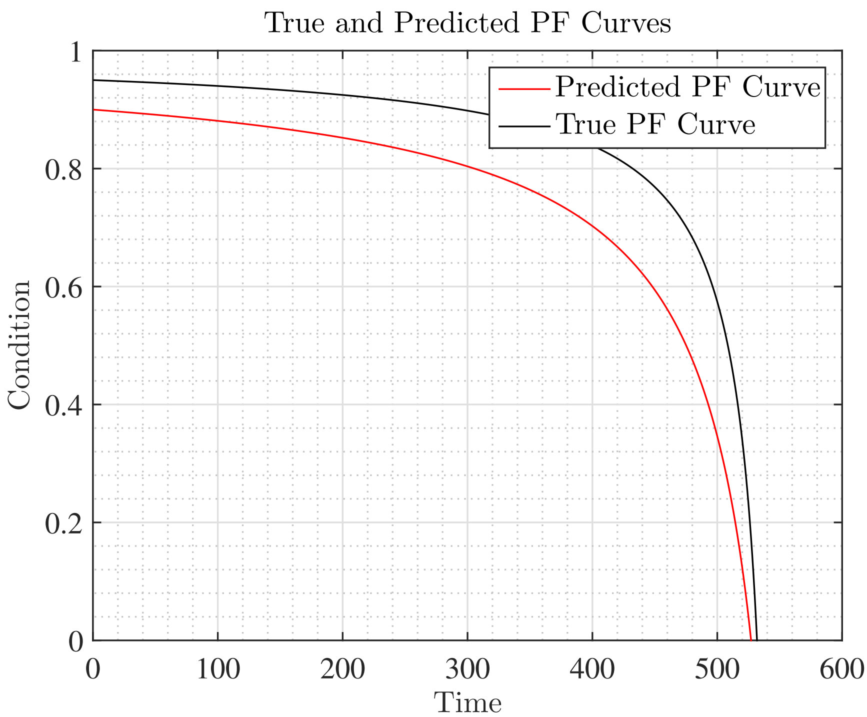

Figure 3.1: Original and Experimental PF Curves

3.3 PF Curve Validation

The validation is achieved by conducting a sensitivity study that compares a component's true PF curve to a range of predicted PF curves resulting from various initial condition values that were estimated. The process is repeated for various component types and therefore various true PF curves, which results in an error surface. The sensitivity study process is depicted step-by-step in figure 3.2 below.

In step 1, a true PF curve is generated with full knowledge of the failure mechanism. Step 2.1 then generates a predicted PF curve with knowledge of failure data, the material type and an estimate with regards to the initial condition or operating condition parameter. The true and predicted PF curves are then validated against each other in step 2.2. In step 2.3 the estimate with regards to initial condition or operating condition parameter is changed and the predicted PF curve generation cycle, shown in red (steps 2.1 to 2.3), is repeated for a certain number of times. Once the validation is completed, the true PF curve characteristics is changed in step 3 and the blue cycle is initiated again. The blue cycle is repeated until enough component types have been generated to represent a wide range of component types and therefore component lifetimes. Keep in mind the relationship between component condition and component defect size:

$$cond = \frac{a_{cr} - a}{a_{cr}} \tag{3.1}$$

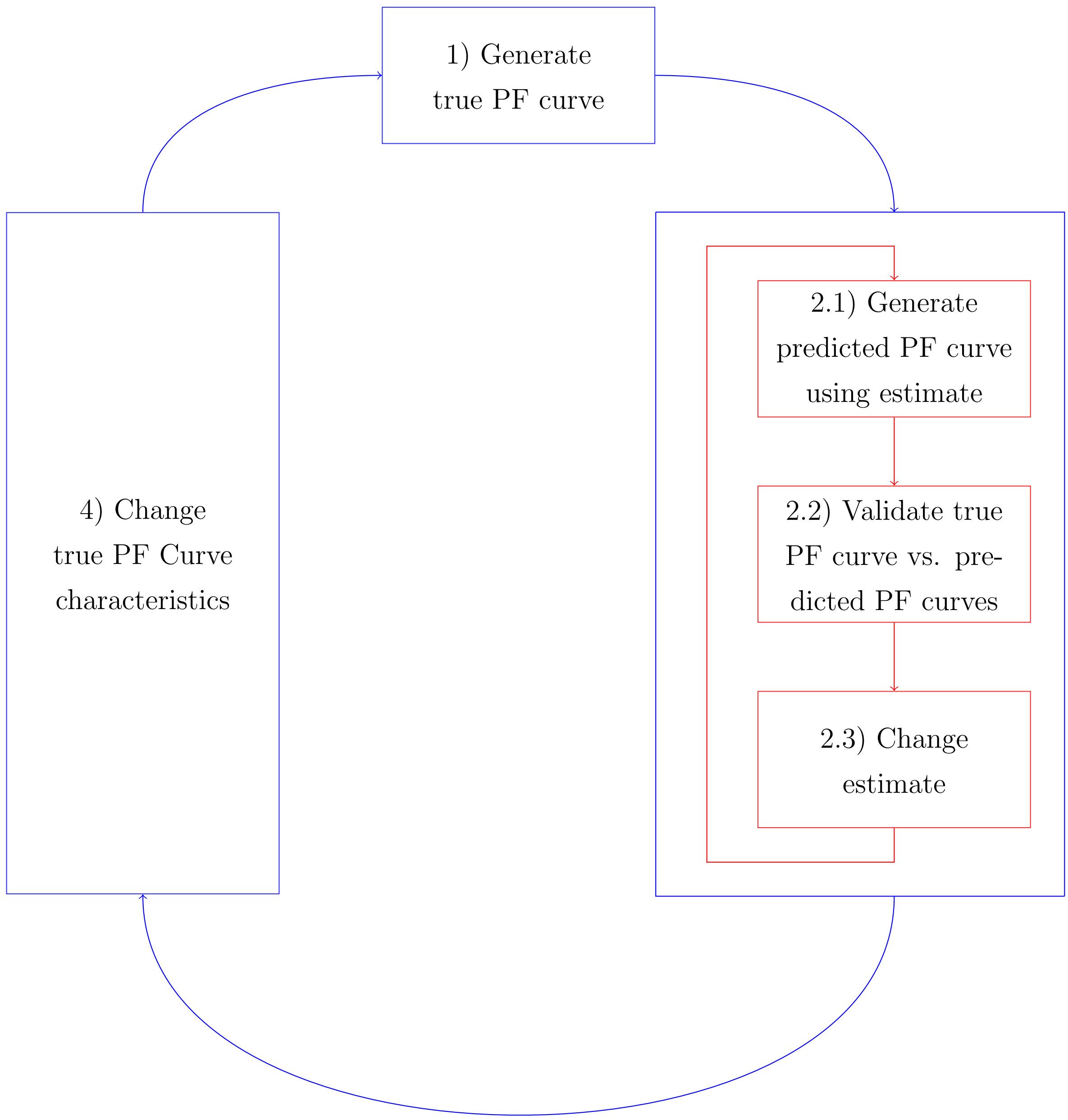

Figure 3.2: Validation of True PF curve vs. Predicted PF Curve

The result of a single validation cycle, as shown in the red cycle in figure 3.2, is referred to as the error. The error is simply the time difference between a true and predicted PF curve at a certain condition as a fraction of the time at that condition of the true PF curve. An error at $cond = 0.5$ is shown in figure 3.3 by the blue horizontal line between the true and predicted PF curves.

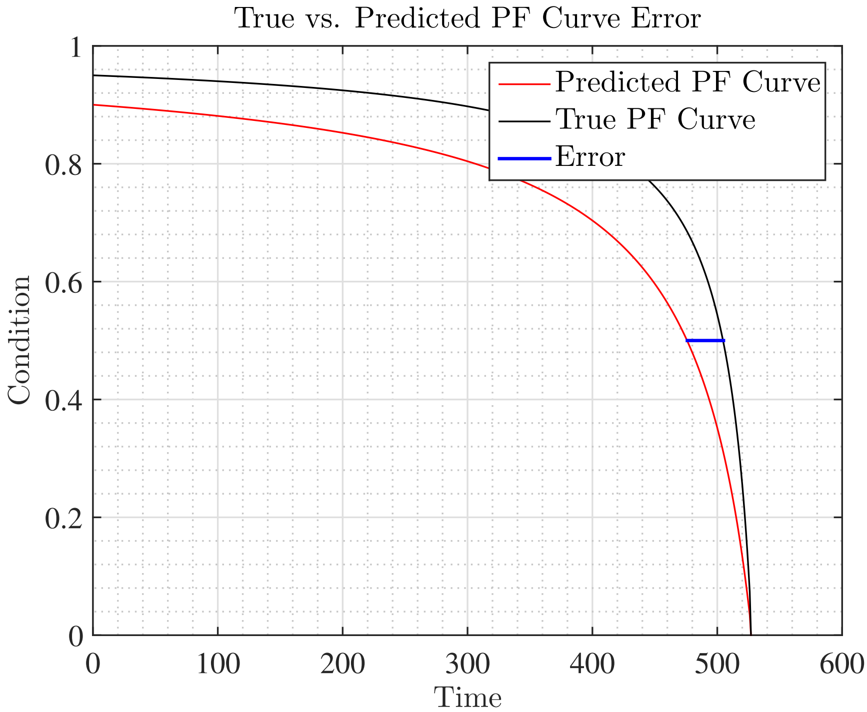

Figure 3.3: Error

In order to explain the numerical experiment validation process, an example where the predicted PF curves are generated by estimating values for initial condition, $cond_{i_{predicted}}$, is shown in figure 3.4. A true PF curve is generated using an initial condition of $cond_{i_{true}} = 0.9$ and the predicted PF curves are generated using initial condition $cond_{i_{predicted}} = 0.9, 0.8, 0.7$. This means that three error values can be calculated as shown in figure 3.3 and these three error values are shown graphically in figure 3.5 where the error is measured at condition $cond = 0.5$. By completing the blue cycle shown in figure 3.2, more true PF curves are generated by changing the true PF curve characteristics. Figure 3.6 shows three true PF curves using initial condition $cond_{i_{true}} = 0.9, 0.8, 0.7$ where each true PF curve is validated against three predicted PF curves with initial condition $cond_{i_{predicted}} = 0.9, 0.8, 0.7$. This develops a third dimension in the error validation plot, shown in figure 3.7 where true initial condition $cond_{i_{true}}$ represents the third dimension planes. Following the logic explained in this paragraph, but with smaller interval sizes in the true and predicted PF curve initial condition ranges, results in figure 3.8 and 3.9.

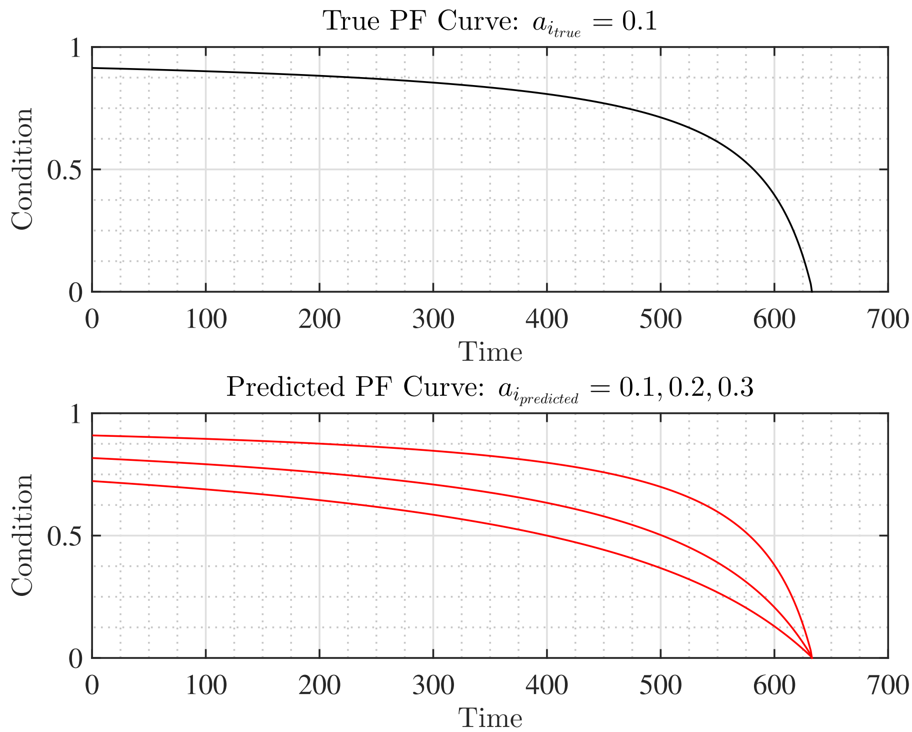

Figure 3.4: Single True PF Curve vs. Multiple Predicted PF Curves

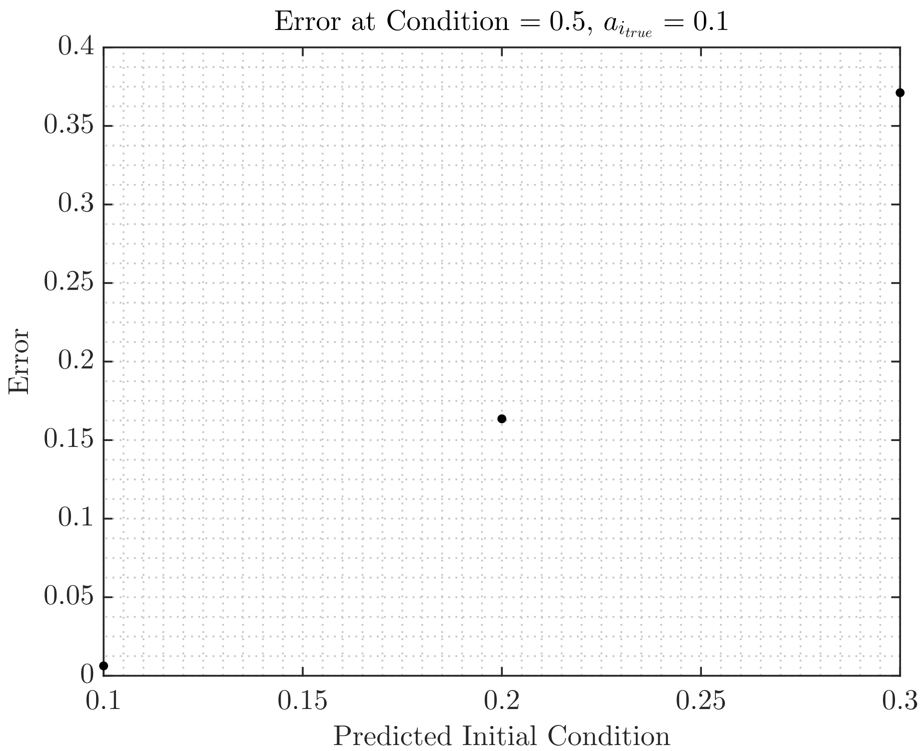

Figure 3.5: Single True PF Curve vs. Multiple Predicted PF Curves Error

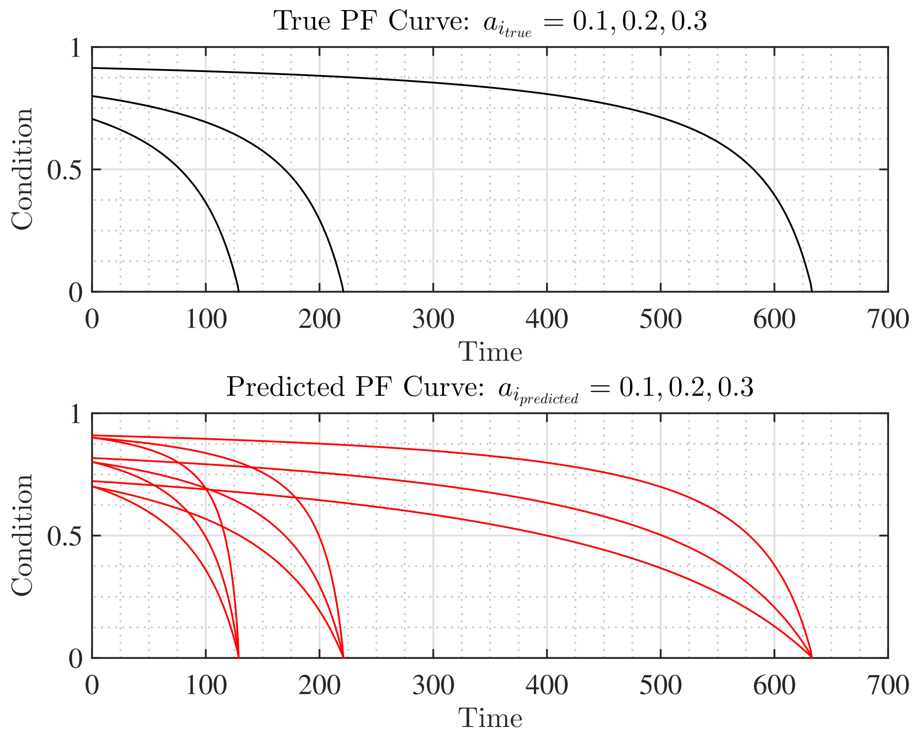

Figure 3.6: Multiple True PF Curves vs. Multiple Predicted PF Curves

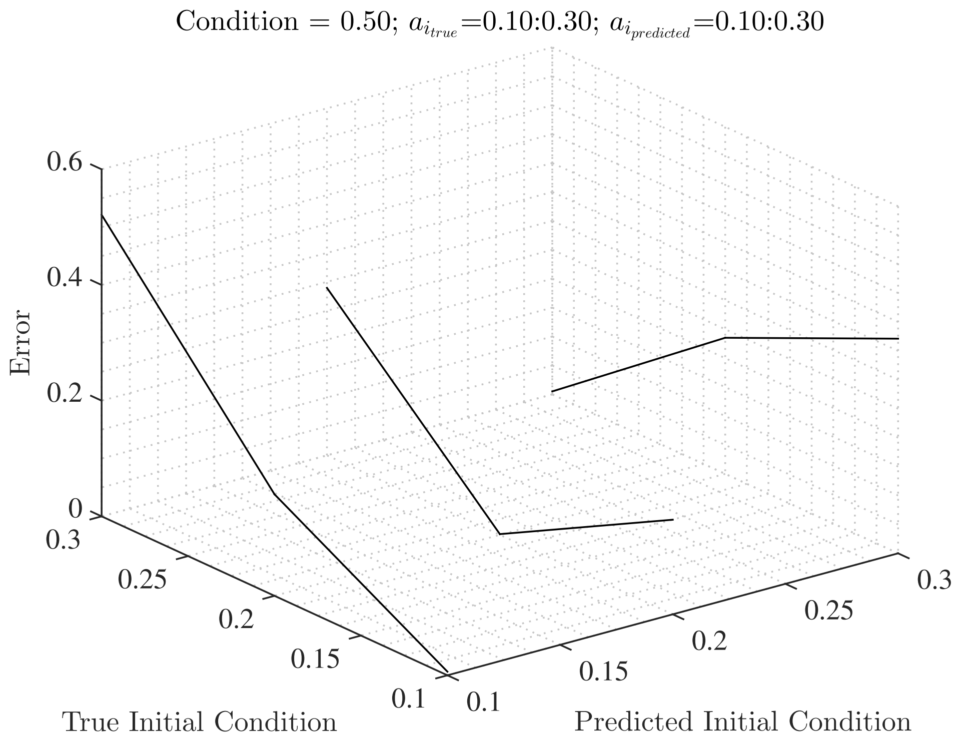

Figure 3.7: Multiple True PF Curves vs. Multiple Predicted PF Curves Error

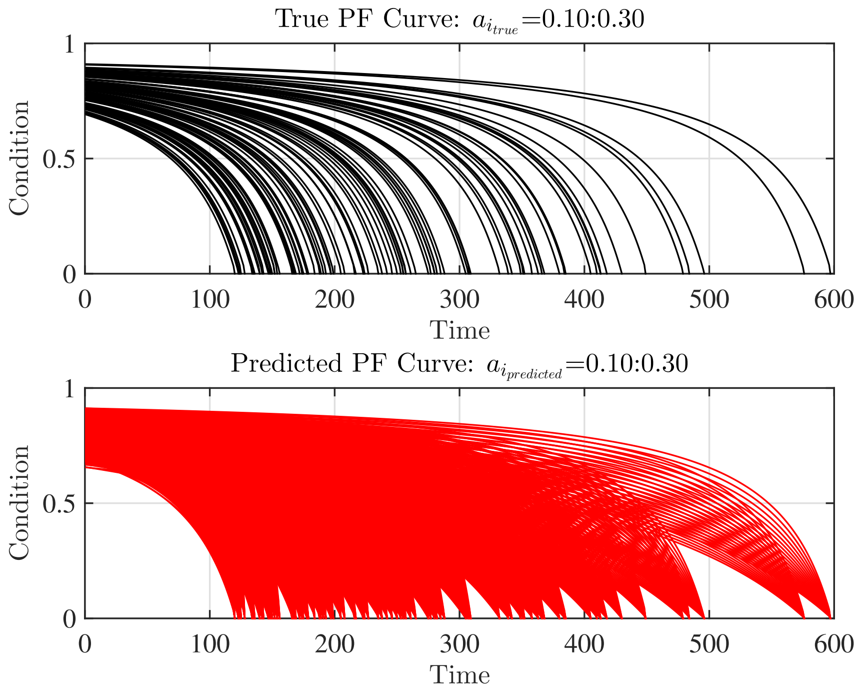

Figure 3.8: Multiple True PF Curves vs. Multiple Predicted PF Curves: Smaller Intervals

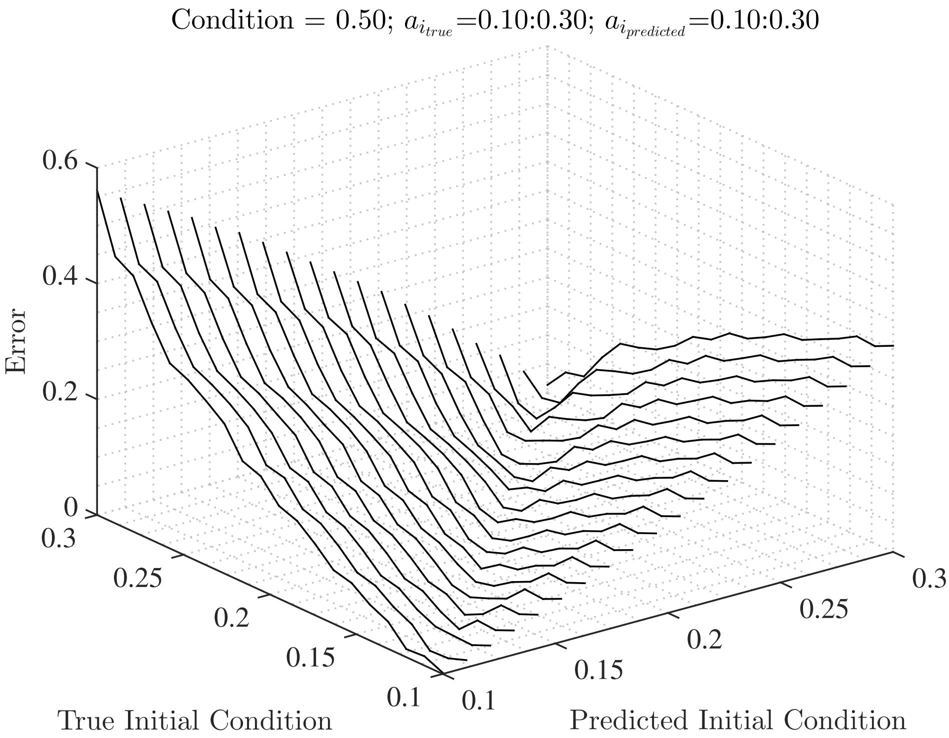

Figure 3.9: Multiple True PF Curves vs. Multiple Predicted PF Curves Error: Smaller Intervals

Figure 3.5, 3.7 and 3.9 shows the resulted error from PF curve validation at condition $cond = 0.5$. The result in figure 3.9 is referred to as an error surface in the remainder of this dissertation. Error surfaces can also be obtained at other component conditions, but in this study $cond = 0.5, 0.4, 0.3, 0.2, 0.1$ are considered.

3.4 Experimental Setup

The numerical experiment assumes that failure data is available by generating it numerically, as discussed in section 3.1. It is also assumed that a component will not have an initial defect size of more than 0.3 of the critical condition, therefore $a_i \leq 0.3(a_{cr})$, or $0.7 \leq cond_i \leq 1$. It is decided to estimate $cond_i$ and calculate C using equation 2.5 for development of predicted PF curves. Two-hundred true PF curves are generated using $cond_{i_{true}} = 0.05 - 0.3$, which are each validated against two-hundred predicted PF curves which are generated using $cond_{i_{predicted}} = 0.05 - 0.3$. This means that each true PF curve is validated against two-hundred predicted PF curves. To bring this into context with regards to figure 3.2, the blue cycle will be completed two-hundred times and for each blue cycle, will the red cycle be completed two-hundred times. Validation will occur place at five conditions, $cond = 0.5, 0.4, 0.3, 0.2, 0.1$ and each of these validations will yield an error surface as shown in figure 3.9.

3.5 Results

The resulting error surfaces are shown in appendix B for $cond = 0.5, 0.4, 0.3, 0.2, 0.1$. Looking at the error surfaces, it can be seen that the overall error decreases as the condition where error is validated decreases. This is due to the fact that a true PF curve and its respective predicted PF curve share the same component life, N_f. The maximum error from each error surface is shown in figure 3.10, which gives a threshold in terms of what the most inaccurate prediction can yield at various conditions.. The maximum error at $cond = 0.5$ is approximately 62%, but it can be seen that the maximum error at $cond = 0.3$ is smaller than 20%. These error values are the absolute worst case scenario at the respective validated condition and in all cases this is achieved by comparing a true PF curve with $a_{i_{true}} = 0.3$ to a predicted PF curve with $a_{i_{predicted}} = 0.05$.

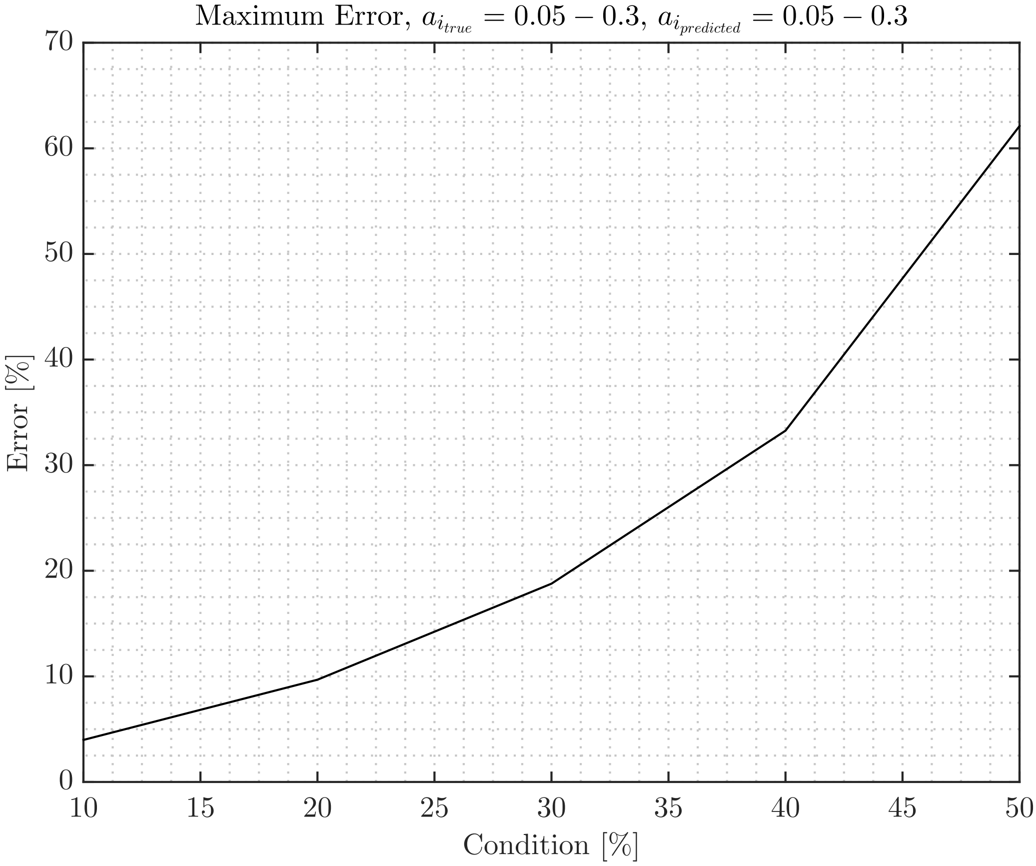

Figure 3.10: Numerical Experiment Results: Maximum Error

3.6 Discussion

The hypothesis stated in this chapter was that a reasonable estimate of a PF curve may be derived from failure data + partial knowledge of the failure mechanism. The failure data was generated numerically and the failure mechanism was partially known: N_f was known from failure data and m was known due to it being a material constant. The sensitivity study mentioned in this chapter involved validation of predicted PF curves.

The first step to validate the error of the estimation method discussed in this chapter entailed evaluating pairs of true and predicted PF curves in terms of time difference at various conditions, $cond = 0.5, 0.4, 0.3, 0.2, 0.1$. Two-hundred true PF curves are generated using two-hundred different true initial condition values, $a_{i_{true}} = 0.05 - 0.3$, and for each of these true PF curves, two-hundred predicted PF curves were generated using initial condition $a_{i_{predicted}} = 0.05 - 0.3$. This is how the error surface is developed.

Two things were observed and learned:

- The error surface has a smooth trend, meaning it has no sharp peaks/values, as was expected. The error is zero when $a_{i_{true}} = a_{i_{predicted}}$ and increases as $a_{i_{predicted}}$ separates from $a_{i_{true}}$. The maximum error is at $cond = 50\%$ where $a_{i_{true}}$ and $a_{i_{predicted}}$ are the furthest apart. The error also decreases as condition reaches $cond = 0\%$ which indicates that the method may be accurate for practical use.

- In practice, however, it will not be possible to know which of the true PF curves represents a specific component at the start of its life. It is, for example, possible that a newly installed component may have a large initial defect ($a_{i_{true}} = 0.3$), or a small one ($a_{i_{true}} = 0.1$) or anything in between. Not knowing which true PF curve to use means that the calculation of the operating condition parameter, C, given a choice of predicted initial condition, $a_{i_{predicted}}$, can not be performed, since the component lifetime, N_f, is unknown. In chapter 4, where the application of the newly developed method is described, a solution to this problem will be presented.

Chapter 4

Application of the Newly Developed Method for Implementation of CBM

4.1 Introduction

This chapter examines whether the newly developed method of PF curve prediction can be applied to other applications, such as modelling of bearing degradation using PF curves. The results from the numerical experiment show that initial conditions for a defect can be chosen within a certain range and the proposed degradation function, or PF curve, would resemble the real component degradation curve relatively closely. In this chapter the application of the new method on bearings is conceptually described.

4.2 Bearing Life Degradation

Bearings are subjected to a certain intensity of repeating stress on their track ring and rolling element even during operation under proper loading, appropriate mounting and sufficient lubrication. A bearing's basic life rating, with a reliability of 90%, is shown by equation 4.1,

$$L_{10} = \left(\frac{C_r}{P_r}\right)^{10/3} \tag{4.1}$$

where L_{10} is the basic life rating, C_r is the basic dynamic load rating and P_r is the dynamic equivalent radial load. Equation 4.1 can be adjusted by taking a reliability correction factor, a_1, a special material property factor, a_2, and a special operating conditions factor, a_3, into account to calculate the corrected bearing life rating. This is shown by equation 4.2,

$$L_{na} = a_1 a_2 a_3 L_{10} \tag{4.2}$$

where L_{na} is the corrected bearing life rating [Nose Seiko, 2016]. The reliability correction factor, a_1, for bearing reliability larger than 90% is depicted in table 4.1.

Table 4.1: Bearing Reliability Factor a_1

Reliability (%)	L_n	a_1
90	L_{10}	1
95	L_5	0.62
96	L_4	0.53
97	L_3	0.44
98	L_2	0.33
99	L_1	0.21

The reliability factors shown in table 4.1 are shown graphically in the first part of figure 4.1. This is in essence the tail of a survival function and the Weibull parameters, β and η, can be extracted from this. The second part of figure 4.1 shows the entire survival function with $\beta = 1.5$ and $\eta = 4.46$.

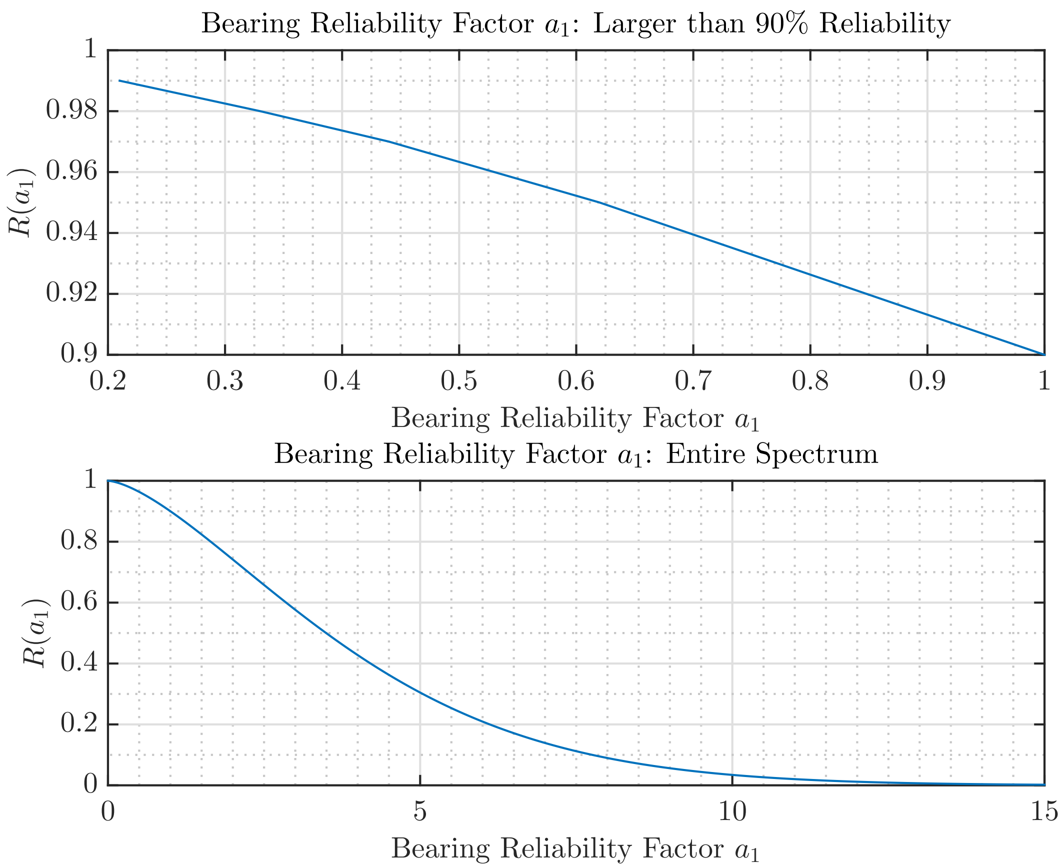

Figure 4.1: Bearing Reliability Factor Survival Function

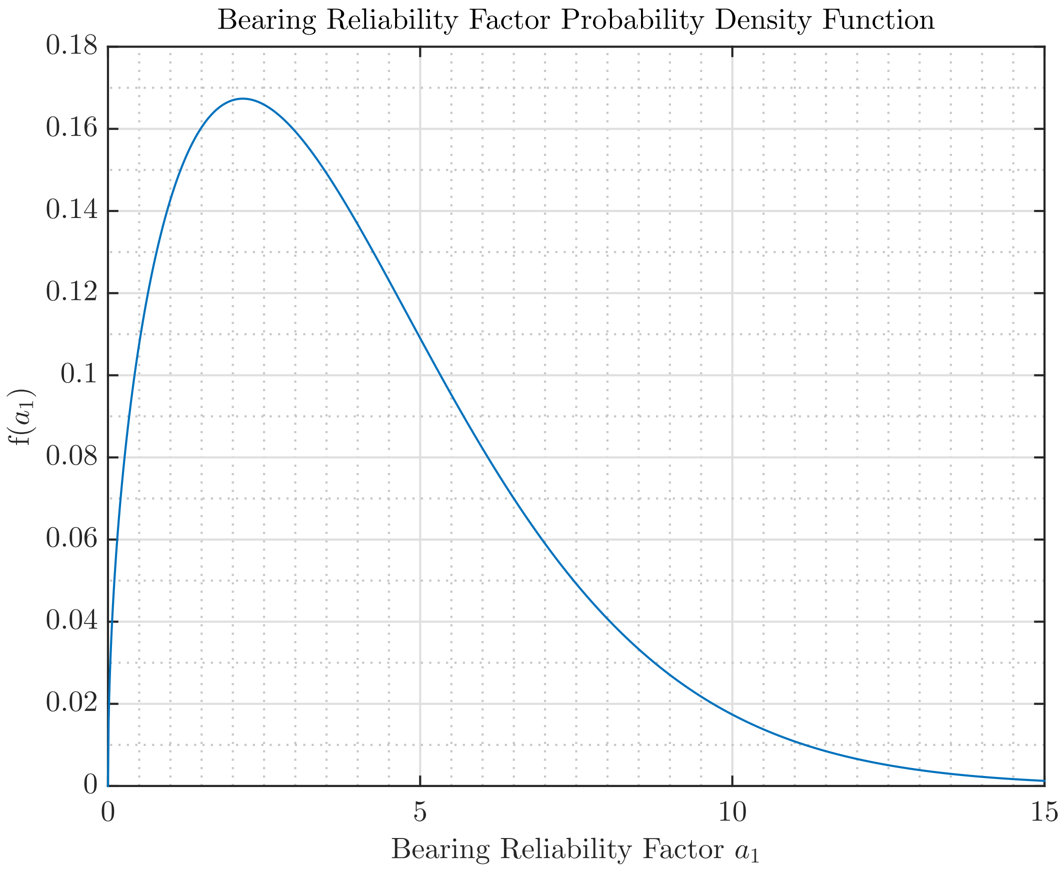

Figure 4.2: Bearing Reliability Factor Probability Density Function

By knowing the basic load rating and the dynamic radial load of an installed bearing, the corrected life rating can be adjusted for the reliability need from 0% to 100% according to the second part of figure 4.1.

Xu et al. investigated the relationship between characteristic values of vibration signals and the variable in the Paris equation which can describe the health of 6205 deep groove ball bearings [Xu et al., 2012]. The historic lives and vibration signals were analysed and the feasibility of this method was investigated. It was found that an improved Paris model considers the change of Root Mean Square (RMS) and Intrinsic Mode Function (IMF) with regards to the fault characteristic frequency and it is suited for online residual fatigue life prediction [Xu et al., 2012].

Li et al. established a stochastic defect-propagation model without the requirement of prior knowledge of bearing characteristics that determines the mean path of defect propagation and its dispersion at any instance [Li et al., 2000]. By employing a random variable to account for time-variant and stochastic character of a defect propagation process and proper known initial conditions, two ordinary differential equations are solved to predict mean path and variance of defect propagation. Using this method, the RUL can be statistically determined for the purposes of optimal maintenance scheduling. By assuming that the vibration level generated by the defect bearing is proportional to defect area, this method was used to forecast vibration RMS. It was found that the proposed approach offers a prediction that accommodates bearing replacement before catastrophic failure occurs [Li et al., 2000].

4.3 Condition-Based Maintenance on Bearings Using the Newly Developed Method

Firstly, the newly developed method requires that the failure mechanism can be described by a power law, which includes a practically measurable condition parameter. For bearings, failing due to fatigue of the rolling surfaces, this is the case and the condition parameter would be based on vibration measurements. The form of the life equation is then known and the value of the exponent can be estimated with reasonable accuracy. Secondly, the method requires knowledge of failure statistics. In practice, should historic failure statistics not be available, the Weibull distribution derived from the published life rating for a certain bearing under a known load, together with the reliability factors, can be used for this purpose.

Chapter 3 validated different component types' PF curve errors at various conditions, but as stated in section 3.6, in practice it would not be known which PF curve represents a component's life, at the beginning of its life. By examination of figure 4.2 can it be seen that a bearing's lifetime distribution is very wide. In chapter 3, the assumption was made that initial defect size would not exceed 30% of the critical defect size, which means that the initial condition, $cond_i$, will be greater than 70% of the critical condition. By taking this and the fact that bearing vibration can be monitored into account, a critical value for vibration can be calculated by dividing the vibration measurement on installation, V_i, by the estimation of condition that has already deteriorated, $cond = 1 - cond_i = 1 - 0.7 = 0.3$. This means that $V_{cr} = \frac{V_0}{0.3}$, which will be a worst case scenario based on the assumption that $cond_i \geq 70\%$.

Consider the following scenario: a bearing is installed and a vibration measurement is taken on installation, $V_i = 10mm/s$. Based on the assumption that $cond_i \geq 70\%$, the worst-case critical vibration, $V_{cr_{predicted}} = \frac{10}{0.3} = 33.33mm/s$, but in actual fact $V_i =$

$10mm/s$ is really only 10% of the critical vibration $V_{cr_{true}} = \frac{10}{0.1} = 100mm/s$. Throughout the life of the component, CM vibration measurements are used to develop a predicted PF curve using the following relation.

$$cond_k = 1 - \frac{V_k}{V_{cr_{predicted}}} \tag{4.3}$$

Bearing lifetime distributions are numerically generated by varying values for initial condition, $cond_i = 0.855, 0.9, 0.945$. Using the minimum, mean and maximum values of bearing life, true PF curves are generated for three components using Paris' power law with $c = 0.02$ and $m = -1.1$. Using the worst case scenario critical vibration, $V_{cr_{predicted}} = 33.33mm/s$, vibration measurements over the the three components' lifetimes are used to build a predicted PF curve with equation 4.3. This is compared to another case where the same methodology is followed, but the bearing lifetime distributions are generated by varying the operating condition parameter instead of the initial condition. This is obtained by using $cond_i = 0.9$, $c = 0.03, 0.02, 0.01$ and $m = -1.1$. The results are shown in figure 4.3, where the error at $cond = 0.5, 0.4, 0.3, 0.2, 0.1, 0$ is shown in figure 4.4.

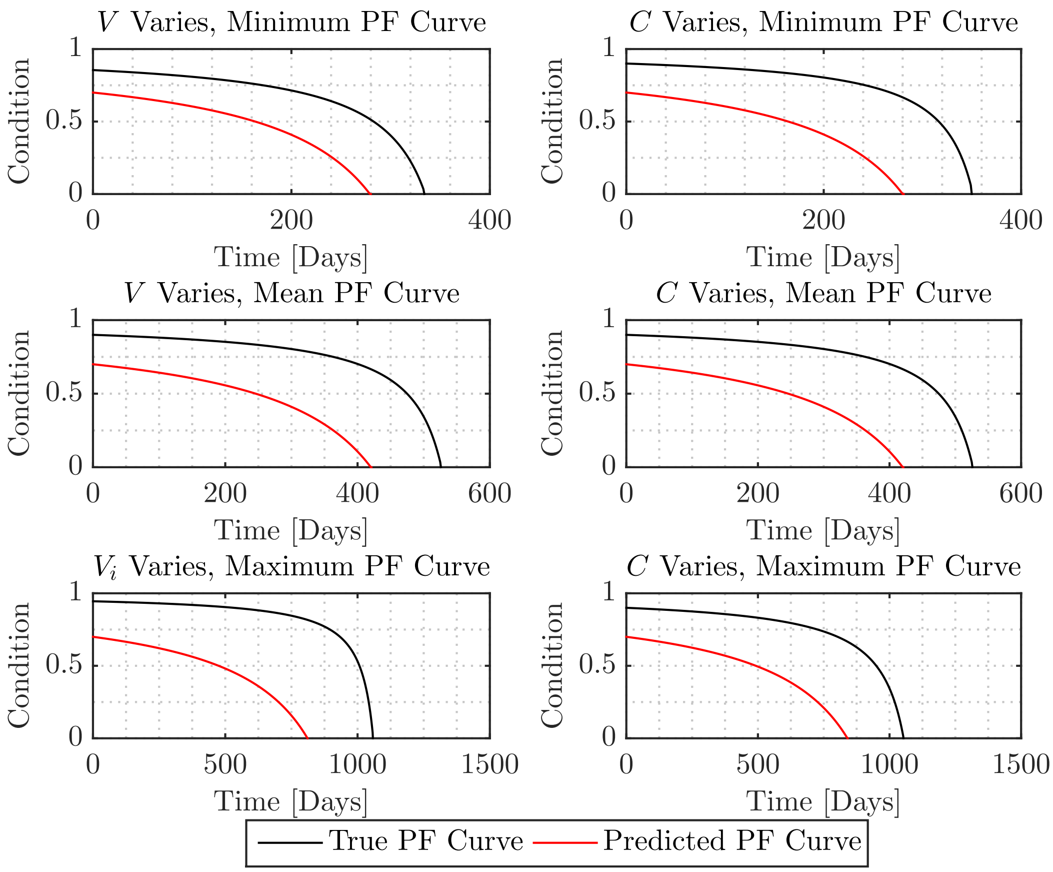

Figure 4.3: Numerical Experiment Part 2

It can be seen that the predicted PF curve estimates the bearing lifetime within 20% of the true bearing lifetime for each case. This is a fair result, due to the fact that using this, maintenance decisions can be made using a conservative PF curve and the bearing lifetime would be estimated within 20%. Recall that this was obtained using the assumption of the worst case scenario. If an initial condition of $cond_i = 0.8$ is used instead of $cond_i = 0.7$, the results are more accurate, as shown in figure 4.5 and figure 4.6. It can be seen that the bearing lifetime is now estimated within 10% of the true bearing lifetime.

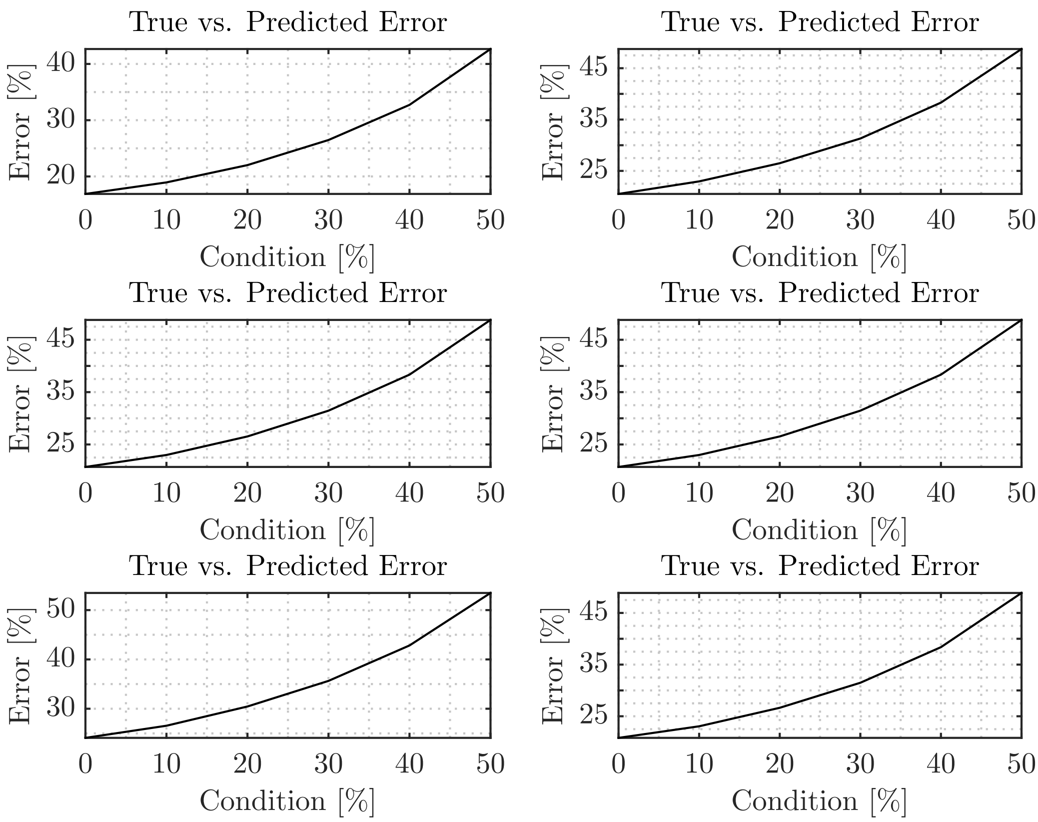

Figure 4.4: Numerical Experiment Part 2 Error

4.4 Summary of Process

Using the knowledge that a vibration level measured on a bearing can be assumed to be proportional to defect size in the bearing [Li et al., 2000], and the results from chapter 4, bearing life degradation can be predicted and PF curves for bearing degradation can be developed. This is possible through the sequence shown in figure 4.7.

4.5 Evolution of the Newly Developed Method

In a practical application, the new method will evolve as more data becomes available. Initially, only failure statistics and some knowledge of the failure mechanism model would be available. In the case of bearings, an initial condition measurement would also be required. CBM decisions would then be based on the PF curves derived using the newly developed method. By definition, CM data will be recorded after application of CBM, which makes it possible to update the PF curve model, using CM histories. The new method therefore evolves to a CBM tactic, as illustrated in figure 4.2.

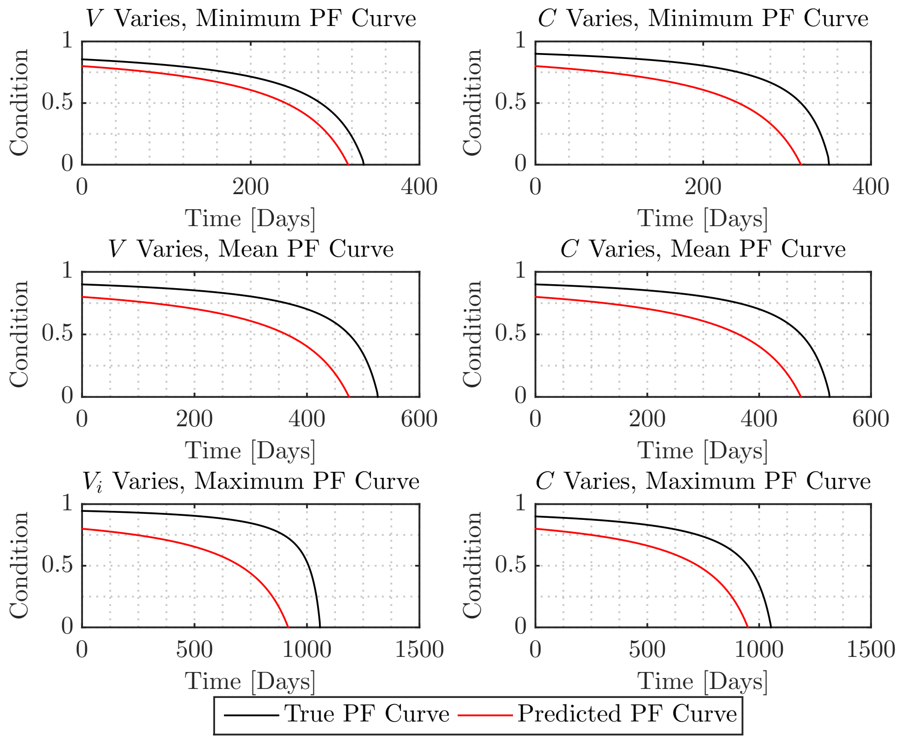

Figure 4.5: Numerical Experiment Part 2

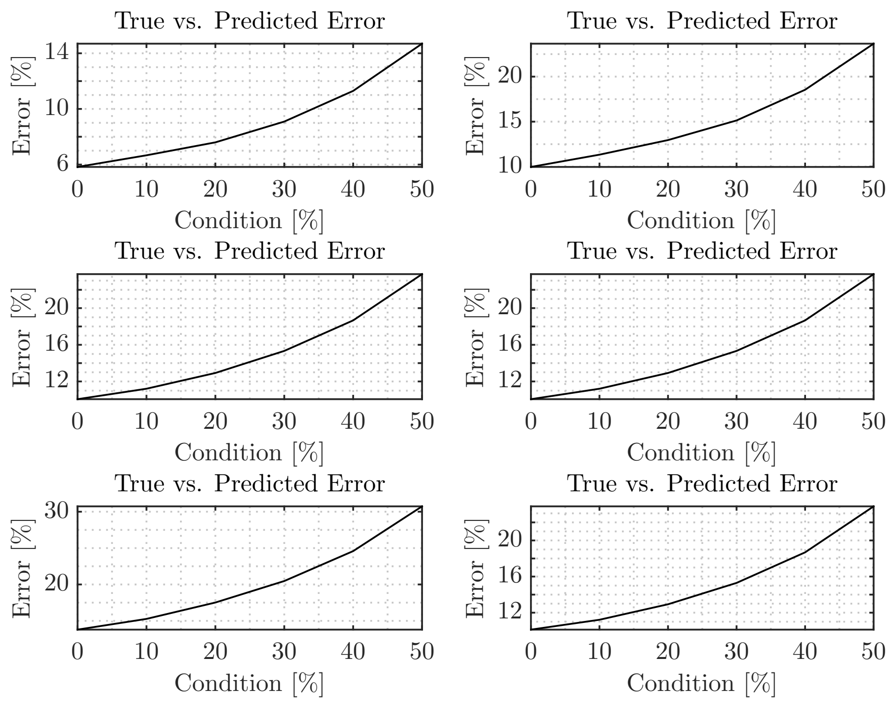

Figure 4.6: Numerical Experiment Part 2 Error

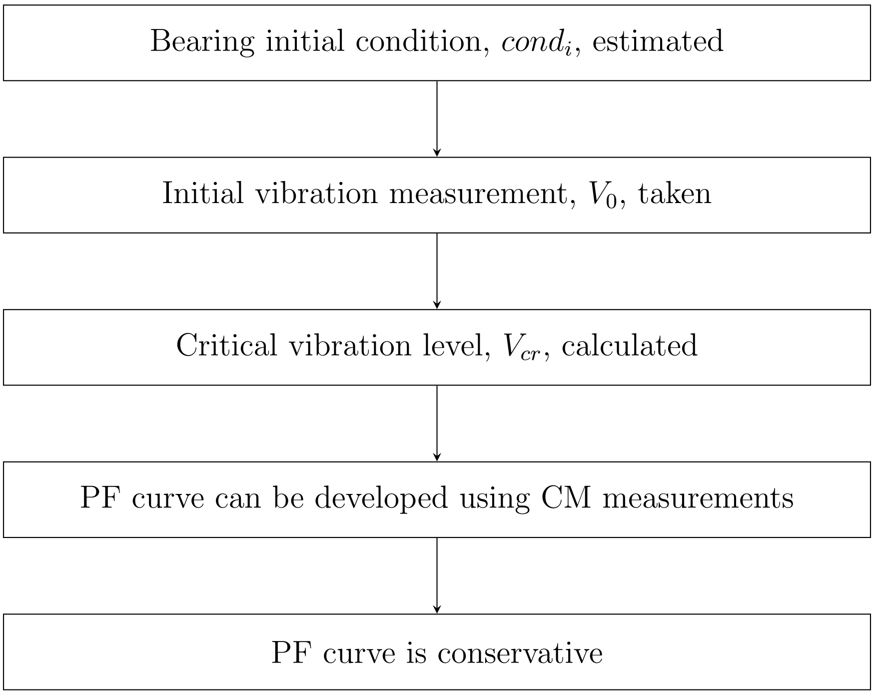

Figure 4.7: Bearing Life Degradation Prediction Sequence

4.6 Conclusion

It is shown that the newly developed method can be applied to various components whose degradation follow that of a power law. In this example, bearing life degradation was considered. It is also shown that the developed method can use physical failure model characteristics to develop a PF curve for bearing degradation by implementing CM measurements. This chapter took the results from chapter 3 and proposed a method for the practical implementation thereof. The method entails estimating a value for initial condition and using CM measurements to build a PF curve. The newly developed method allows the implementation of CBM without knowledge of historic CM data, as shown in this chapter.

Table 4.2: Proactive Maintenance Spectrum

	Ideal CBM	**This Study**	**PHM**	**Reliability Theory**
Failure Statistics	Yes	Yes	Yes	Yes
Failure Mechanism	Yes	Yes	No	No
Condition Monitoring Possible	Yes	Yes	Partially	N.A
Condition Monitoring History	Yes	No	Yes	No
Mainte-nance Approach	Predictive Maintenance	Predictive Maintenance	Predictive Maintenance	Preventative Maintenance
Method	Physical Failure Model	**Failure Data + Partial Knowledge of Failure Mechanism**	PHM	Time/Use-Based

Chapter 5

Economic Benefit of the Newly Developed Method: A Simulated Case Study

5.1 Introduction

The case study discussed in this chapter has two goals: firstly, it shows how the newly developed method allows CBM to be implemented without knowledge of historic CM data. Secondly, it shows the benefit of a proactive maintenance approach, implemented with the use of CBM, compared to a preventative approach and a reactive approach. This is shown with use of a simulation that implements components, each with various initial conditions, in a system and allowing the components to degrade over time according to Paris' power law. The three maintenance approaches mentioned are then applied to the system and at the end of a simulation period of ten years are the outcomes extracted in the form of maintenance events, maintenance time and maintenance cost for each maintenance approach.

5.2 System Specification

The tested system consists of four component types, of which ten of each component is implemented. One component failure does not influence another and can be replaced on failure without altering the production of the other components. The components are specified as follows and shown in figure 5.1 where equation 2.5 is used to calculate the component lifetimes, N_f using $C = 0.02$ and $m = -1.1$.

Table 5.1: Case Study Component Initial Condition Specification

Component	a_i **Mean**	a_i **Standard Deviation**
1	0.1	0.07
2	0.3	0.03
3	0.05	0.008
4	0.23	0.15

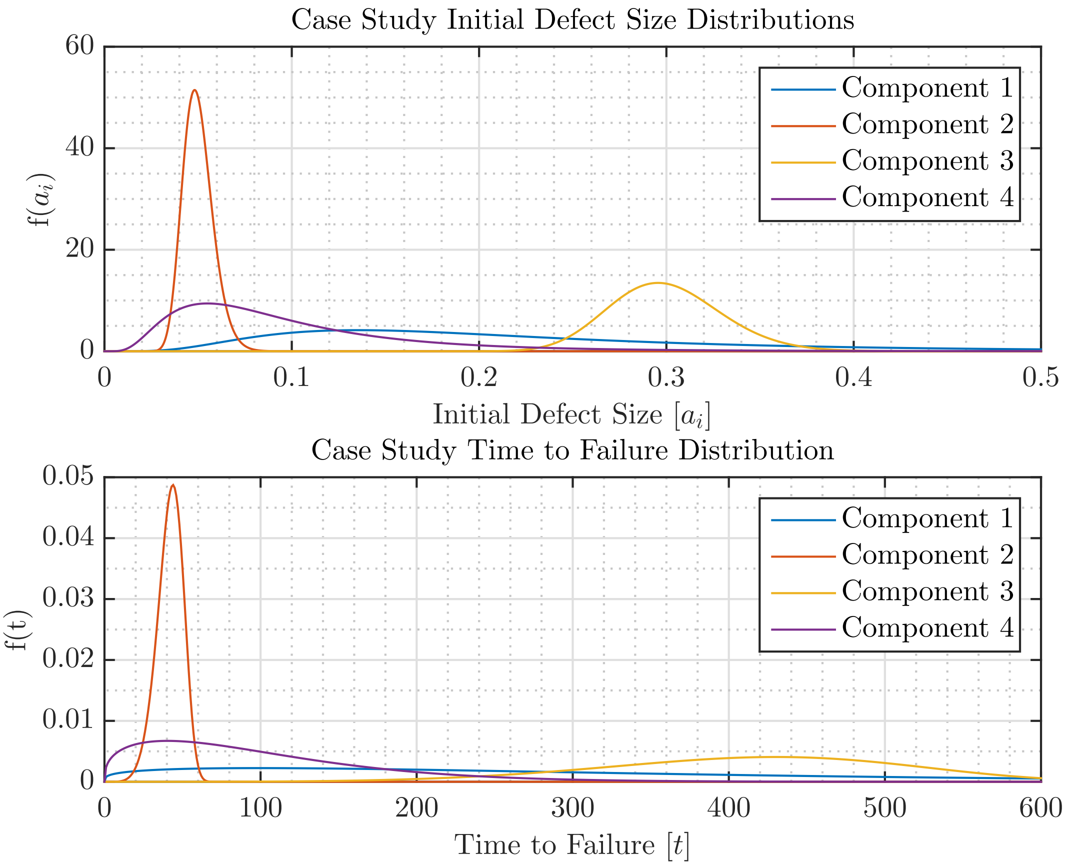

Figure 5.1: Case Study Component Specification

In a group of components, all that change are the initial conditions and therefore the times to failure The component lifetime densities, which are shown in figure 5.1 are used to estimate Weibull parameters, which are used to determine the respective reliability functions and optimal preventative replacement time-based on cost and time of preventative and reactive replacements. 5.1

The cost and time for preventative and reactive replacements (C_p, C_f, T_p and T_f respectively) are shown below. The assumption is made that a reactive replacement will cost between 5 and 10 times more, while taking 3 to 6 times longer, than a preventative replacement. A Matlab function has been built to select a random multiplier within these ranges.

Table 5.2: Life Cycle Optimisation

Component	**Cost**		**Time**	
	C_p	C_f	T_p	T_f
1	20	$5(C_{p_1}) < C_{f_1} < 10(C_{p_1})$	3	$3(T_{p_1}) < T_{f_1} < 6(T_{p_1})$
2	30	$5(C_{p_2}) < C_{f_2} < 10(C_{p_2})$	2	$3(T_{p_2}) < T_{f_2} < 6(T_{p_2})$
3	10	$5(C_{p_3}) < C_{f_3} < 10(C_{p_3})$	4	$3(T_{p_3}) < T_{f_3} < 6(T_{p_3})$
4	15	$5(C_{p_4}) < C_{f_4} < 10(C_{p_4})$	1.5	$3(T_{p_4}) < T_{f_4} < 6(T_{p_4})$

5.3 Results

The cost and time of preventative and reactive replacements are shown in table 5.3 for one component replacement. Time and cost of replacements are normalised and not expressed in a certain monetary unit. CBM implemented by using the newly developed method in this study is compared to two maintenance tactics: run to failure, where all replacements are reactive, and time-based, where replacements are based on an optimal replacement policy driven by the algorithm depicted in section 1.2.1.3. The fitted Weibull parameters (shape parameter, β, and scale parameter or characteristic life, η) and optimal preventative replacement times for each component are shown in table 5.4.

Table 5.3: Component Replacement Cost and Time

Component	**Cost**		**Time**	
	C_p	C_f	T_p	T_f
1	20	131.3	3	11
2	30	155.3	2	8
3	10	75	4	21.5
4	15	99.9	1.5	6.7

Table 5.4: Optimal Preventative Replacement Times

Component	**Shape Parameter**	**Characteristic Life**	**Optimal Replacement Time**
1	1.36	319.3	163
2	6.75	46	30
3	6	431.4	251
4	1.19	104.2	92

Figure 5.2 and 5.3 show the respective components' survival and hazard rate functions.

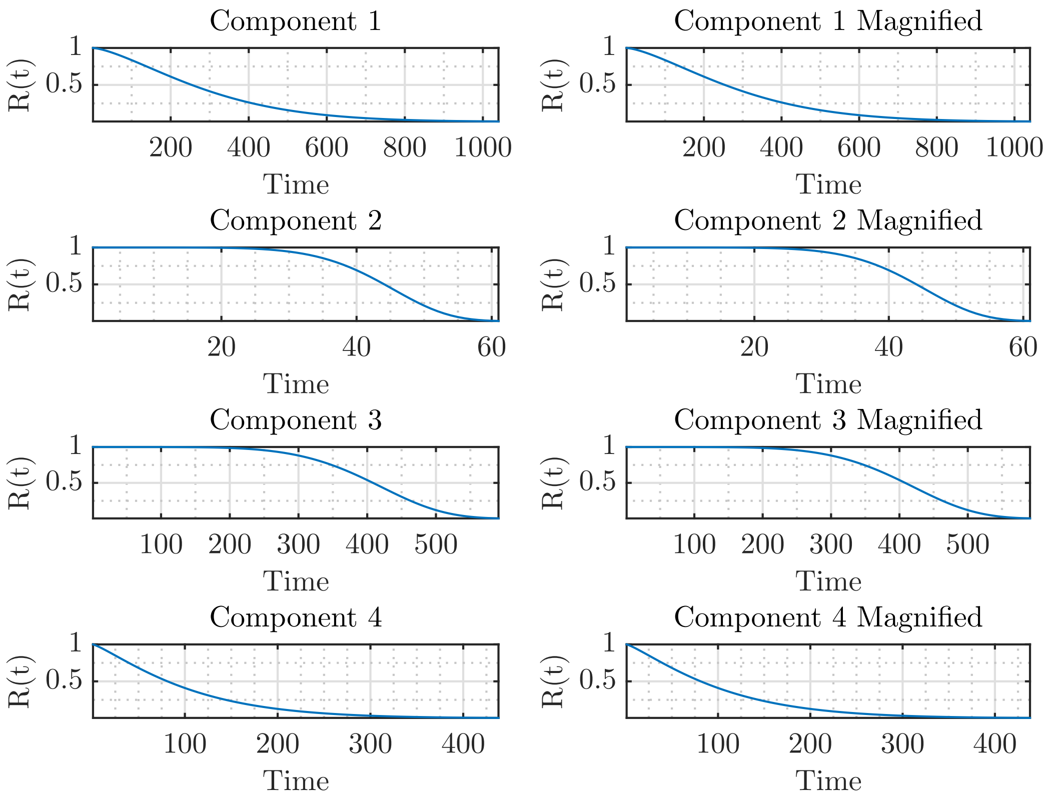

Figure 5.2: Survival Functions

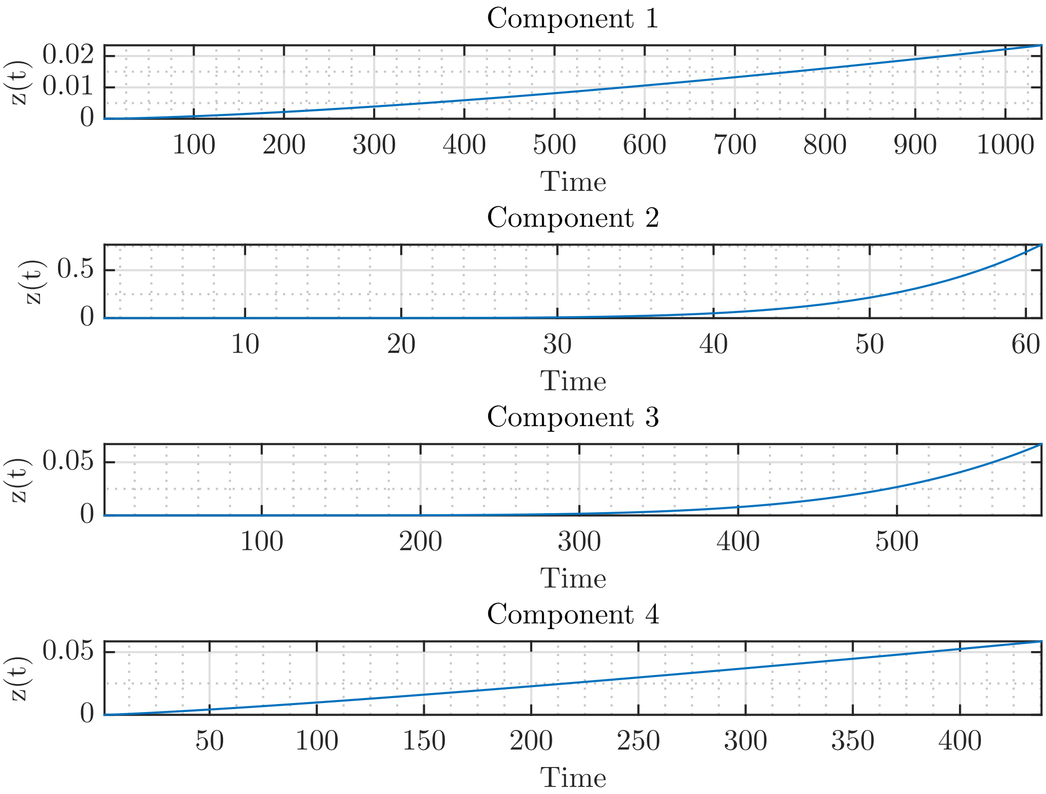

Figure 5.3: Hazard Rate Functions

It can be seen that the probability of failure (survival) is 63.2% (36.8%) on or before the characteristic life η in all components' cases, which is an attribute of the survival function [Coetzee, 1997]. One would therefore expect 63.2% of all components to fail before or on the characteristic life (36.8% will survive up to this life). It can be seen that components 1 and 4 have close to linearly increasing hazard rates while components 2 and 3 have concave increasing hazard rates. Figure 5.4 and 5.5 show the results of the three applied maintenance approaches that is applied to a system that runs for ten years. In figure 5.4, the green bars resemble components that have been replaced before failure and the red bars resemble components that have been replaced after failure. The blue bars resemble production that is lost with each approach. These results are summarised and shown in figure 5.5.

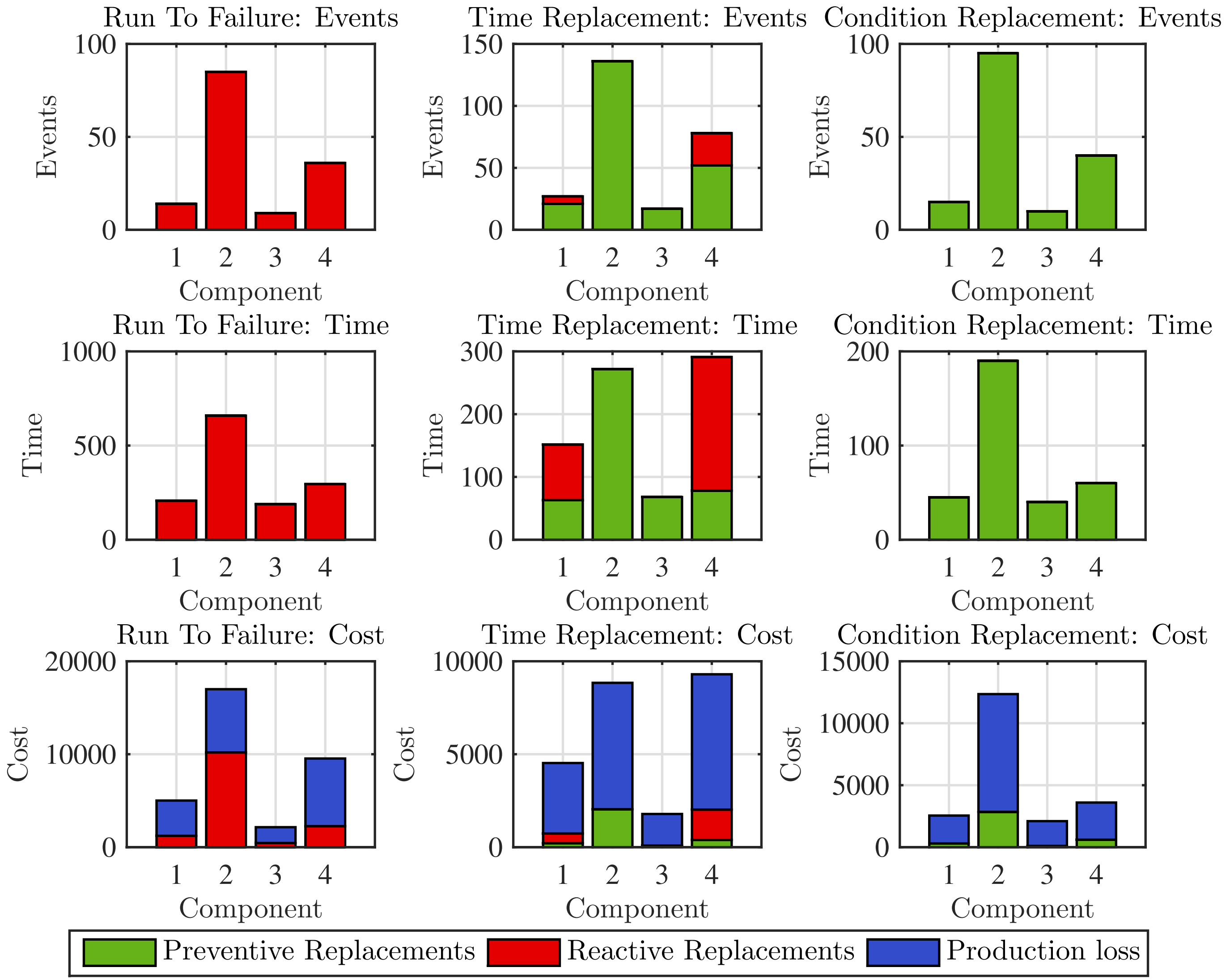

Figure 5.4: Case Study Results

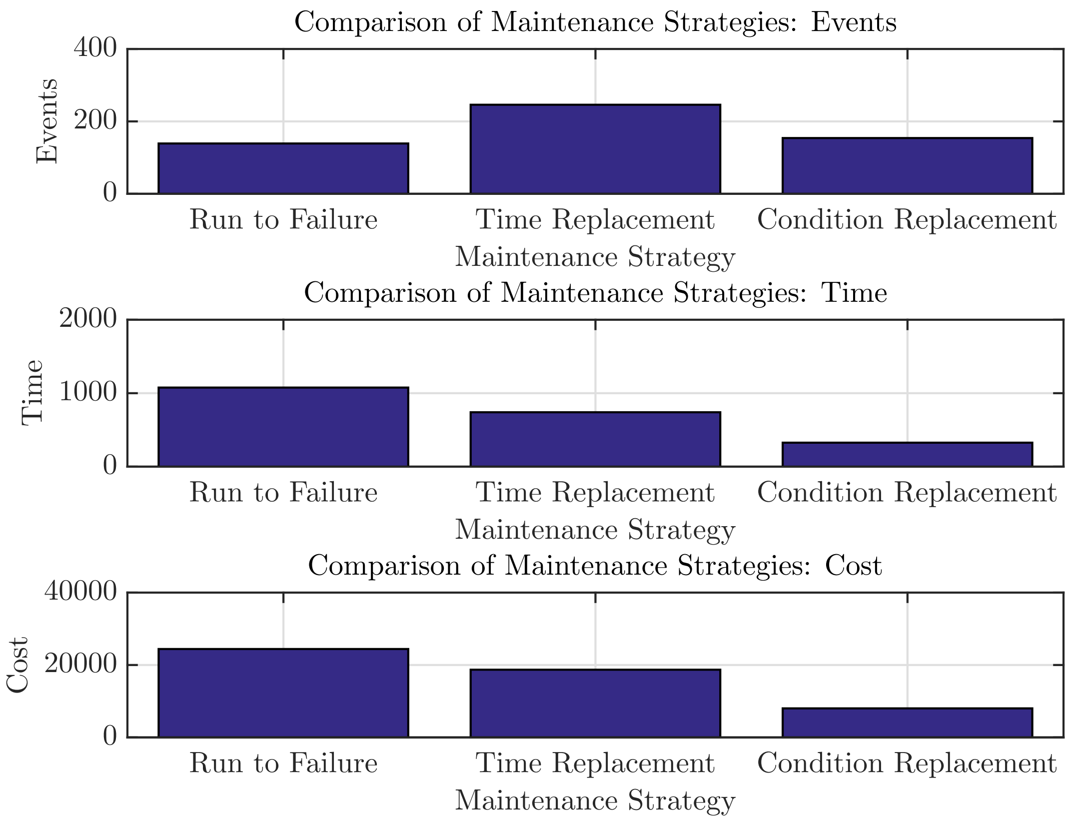

Figure 5.5: Case Study Results Summary

The three scenarios are compared in figure 5.4 within the three columns with regards to events, time and cost. These results are summarised in figure 5.5 which compares overall performance with regards to events, time and cost. The first scenario depicts a run to failure tactic, where all replacements are reactive. The second scenario's replacements are based on the life cycle cost optimisation and the third scenario is an implementation of CBM with the new method developed in this study.

It can be seen that the reactive replacements in scenario one result in high downtime and cost, while having more events than the other scenarios. This is due to components having a longer effective life, which is the time it has been installed and contributed to overall system production. The component failures do however yield less desirable behaviour of the system, as replacement time and cost increases drastically compared to preventative replacements. The second scenario, where a time-based maintenance tactic has been applied, shows more preventative replacements relative to reactive replacements. This is due to some components having initial conditions that lies beyond a normal standard deviation of the initial condition density. The few reactive replacements make a drastic difference in downtime and cost. The last scenario shows that all components have been replaced pro-actively, which causes a drastic reduction in downtime and cost relative to the other scenarios. It is evident that the events in scenario two and three are not very different, but scenario three, encompassing only preventative replacements, causes the downtime and cost to be much lower than in the case of scenario two.

Table 5.5: Simulated Case Study Results

Maintenance Tactic	**Events**	**Time**	**Cost**
Run to Failure	146	1582.6	66395
Time-Based	236	809.7	51480
Condition-Replacement	166	355	21740

Table 5.6: Case Study Maintenance Tactic Relative Improvement

		Relative Improvement (%)
Run to Failure	Events	113.70
	Time	22.43
	Cost	32.74
Time-Based	Events	70.34
	Time	43.84
	Cost	42.23

5.4 Conclusion

The goal of the simulated case study that was conducted is to showcase the benefit of CBM over run to failure and time-based maintenance tactics, and to implement the CBM tactic using the newly developed method in this study. Implementation of the run to failure maintenance tactic consists of components running until failure, which means that all replacements are reactive. Time-based replacements are based on a life cycle optimisation algorithm that selects the optimal time for replacement based on downtime and cost due to preventative and reactive replacements. The method developed in this study estimates condition of components based on an estimate of initial condition and condition monitoring. In this case it is obviously desirable to take as many CM measurements as possible, but an increase in CM measurements results in an increase in cost as well, which is included when calculating the cost of replacements.

The results show a dramatic decrease in downtime and cost by applying CBM, compared to a run to failure or time-based maintenance tactic. Although more events occur compared to a run to failure tactic, the downtime and cost improvements are large. This shows that efficient maintenance planning has a great impact on the system, although it might not be obvious when considering the number of components replaced. Replacements based on component condition certainly yields the best results for the organisation, although it might have high costs related to it.

The model discussed in this chapter simulates a period of ten years and replacements are made according to the applied maintenance tactic. Compared to a reactive approach, the predictive approach resulted in 78% less downtime and 67% less expenditure. Compared to a preventative approach, the predictive approach resulted in 56% less downtime and 57% less expenditure. These promising results would assist in making a business case for the implementation of CBM in practical applications.

Chapter 6

Time-Based Maintenance Approach Simulation: Case Study

6.1 Introduction

In chapter 2 a maintenance approach simulation, which initially simulated a non-real system with dummy data, was discussed and in section 2.3 a problem was encountered that acted as a major obstruction when attempting to model a real-life system using obtained failure data. The problem entailed not being able to describe component degradation with a Paris power law, shown in equation 2.5. This is due to the lack of CM history, and therefore the lack of knowledge of initial condition of a component. Access to failure data is, however, not restricted. It led to the discovery that two variables in the Paris power law, equation 2.5, were unknown and impossible to solve. Chapter 3 aimed to solve this problem by estimating one of the unknown variables and using equation 2.5 to solve the other. In this case, the initial condition, a_i, was estimated and the operating condition parameter, C, was solved. Chapter 3 acted as a sensitivity study in order to establish whether it would be viable to follow this approach by calculating an error between a component's "real" and "predicted" PF curves. The numerical experiment has shown promising results and through development of the new method in the preceding chapters it is seen that this method might become useful in the implementation of a CBM tactic.

In this chapter the system that is simulated is discussed and real failure data is applied to the simulation. The failure data is not of a dense nature and Bayesian statistics is used to attempt to solve this problem. Based on the findings from chapter 3, PF curves are predicted for each component and replacements are simulated accordingly to the applied maintenance tactic.

6.2 System Specification

Failure data from a ball mill at an Anglo Platinum mine in Mogalakwena, Limpopo (RSA), is obtained and used in the time-based maintenance approach simulation. The goal is to simulate the effect of maintenance tactics on the system. A simplified version of the entire milling system is represented in figure 6.1 and it is assumed that all components' degradation follow that of a power law, derived in section 2.2.2. Five components are used to represent a basic depiction of the system.

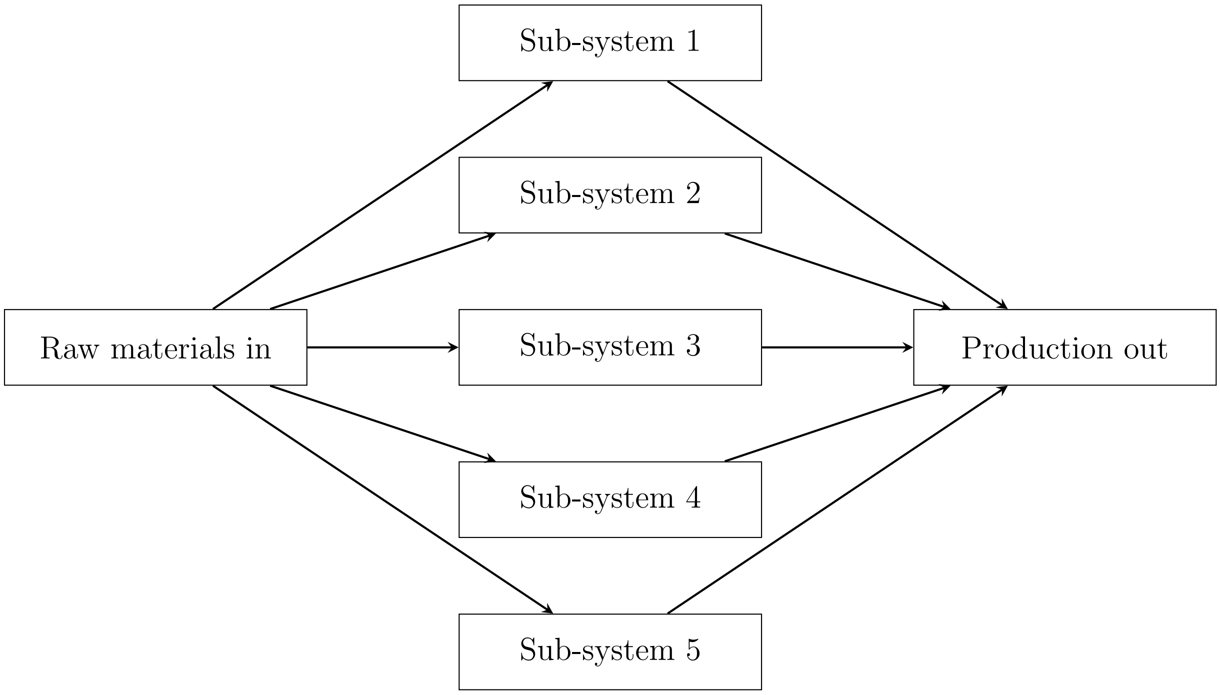

Figure 6.1: Ball Mill Basic Representation

Due to the statistical failure data not being of a dense nature, it resulted in the standard deviation for each component lifetime distribution being too large to use in the simulation. Therefore, Bayes' theorem is applied to it to develop component lifetime distributions with acceptable standard deviations. The data would be used to update a prior belief of the characteristics of the respective components of the system. Bayes' theorem is useful in a case where data is continuously accessible, resulting in the prior belief of the failure characteristics being updated constantly. The five sub-systems shown in figure 6.1 have component lifetime distributions that are developed using Bayes' theorem, shown in figure 6.2 (an example calculation using Bayes' theorem is shown in appendix C. Each sub-system consists of 40 components that possesses the same characteristics with regards to initial condition, a_i, operating condition, C, material property, m, and lifetime distribution, a normally distributed N_f.

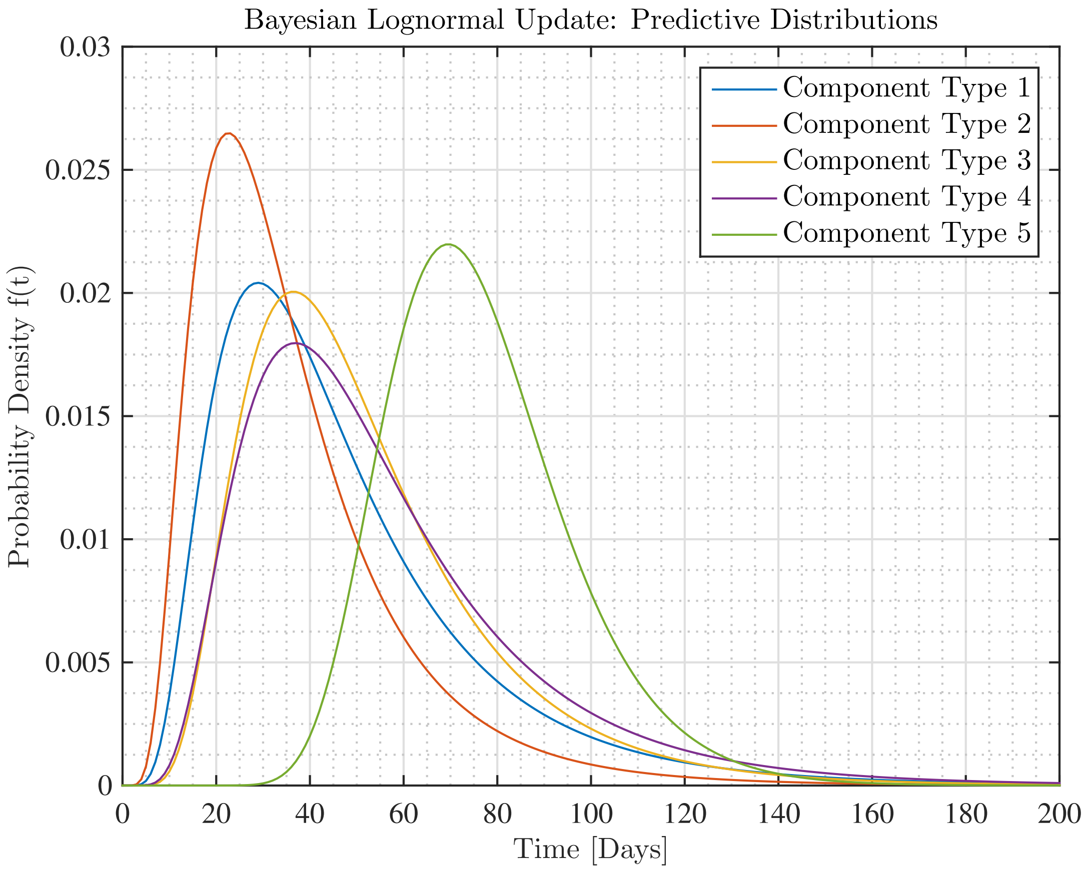

Figure 6.2: Bayesian Lognormal Update: Predictive Distributions

Table 6.1: Time-Based Case Study Component Specification

Component	a_i mean	a_i standard deviation	C	m
1	0.1	0.029	0.27	-1.1
2	0.1	0.029	0.35	-1.1
3	0.1	0.025	0.23	-1.1
4	0.1	0.027	0.25	-1.1
5	0.1	0.04	0.19	-1.1

The failure distributions as they are used in the time-based maintenance approach simulation are shown in figure 6.3.

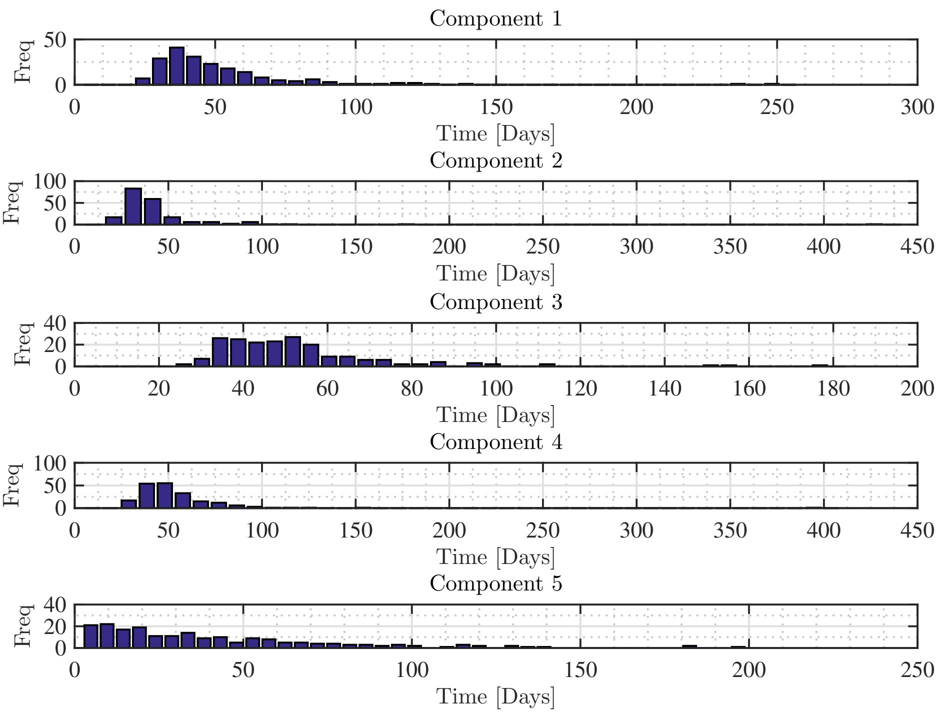

Figure 6.3: Component Details

The component lifetime distributions have the same shape as that of its respective initial condition distribution, due to the operating condition parameter, C, remaining constant for all component initial conditions generated from its normal distribution. Figure 6.4 and 6.5 show the maintenance consequences of all maintenance tactics in terms of downtime and maintenance cost respectively. The component replacement properties are shown in table 6.2.

Table 6.2: Component Replacement Properties

Component	1		2		3		4		5	
Tactic	Hours	Cost	Hours	Cost	Hours	Cost	Hours	Cost	Hours	Cost
Run to Failure	20	800	5	100	11	500	13	5000	2	2000
Corrective	12	800	3	100	8	500	10	5000	4	2000
Time-Based	12	800	3	100	8	500	10	5000	4	2000
Servicing	12	800	3	100	8	500	10	5000	4	2000
CBM	12	800	3	100	8	500	10	5000	4	2000
Design-Out	12	800	3	100	8	500	10	5000	4	2000

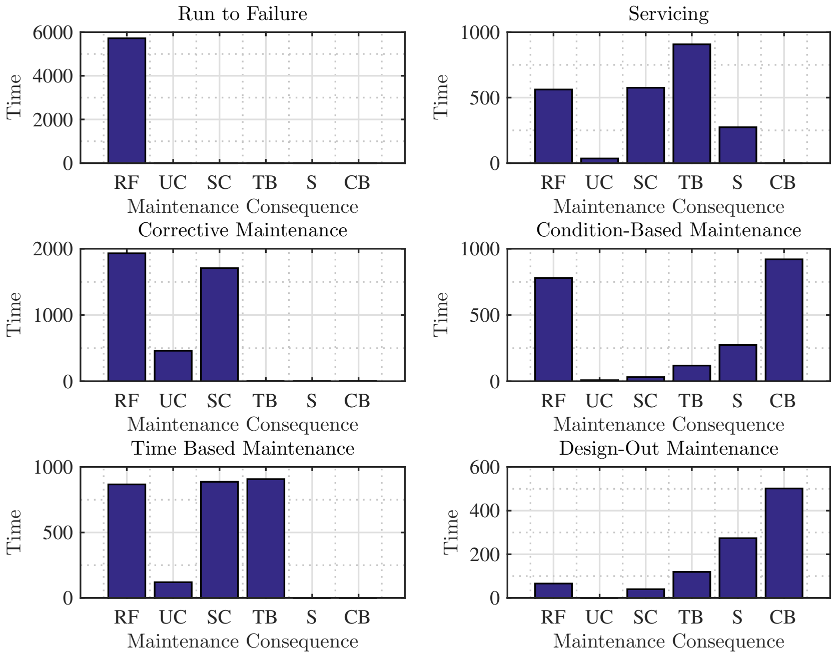

Figure 6.4: Maintenance Consequences of Respective Maintenance Tactics

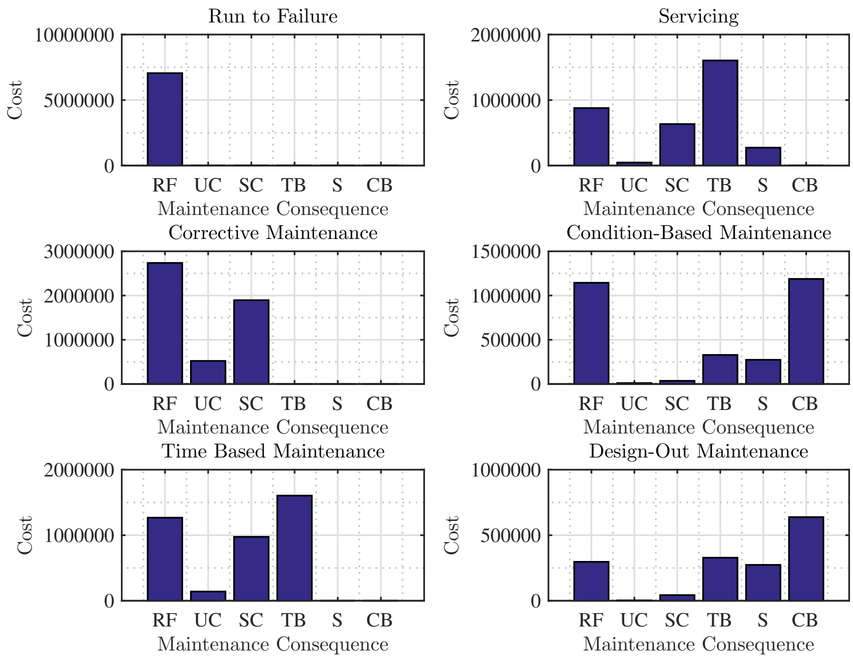

Figure 6.5: Maintenance Consequences of Respective Maintenance Tactics: Cost

6.3 Results

The theoretical daily production, in tons, forms a Weibull distribution with $\eta = 1000$ and $\beta = 20$. The theoretical production is naturally affected by the replacements based on the applied maintenance tactics. The results from the case study include a chart showing daily production with a fitted trend-line, a daily production histogram, and a summary of the maintenance consequences in terms of downtime and maintenance cost. The model simulates a period from the beginning of 2013 to the end of 2015 and the applied maintenance tactics are as follows.

- 2013: Corrective Maintenance

- 2014: Time/Use-Based Maintenance

- 2015: Condition-Based Maintenance

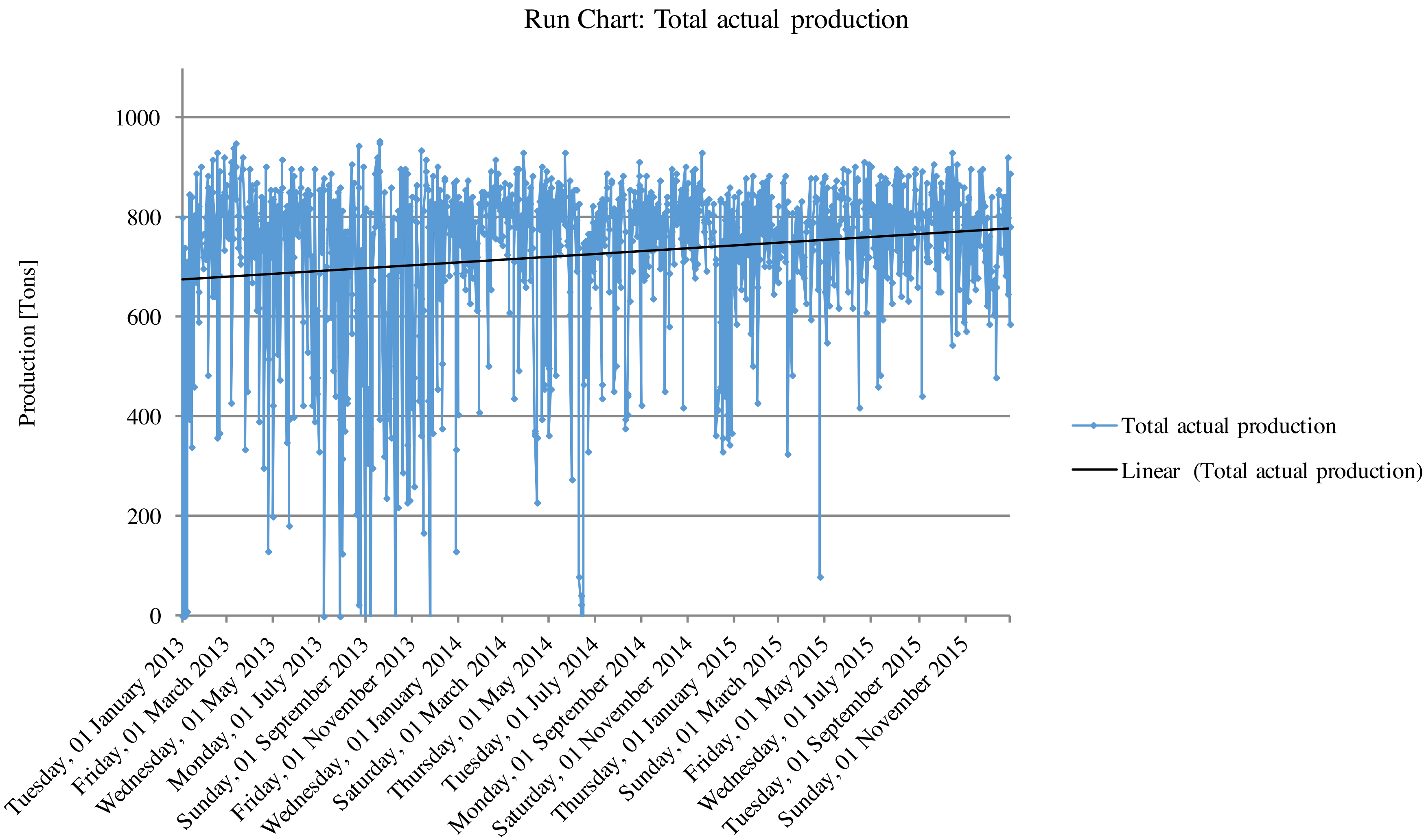

Figure 6.6: Run Chart: Total Daily Production

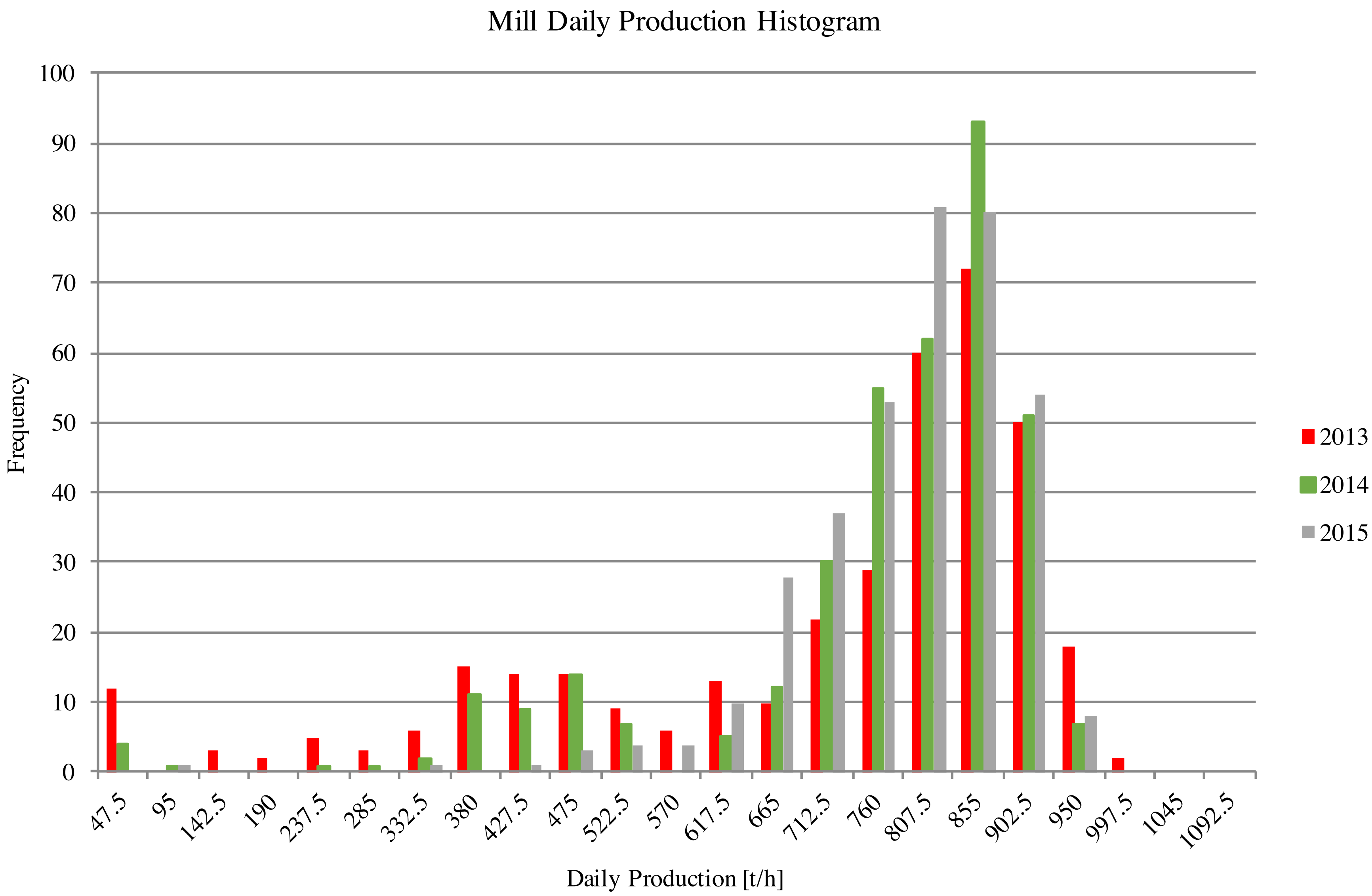

Figure 6.7: Daily Production Histogram

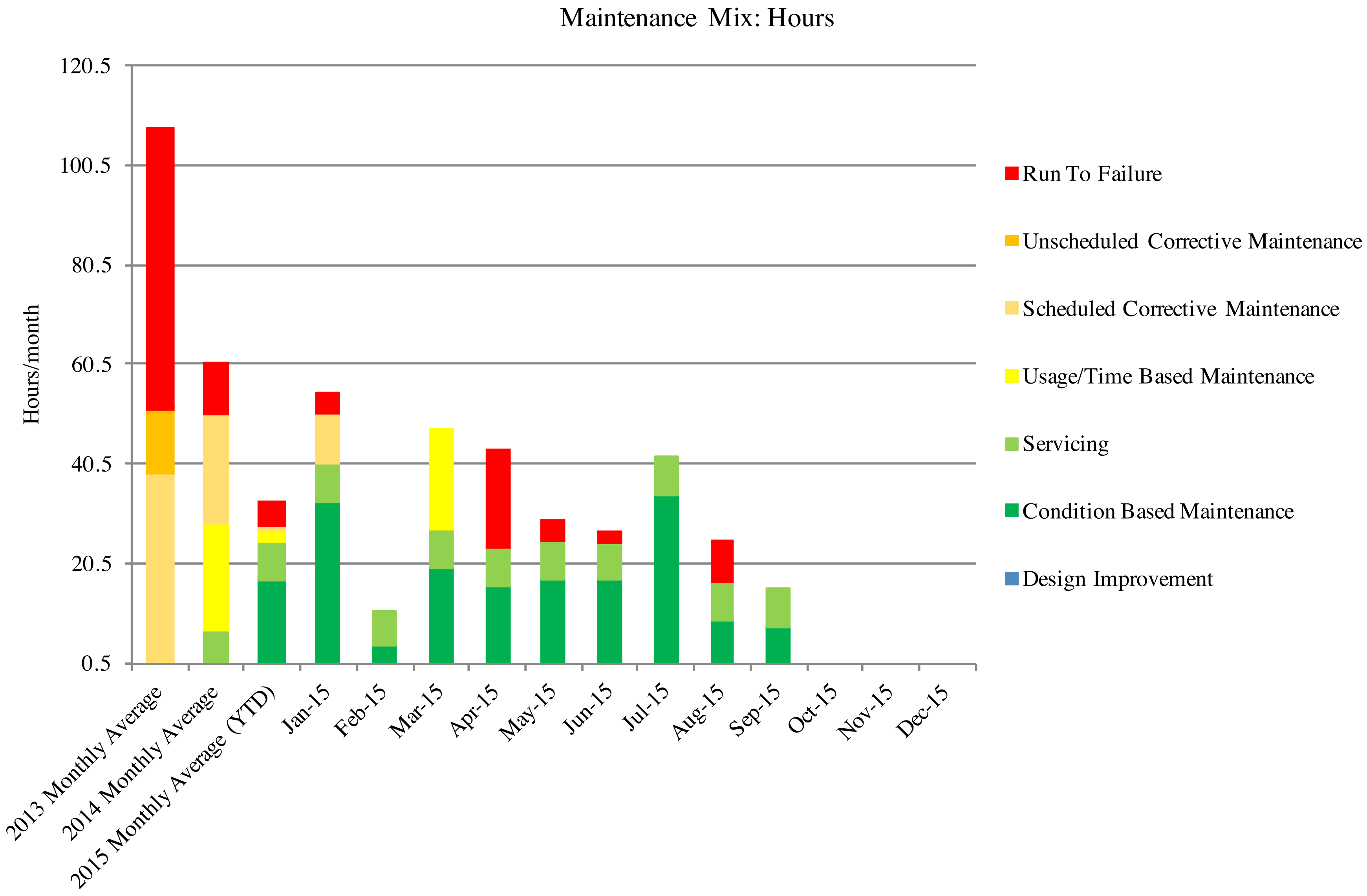

Figure 6.8: Maintenance Mix: Hours

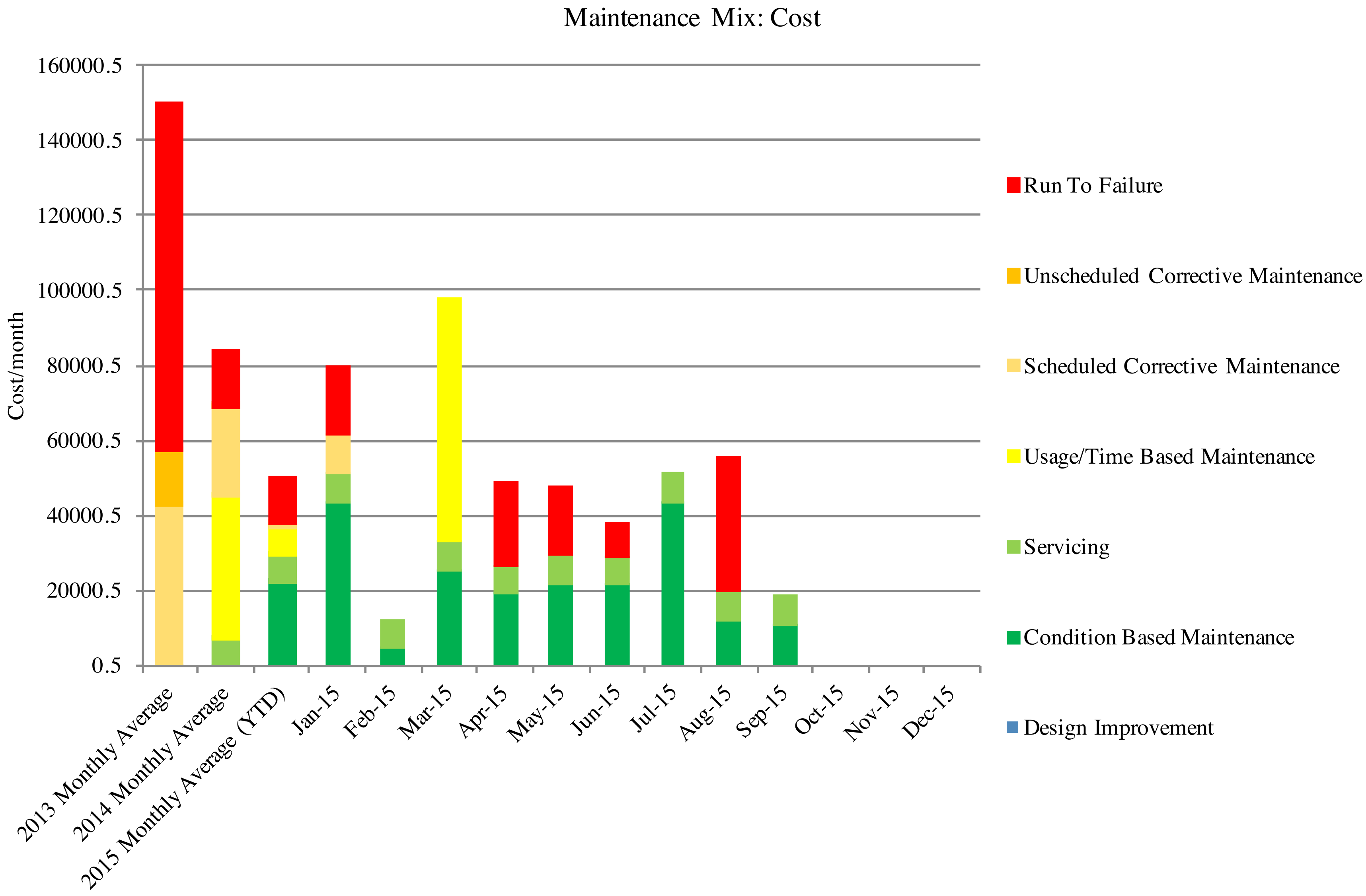

Figure 6.9: Maintenance Mix: Cost

6.4 Conclusion

In chapter 2 the time-based maintenance approach simulation developed by Wannenburg was discussed and an attempt was made to apply statistical failure data from a mill to the model in order to obtain an optimum maintenance mix for keeping the production rate at a maximum. It was discovered that this would be impossible, as parameters needed to represent component degradation with a power law could not be obtained by only using statistical failure data. The failure data was, however, used to develop relatively narrow failure distributions using Bayes' theorem.

The findings from chapter 3 and 4 have shown that it is possible to develop PF curves to use in a CBM application, without knowledge of historic CM data, by estimating parameters in Paris' power law. The model simulates a period from the beginning of 2013 to the end of 2015. For the first year, a corrective maintenance tactic is applied, for the second year a time/use-based tactic is applied and in the final year a condition-based tactic is applied. Figure 6.6 shows that the production increases over the three years and figure 6.7 shows that the mean production over the period is close to that of theoretical production, when all is working perfectly, which is 1000 tons/hour.

Chapter 7

Conclusion and Recommendations

7.1 Conclusion

In this study an attempt was made to develop a condition degradation modelling tool that minimizes condition monitoring and estimates component condition based on an initial condition assumption. The physical failure model that was implemented is of a fracture mechanics nature and considers crack growth in components. The problem that was noticed is that the ideal case for CBM normally depends on uninterrupted monitoring of component condition, which is an expensive exercise. By applying reliability theory, optimal component replacement can be determined based on failure statistics and replacements could be planned based on a time-based tactic. This is more cost effective, although not as robust as a maintenance tactic that takes component condition into account. PHM exists, which determines optimal component replacement times based on a developed component age and relies on failure statistics. The main goal of this project was to develop a robust method that allows a CBM implementation without knowledge of CM history. This was achieved an it was found that the newly developed method can potentially be very useful. The following contributions are made by this study:

- The method developed in this study aims to combine a physical failure model and statistical theory to obtain a tool that estimates component condition over time. This is achieved by deriving the PF curves necessary for CBM implementation, which may be employed when only statistical failure data and some knowledge of the failure model is available. The method entails estimating the values of initial condition parameters and calculating the remaining parameters and has proven to be robust with sufficient accuracy to allow effective implementation of CBM. Figure 1.2 shows the identified opportunity for a new method.

- It is shown that the newly developed method can be employed for any failure mechanism where a power law governs the failure rate and where the exponent of the power law is known with reasonable accuracy. Chapter 4 shows that it is possible to apply the newly developed method to bearing life degradation prediction by measuring bearing vibration and using it to develop PF curves, as it is known that bearing vibration and the defect size within a bearing are related.

- Using Bayesian statistics, it is shown that sparse knowledge of failure statistics can be augmented. Bayesian statistics can also be used to continuously update a belief regarding component RUL as a component degrades, which increases the accuracy of a developed PF curve.

- The possible economic benefits of employing the newly developed method over other maintenance tactics is demonstrated through simulation. The newly developed method is compared to a run to failure tactic, which only consists of reactive replacements, and a time-based tactic, which bases replacements on an optimal replacement time. The initial conditions are known and the component degradation is based on Paris' law. The system is run for ten years and replacements are made according to the respective maintenance tactics. The results show a dramatic decrease in system downtime and maintenance cost, as all replacements are made preventatively. Relative to a run to failure tactic, CBM yields a 77.6% improvement in downtime and a 67.3% improvement in maintenance cost. Relative to a time-based tactic, CBM yields a 56.2% improvement in downtime and a 57.8% improvement in maintenance cost.

- It is shown how the knowledge of PF curves derived using the new method, can be used to optimise the maintenance approach on a complex system by time-based simulation. A complex system is presented using the time-based maintenance approach simulation discussed in chapter 2.

The second column in table 7.1 is now solved and it is shown that it may be possible to implement a CBM tactic without the need of CM history, and with only access to failure data.

Table 7.1: Proactive Maintenance Spectrum

	Ideal CBM	**This Study**	**PHM**	**Reliability Theory**
Failure Statistics	Yes	Yes	Yes	Yes
Failure Mechanism	Yes	Yes	No	No
Condition Monitoring Possible	Yes	Yes	Partially	N.A
Condition Monitoring History	Yes	No	Yes	No
Maintenance Approach	Predictive Maintenance	Predictive Maintenance	Predictive Maintenance	Preventative Maintenance
Method	Physical Failure Model	**Failure Data + Partial Knowledge of Failure Mechanism**	PHM	Time/Use-Based

7.2 Recommendations for Further Work

The following is recommended for a continuation of this project:

- Real, workable, and relevant failure data must be obtained in order to establish the lives of components and what lifetimes to model.
- A comparison between application of CBM using the newly developed method and PHM must also be drawn.
- A maintenance optimiser must be built for the maintenance approach simulation, which would replace a trial-by-error approach in order to find the optimal maintenance mix.
- The process for improving the PF curve model parameters as more CM data becomes available, should be developed.
- It may be of value to to a physical experiment on bearings to validate the method that is further developed in chapter 4.

Bibliography

Arthur, N. (2005). Optimization of vibration analysis inspection intervals for an offshore oil and gas water injection pumping system TT -. *Proceedings of the I MECH E Part E Journal of Process Mechanical Engineering*, 219(3):251–259.

Bayes, T., Laplace, P. S., and Jeffreys, H. (2015). Bayes ' theorem. pages 1–17.

Blann, D. (2013). Maximizing the P-F Interval Through Condition-Based Maintenance.

Budynas, R. and Nisbett, J. (2011). *Shigley's Mechanical Engineering Design*. McGraw Hill Higher Education, New York City, NY, 9 edition.

Carnero, M. (2009). Selection of condition monitoring techniques using discrete probability distributions: A case study. *Proceedings of the Institution of Mechanical Engineers, Part O: Journal of Risk and Reliability*, 223(1):99–117.

Coetzee, J. L. (1997). *Maintenance*. Maintenance Publishers, Vanderbijlpark.

Coetzee, J. L. (2015). *RCM ProAktiv*. Maintenance Publishers, Vanderbijlpark.

Cox, D. R. (1992). Regression Models and Life-Tables. *Journal of the Royal Statistical Society*, 34(2):527–541.

Drenick, R. (2012). The Failure Law of Complex Equipment. *Journal of the Society for Industrial and Applied Mathematics*, 8(4):680–690.

Fiix (2016). Condition Based Maintenance and Monitoring Software.

Fredriksson, G. and Larsson, H. (2012). An analysis of maintenance strategies and development of a model for strategy formulation-A case study. *Göteborg: Chalmers University of Technology*.

García Márquez, F. P., Tobias, A. M., Pinar Pérez, J. M., and Papaelias, M. (2012). Condition monitoring of wind turbines: Techniques and methods. *Renewable Energy TA -*, 46(3):169–178.

Gelman, A. (2002). Prior distribution. *Encyclopedia of Environmetrics*, 3:1634–1637.

Ghasemi, A., Yacout, S., and Ouali, M. S. (2007). Optimal condition based maintenance with imperfect information and the proportional hazards model. *International Journal of Production Research*, 45(4):989–1012.

Glickman, M. and van Dyk, D. (2007). Basic Bayesian methods. *Methods in molecular biology (Clifton, N.J.)*, 404:319–338.

Hameed, Z., Hong, Y. S., Cho, Y. M., Ahn, S. H., and Song, C. K. (2009). Condition monitoring and fault detection of wind turbines and related algorithms: A review. *Renewable and Sustainable Energy Reviews*, 13(1):1–39.

Jacobs, R. (2008). Introduction to Applied Bayesian Statistics and Estimation for Social Scientists . 2(5):1–3.

Joyce, D. (2009). A short introduction to Bayesian statistics , part I. pages 1–3.

Judd, M. D., McArthur, S. D. J., McDonald, J. R., and Farish, O. (2002). Intelligent condition monitoring and asset management. Partial discharge monitoring for power transformers. *Power Engineering Journal*, 16(6):297–304.

Kobbacy, K. A. H., Fawzi, B. B., Percy, D. F., and Ascher, H. E. (1997). A Full History Proportional Hazards Model. *Quality And Reliability Engineering International*, 13(4):187–198.

Lasky, R. (2012). Electronics Failure Analysis for Pb- and Pb-Free Solder Joints.

Li, Y., Kurfess, T., and Liang, S. (2000). Stochastic Prognostics for Rolling Element Bearings. *Mechanical Systems and Signal Processing*, 14(5):747–762.

Liao, L. and Köttig, F. (2014). Review of hybrid prognostics approaches for remaining useful life prediction of engineered systems, and an application to battery life prediction. *IEEE Transactions on Reliability*, 63(1):191–207.

Makis, V. and Jardine, A. (1991). Optimal replacement in the proportional hazards model. *Department of Industrial Engineering, University of Toronto*, pages 172–183.

Mobley, R. K. (2004). Maintenance 2nd Edition. (2):2–3.

Neale, M. and Woodley, B. (1975). Condition Monitoring Methods and Economics. *Symposium of the Society of Environmental Engineers*.

Nederlof, M. (2010). Bayesian update of a prior normal distribution with new sample information.

Nose Seiko (2016). Bearing Life and Load Rating.

Ondrasovic, M. and Ondrasovicova, O. (2009). Normal Distribution. page 1983.

ReliaSoft (2016). On-Condition Maintenance Using P-F Interval or Failure Detection Threshold (FDT).

Samrout, M., Châtelet, E., Kouta, R., and Chebbo, N. (2009). Optimization of maintenance policy using the proportional hazard model. *Reliability Engineering & System Safety*, 94(1):44–52.

Saravanan, S., Altaf, M., and Udaiappan, M. (2014). Profitable Condition Monitoring. *National Conference on Condition Monitoring (NCCM)*, pages 133–142.

Schreurs, P. (2012). Fracture Mechanics. *Lecture notes: Fracture Mechanics TUe.*

Tchakoua, P., Wamkeue, R., Ouhrouche, M., Slaoui-Hasnaoui, F., Tameghe, T. A., and Ekemb, G. (2014). Wind turbine condition monitoring: State-of-the-art review, new trends, and future challenges. *Energies*, 7(4):2595–2630.

Tian, Z. and Liao, H. (2011). Condition based maintenance optimization for multi-component systems using proportional hazards model. *Reliability Engineering & System Safety*, 96(5):581–589.

Vlok, P., Coetzee, J., Banjevic, D., Jardine, A., and Makis, V. (2002). Optimal component replacement decisions using vibration monitoring and the proportional-hazards model. *Journal of the Operational Research Society*, 53(53):193–202.

Xu, D., Huang, J. E., Zhu, Q., Chen, X., Xu, Y. C., and Wang, S. (2012). Residual Fatigue Life Prediction of Ball Bearings Based on Paris Law and RMS. *Chinese Journal of Mechanical Engineering*, 25(2):320–327.

Zhou, R. R., Serban, N., and Gebraeel, N. (2011). Degradation modeling applied to residual lifetime prediction using functional data analysis. *The Annals of Applied Statistics*, 5(2B):1586–1610.

Appendix A

Numerical Experiment Preparation

A.1 Experimental Preparation

A.1.1 Mathematical Preparation

The mathematical preparation is that shown in section 2.2.2 and it is known that it would be impossible to solve all three unknown variables analytically. The numerical experiment is the link to solving these variables. In order to execute a successful experiment, it is required to know which fixed parameters exist. N_f and m are both known due to the fact that N_f, the component lifetime, can be estimated using a combination of physical RUL techniques and historic data, and m is a known material property. C and a_i are unknown because the normalised operating condition parameter, C, can not be quantified using physical principles and the initial condition parameter, a_i, is not known when a component is placed in service. Table A.1 therefore summarises the current knowledge of the problem encountered within equations 2.5 and 2.6.

Table A.1: Paris Equation Parameters

N_f	Known from failure data
m	Known - material property
a_i	Unknown - initial condition
C	Unknown - operating condition

A.1.2 Methods to Solve for Unknown Parameters

The next step is to determine which of the unknown parameters to fix. Within the numerical experiment, one of the parameters would be randomly selected out of a given distribution and the other unknown parameter would be either given or calculated using the Paris equation. It is known that when the failure data forms a distribution on the time axis, the initial conditions for each of the failure data entries would form a distribution as well. This can be proved by using various components of a single type that all operate under the same conditions, e.g. they have the same C parameter. If all of these components have different initial conditions, this would result in different failure times, as C and m remain fixed. In order to determine which parameters to fix and which to calculate, a tool has been developed that calculates an error between the two methods.

This tool entails calculating the Coefficient of Variance (CV) = ratio of standard deviation to mean between the initial condition and failure distributions for each method. The following stepwise approach is followed:

Table A.2: Numerical Experiment Preparation Methods

	Method 1: a_i Distributed, C Fixed	**Method 2: C Distributed, a_i Fixed**
1	Generate 100 a_i samples from a distributed initial condition and calculate respective N_f values for a fixed C value	Generate 100 C samples from a distribution of C and calculate respective N_f values for a fixed initial condition
2	Calculate the ratio of mean and standard deviation for both a_i and N_f distributions and compare the ratios	Calculate the ration of mean and standard deviation for both C and N_f distributions and compare the ratios
3	Repeat step 1-2 with a_i standard deviation increasing to develop narrow normal, wide normal and exponential distributions	Repeat step 1-2 with C increasing to develop narrow normal, wide normal and exponential distributions
4	Repeat step 1-3 with various C values	Repeat step 1-3 with various initial conditions

For this experimental investigation, the narrow normal, wide normal and exponential distributions are classified as follows:

Table A.3: Normal Distribution Range Rationale

Narrow Normal	$0.01(\mu) \leq \sigma < 0.1(\mu)$
Wide Normal	$0.1(\mu) \leq \sigma < \mu$
Exponential	$\mu \leq \sigma$

A.1.2.1 Method 1

Here follows a brief explanation of the implementation of the reasoning, whereafter the actual results will follow. Figure A.1 represents step 1-3 in table A.2 and shows the ratio comparison for the whole spectrum of distributions that are used for a single initial condition mean: the narrow normal, wide normal and exponential distributions.

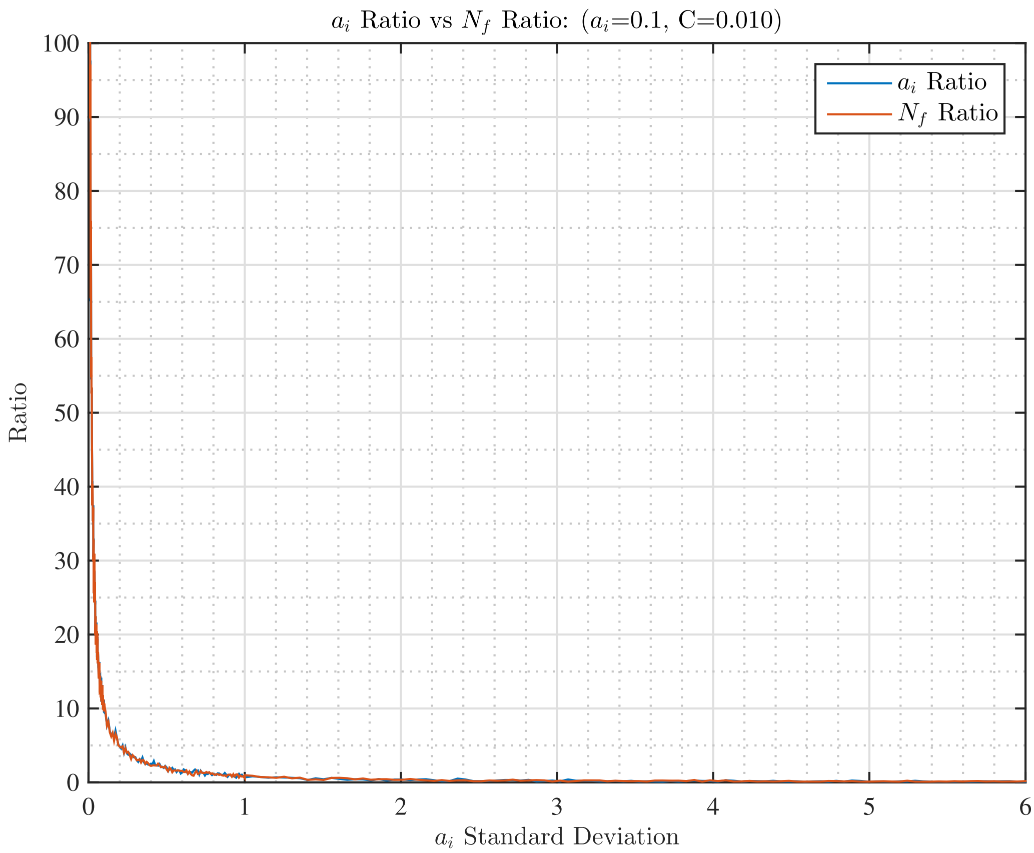

Figure A.1: Ratio Comparison Plot

A problem is encountered here, in that the two plotted functions cannot be differentiated from one another in figure A.1, therefore the narrow normal, wide normal and exponential distributions are separated and plotted individually with the rationale stated in table A.3. Figure A.2 shows this.

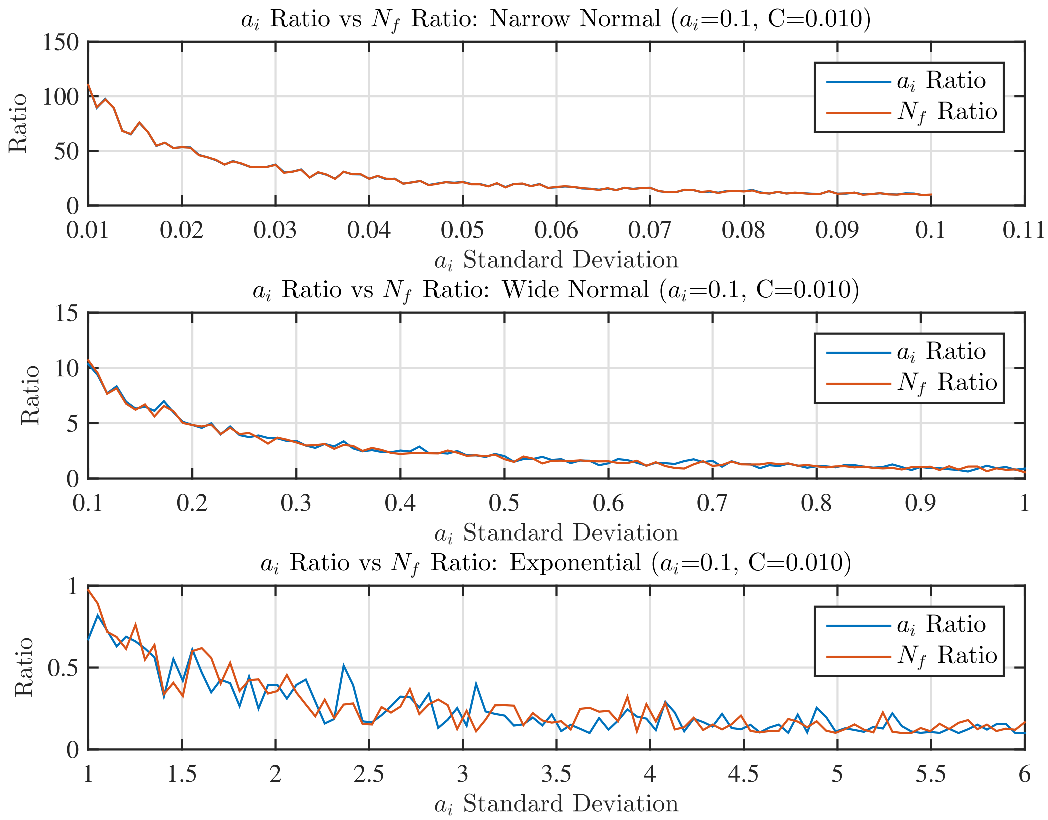

Figure A.2: Ratio Comparison Plot Split

The two ratio functions can now easily be graphically differentiated from one another. Step 4 in table A.2 takes this further by changing the fixed parameter, turning the ratio comparison plot into a ratio comparison surface. This is very helpful due to both parameters increasing simultaneously and graphical estimations being easier to make. Each plane resembles that which is plotted in figure A.2. This surface is shown below.

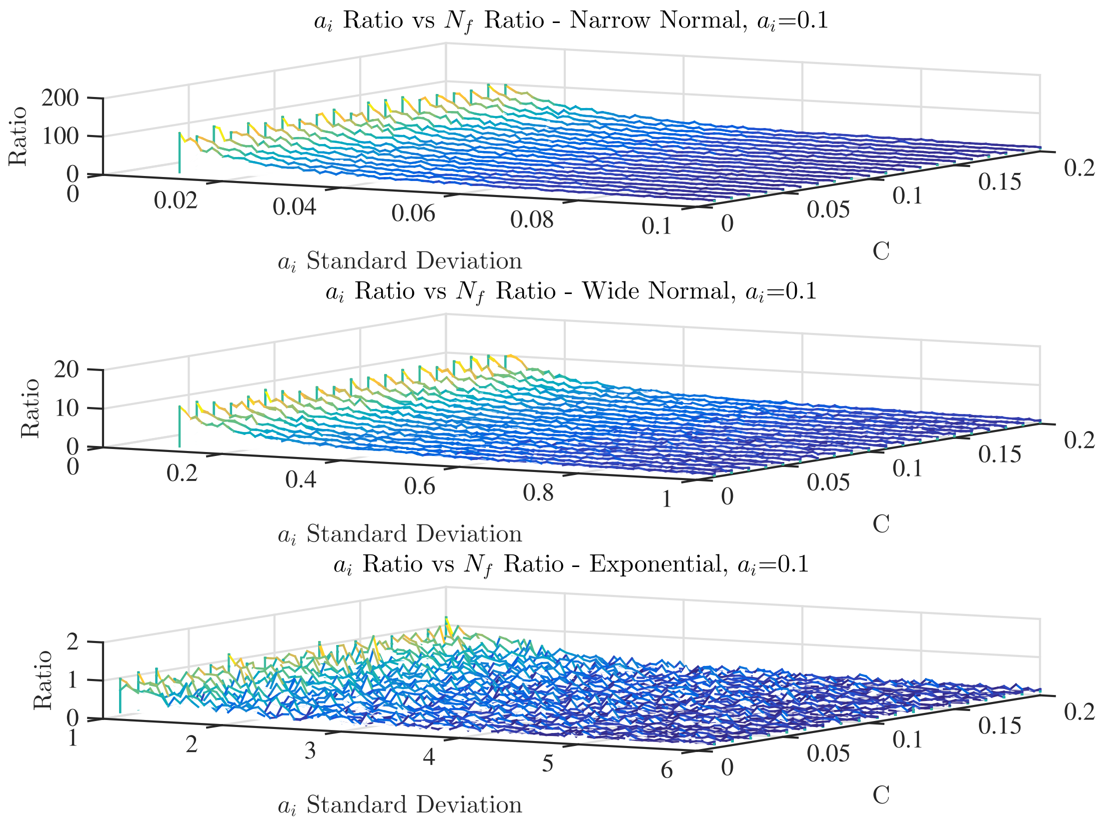

Figure A.3: Ratio Comparison Surface

This entire process is repeated for 3 different mean values of the distributed parameter. In this case, the three mean values would be $a_{i_{mean}} = [0.1; 0.2; 0.3]$. An error would be calculated over the entire standard deviation spectrum for all three cases of initial condition. The error is the average difference of the ratio of the two functions that are plotted against each other. In this case:

$$Error = \frac{a_i \ \ Ratio - N_f \ \ Ratio}{N_f \ \ Ratio} \tag{A.1}$$

The results obtained for the three mean values for initial condition are stipulated in table A.4. The graphical results obtained are reported in Appendix A.

Table A.4: Method 1 Results

Mean Initial Condition	**Error** (%)
0.1	0.411
0.2	0.446
0.3	0.451

A.1.2.2 Method 2

The same principle as in method 1 applies to method 2. In this case, however, four instances of the distributed parameter's mean are used. This is to involve scenarios where component lifetimes fall within a wide range, from a number of days to a number of years. In this case the distributed parameter is C and the range of mean for it is stated below. The complete results are shown in Appendix A.

Table A.5: Method 2 Results

Mean Operating Condition Parameter	**Error** (%)
0.002	0.411
0.02	0.458
0.2	0.482
1	0.514

A.1.3 Conclusion

It is evident in table A.4 and A.5 that the difference in the CV between the assumed parameter and the time to failure distributions yield the same error in method 1 and method 2. This means that either one of the unknown parameters could be assumed, due to the fact that both parameters have the same influence on the component lifetime distribution. It is decided to assume the initial condition parameter, a_i and calculate the operating condition parameter, C, due to the fact that initial condition is a simpler concept to visualise in a physical context than the operating condition.

A.2 Numerical Experiment Preparation: Method 1

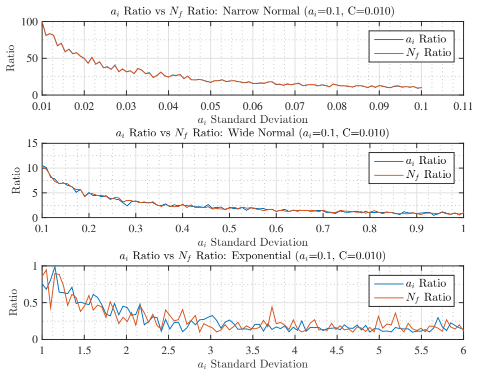

(a) $a_{i_{mean}} = 0.1, \;\; C = 0.01$

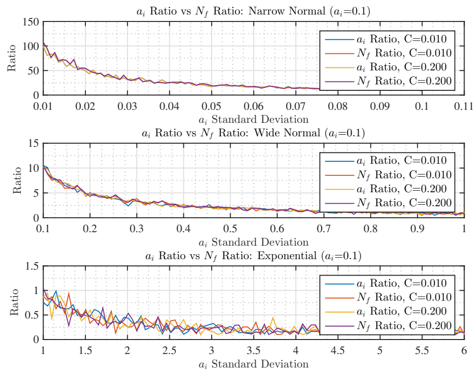

(b) $a_{i_{mean}} = 0.1, \;\; C = 0.01 \;\; \& \;\; C = 0.2$

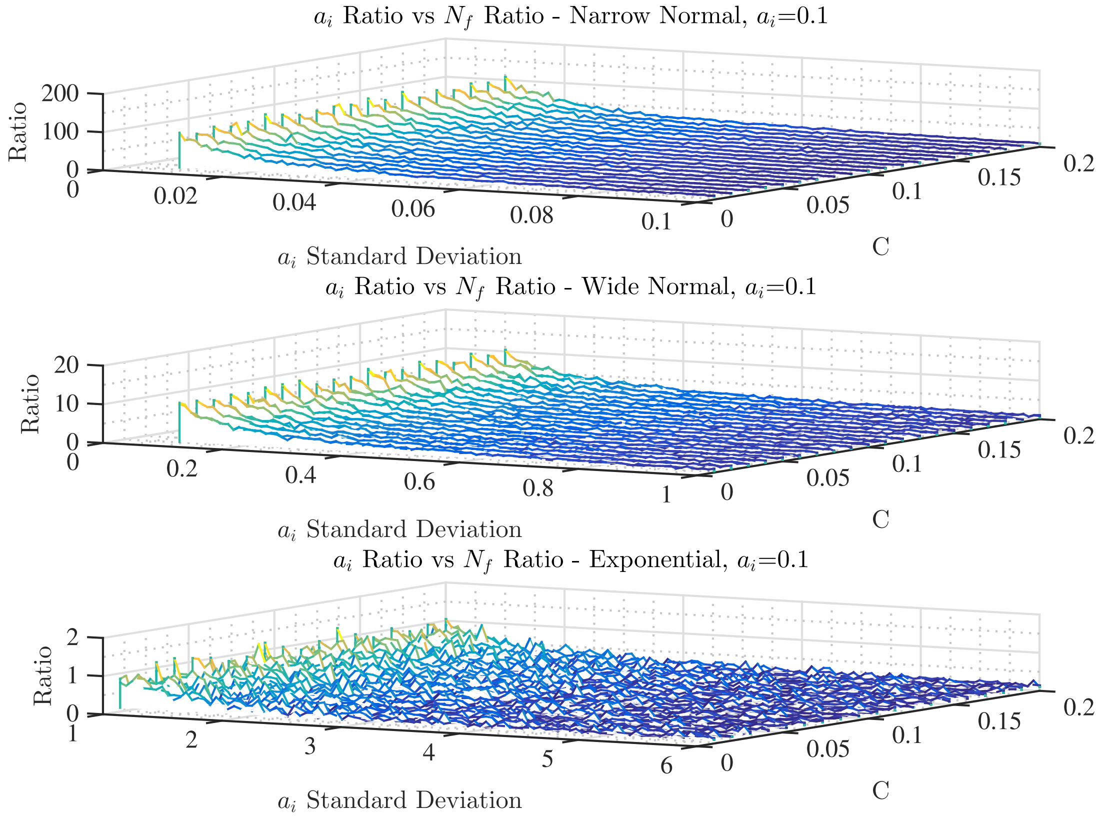

(c) $a_{i_{mean}} = 0.1, 0.01 \leq C \leq 0.2$

Figure A.4: Experimental Preparation for $a_{i_{mean}} = 0.1$

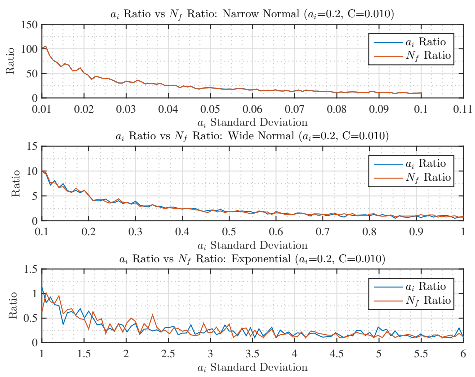

(a) $a_{i_{mean}} = 0.2,\ \ C = 0.01$

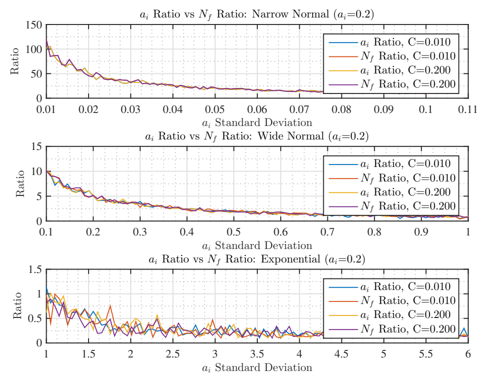

(b) $a_{i_{mean}} = 0.2,\ \ C = 0.01\ \ \&\ \ C = 0.2$

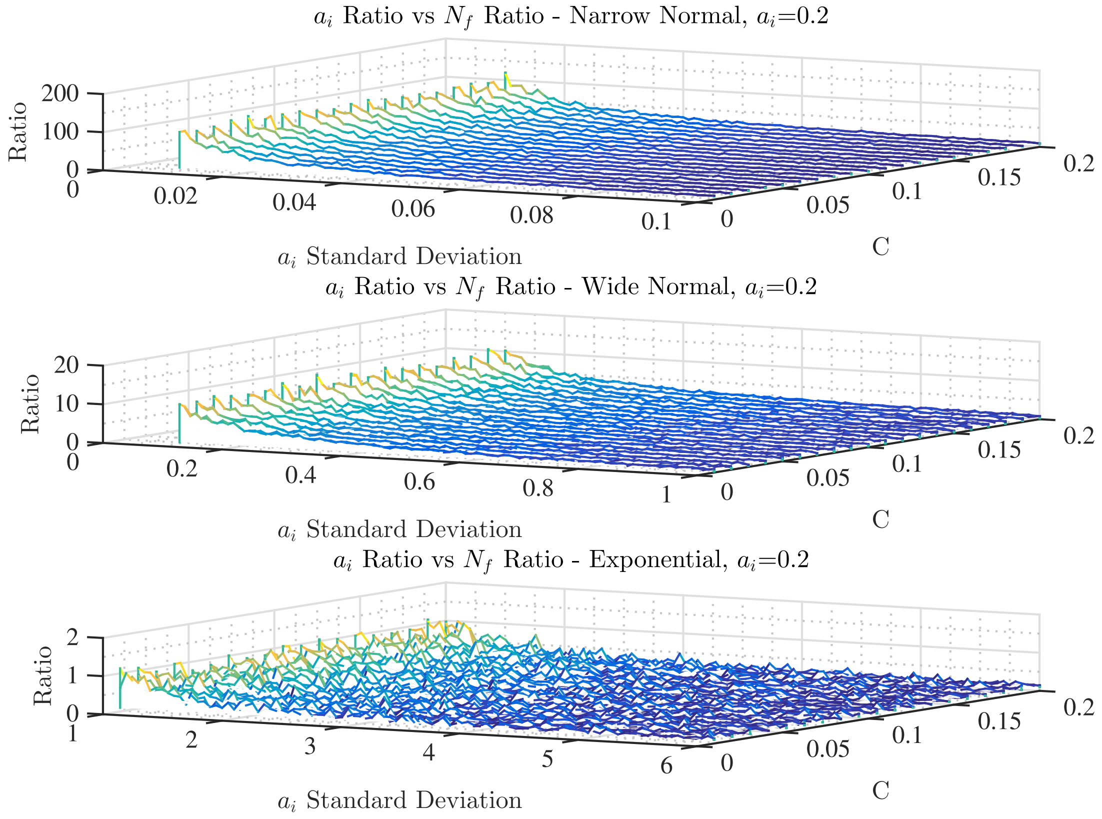

(c) $a_{i_{mean}} = 0.2, 0.01 \leq C \leq 0.2$

Figure A.5: Experimental Preparation for $a_{i_{mean}} = 0.2$

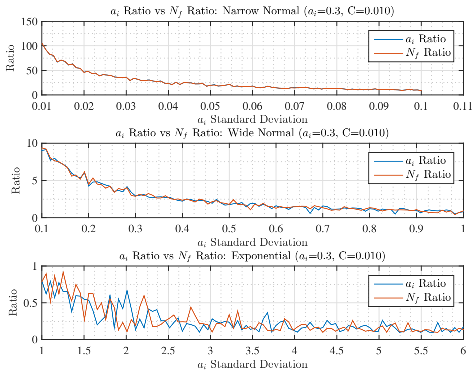

(a) $a_{i_{mean}} = 0.3, \;\; C = 0.01$

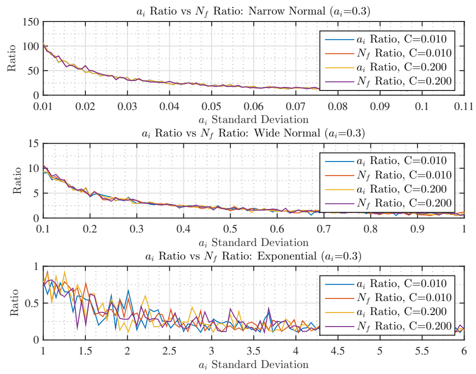

(b) $a_{i_{mean}} = 0.3, \;\; C = 0.01 \;\; \& \;\; C = 0.2$

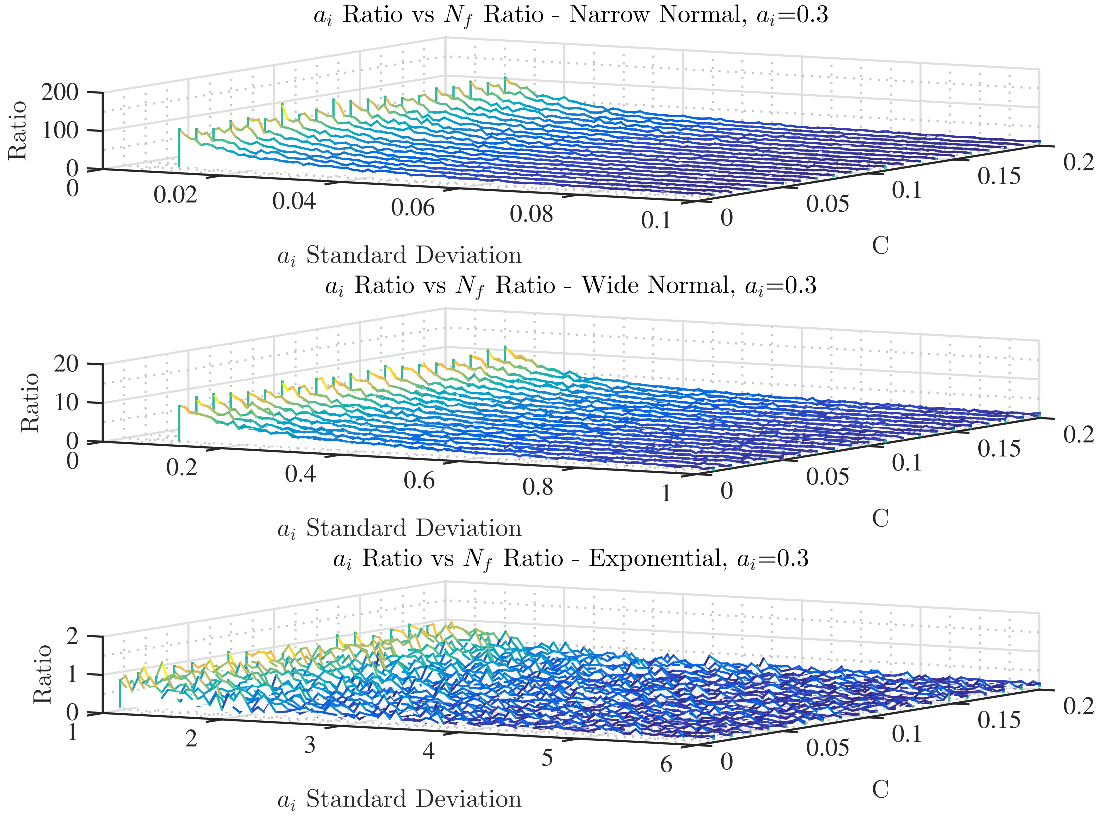

(c) $a_{i_{mean}} = 0.3, 0.01 \leq C \leq 0.2$

Figure A.6: Experimental Preparation for $a_{i_{mean}} = 0.3$

A.3 Numerical Experiment Preparation: Method 2

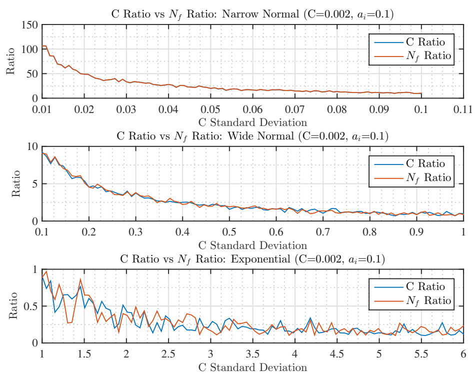

(a) $C_{mean} = 0.002, \;\; a_i = 0.1$

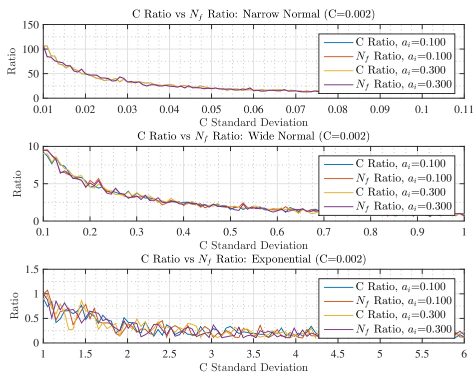

(b) $C_{mean} = 0.002, \;\; a_i = 0.1 \;\; \& \;\; a_i = 0.3$

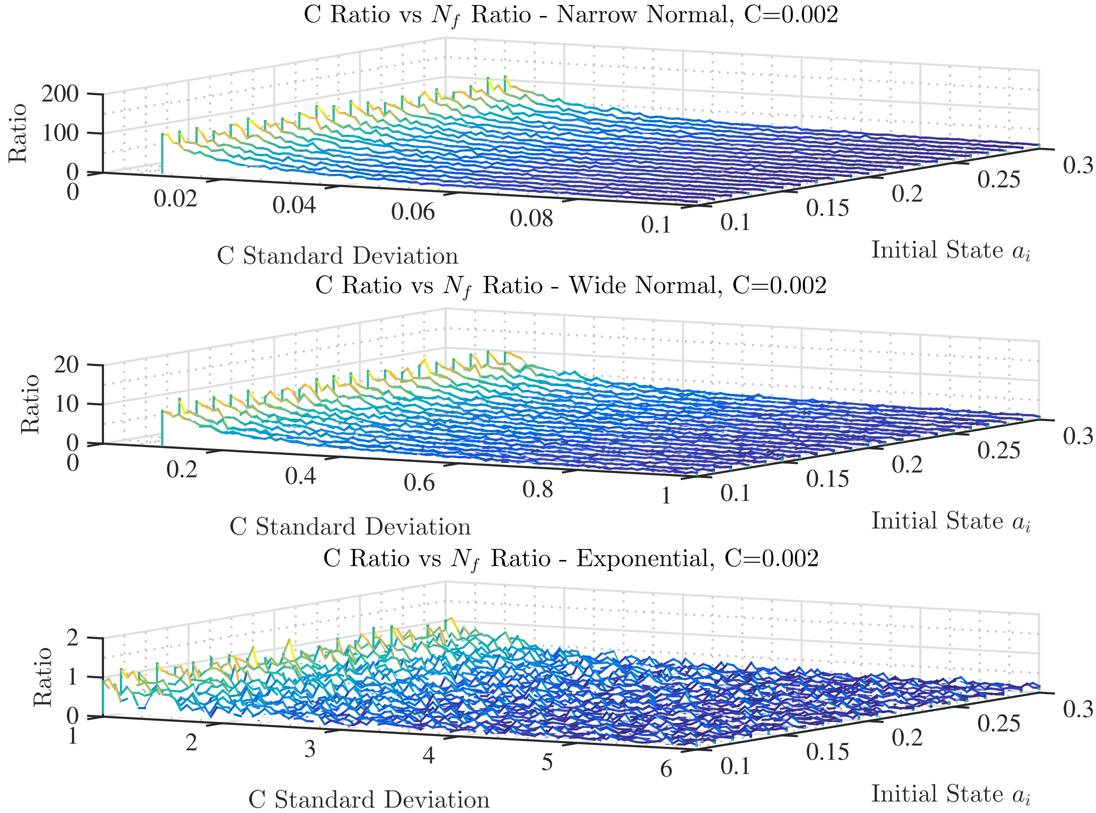

(c) $C_{mean} = 0.002, \;\; 0.1 \leq a_i \leq 0.3$

Figure A.7: Experimental Preparation for $C_{mean} = 0.002$

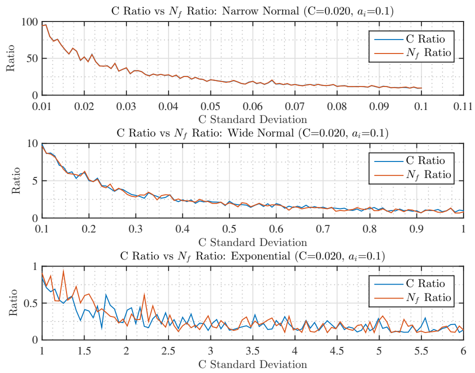

(a) $C_{mean} = 0.02, \;\; a_i = 0.1$

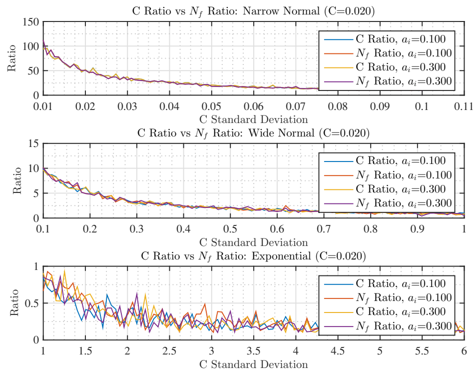

(b) $C_{mean} = 0.02, \;\; a_i = 0.1 \;\; \& \;\; a_i = 0.3$

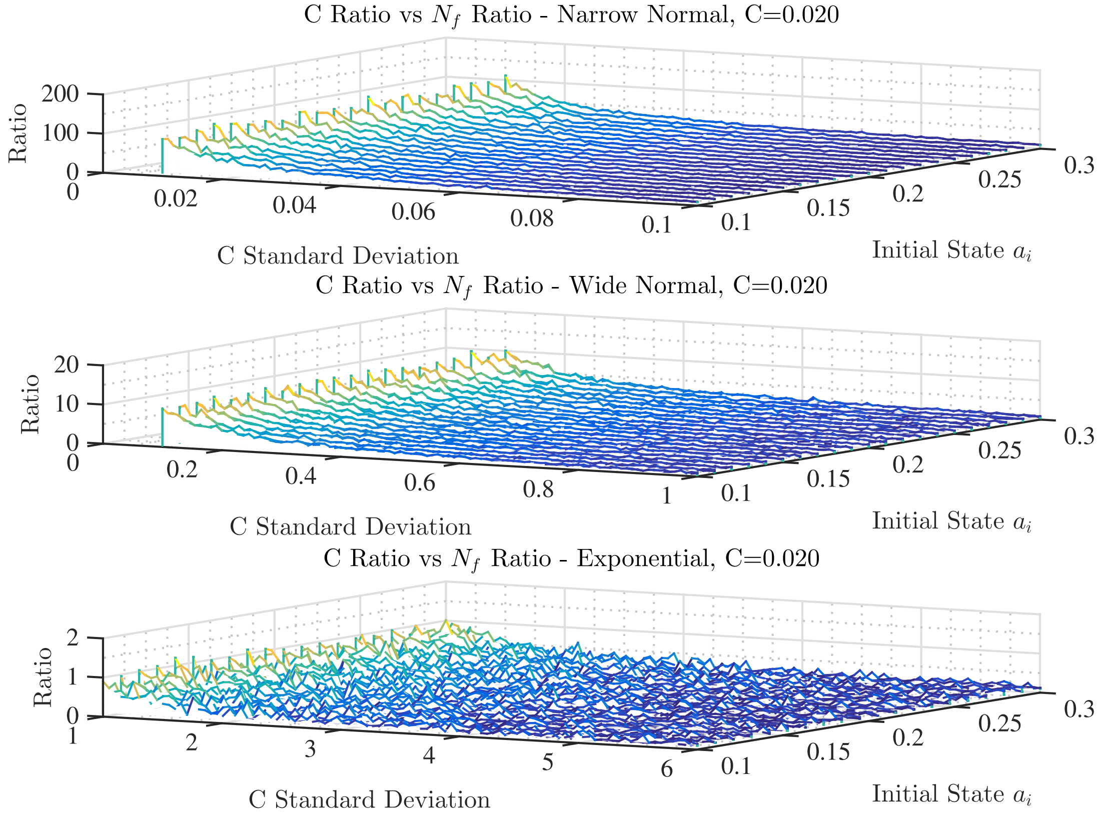

(c) $C_{mean} = 0.02, \;\; 0.1 \leq a_i \leq 0.3$

Figure A.8: Experimental Preparation for $C_{mean} = 0.02$

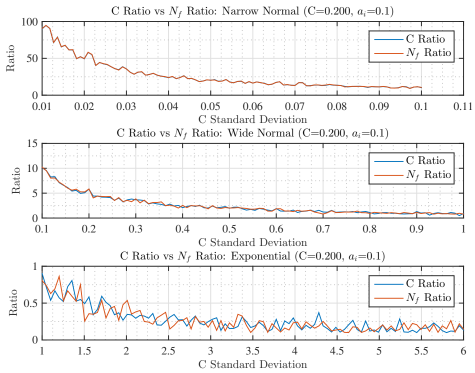

(a) $C_{mean} = 0.2, \;\; a_i = 0.1$

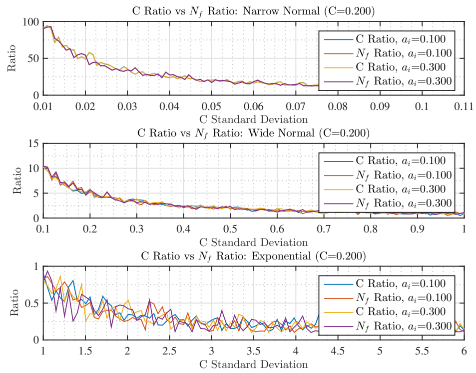

(b) $C_{mean} = 0.2, \;\; a_i = 0.1 \;\; \& \;\; a_i = 0.3$

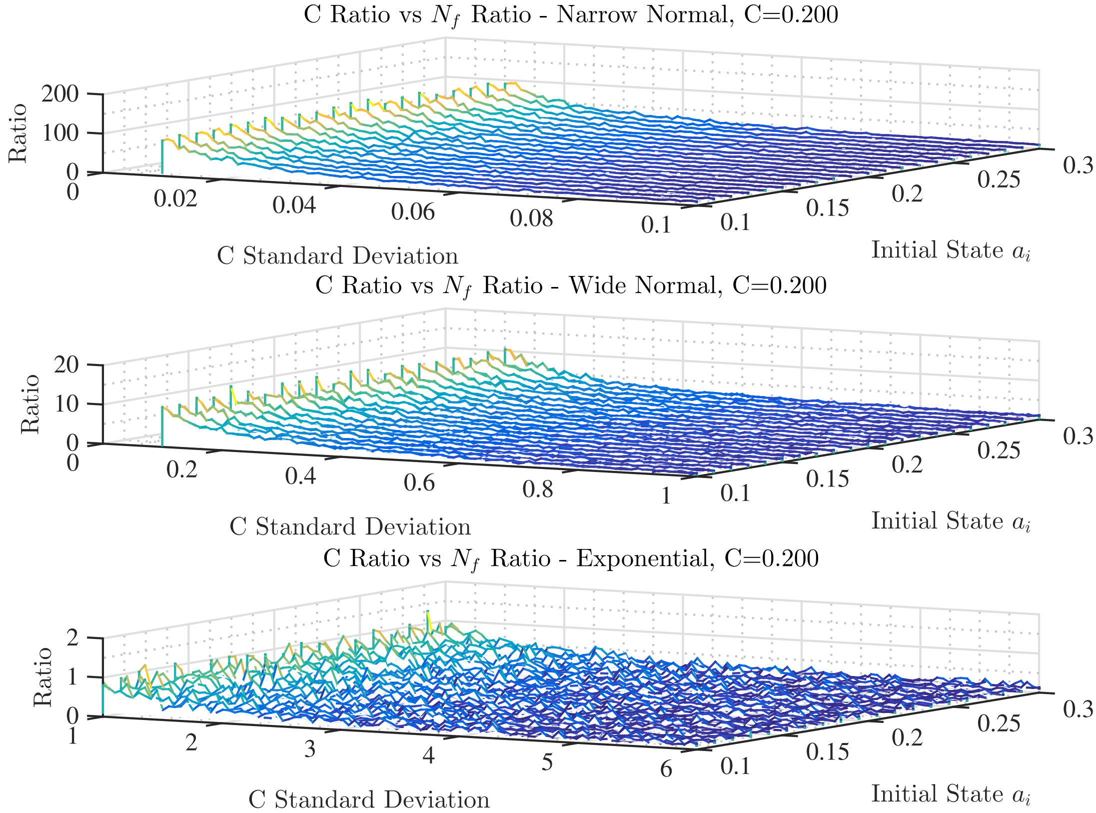

(c) $C_{mean} = 0.2, \;\; 0.1 \leq a_i \leq 0.3$

Figure A.9: Experimental Preparation for $C_{mean} = 0.2$

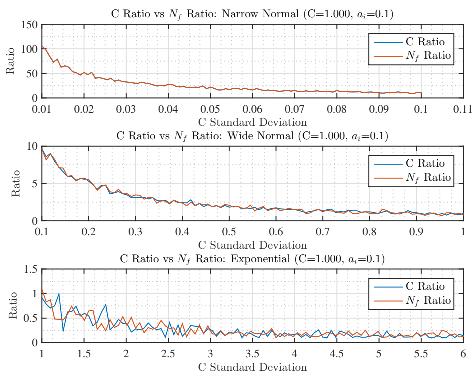

(a) $C_{mean} = 1, \;\; a_i = 0.1$

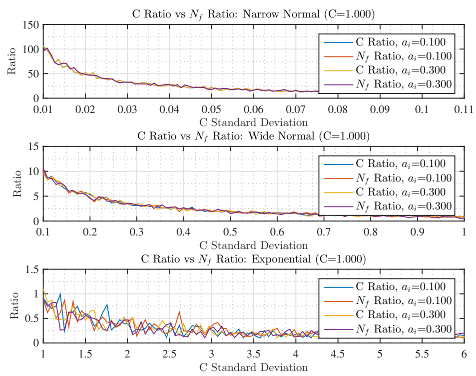

(b) $C_{mean} = 1, \;\; a_i = 0.1 \;\; \& \;\; a_i = 0.3$

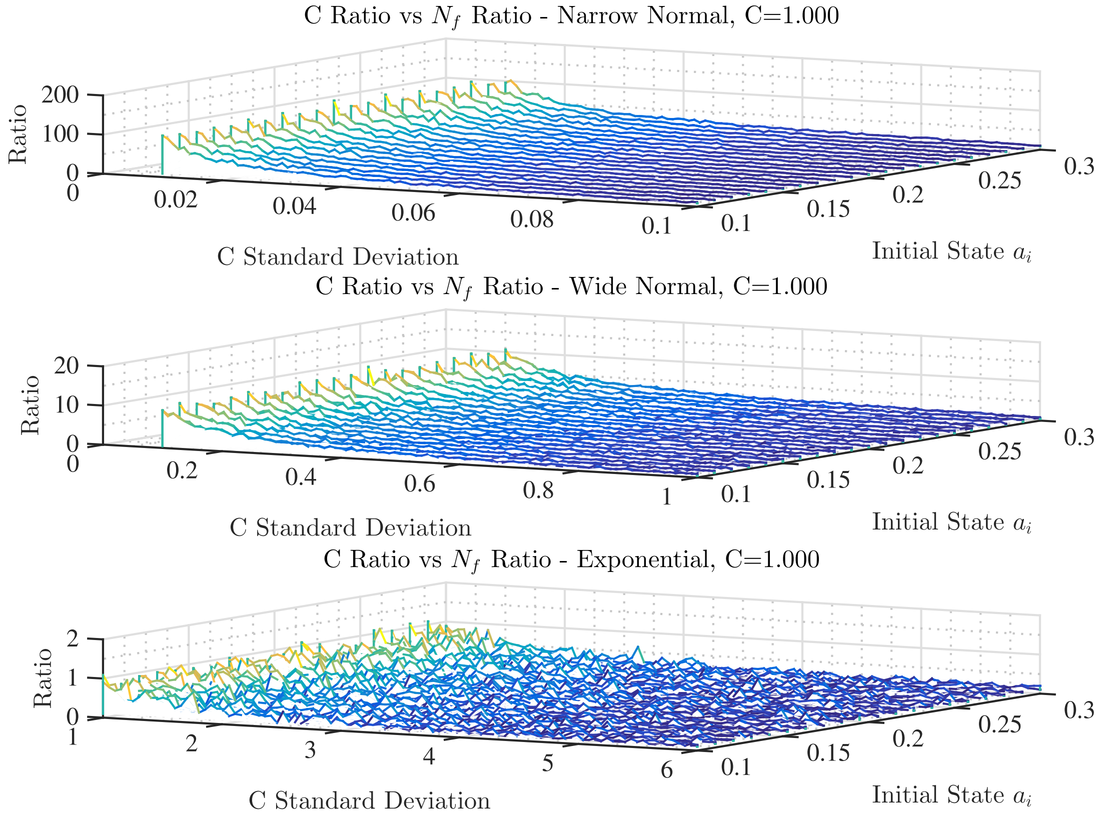

(c) $C_{mean} = 1, \;\; 0.1 \leq a_i \leq 0.3$

Figure A.10: Experimental Preparation for $C_{mean} = 1$

Appendix B

Numerical Experiment Results

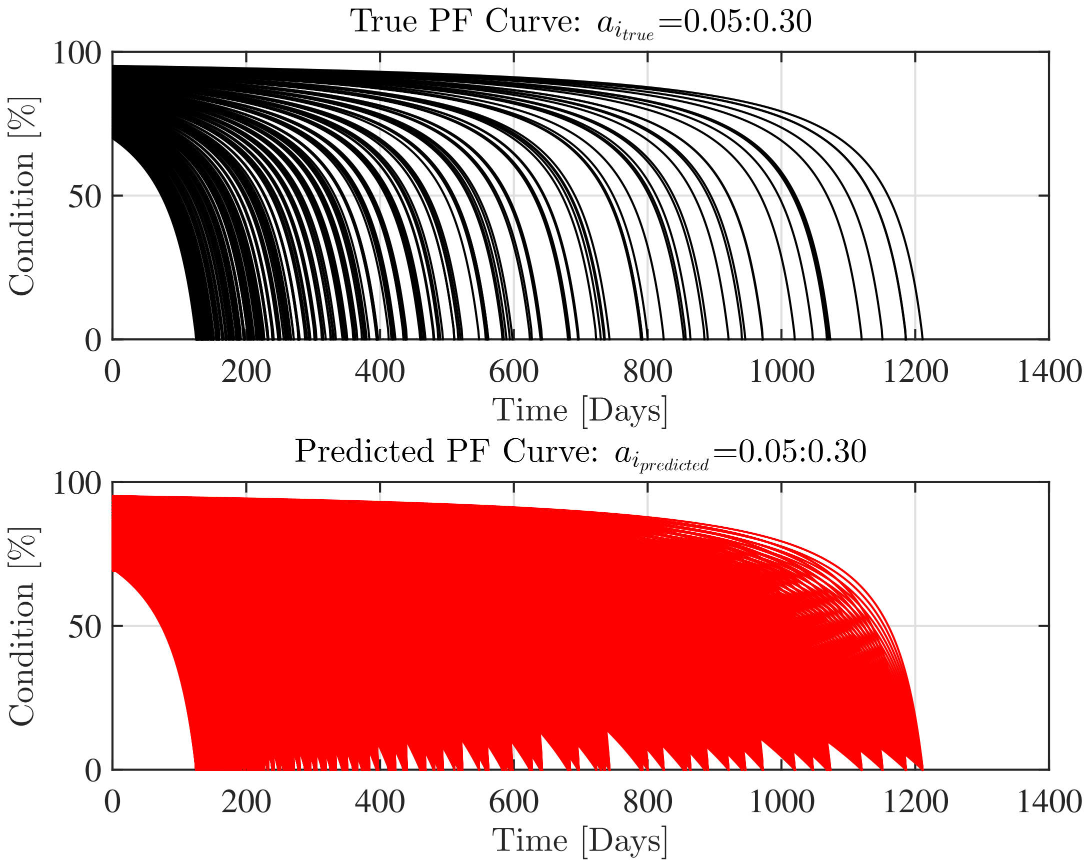

Figure B.1: Numerical Experiment Results: True vs. Predicted PF Curves

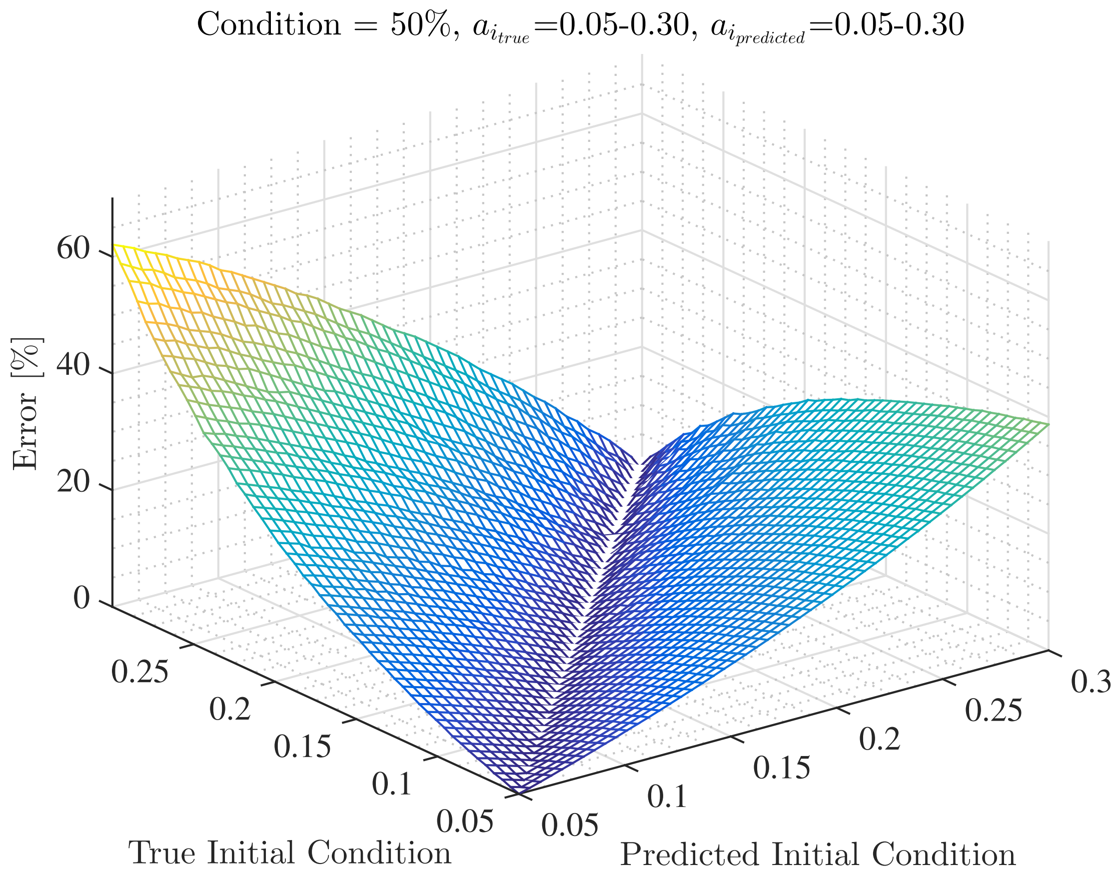

Figure B.2: Numerical Experiment Results: Error Surface at 50% Condition

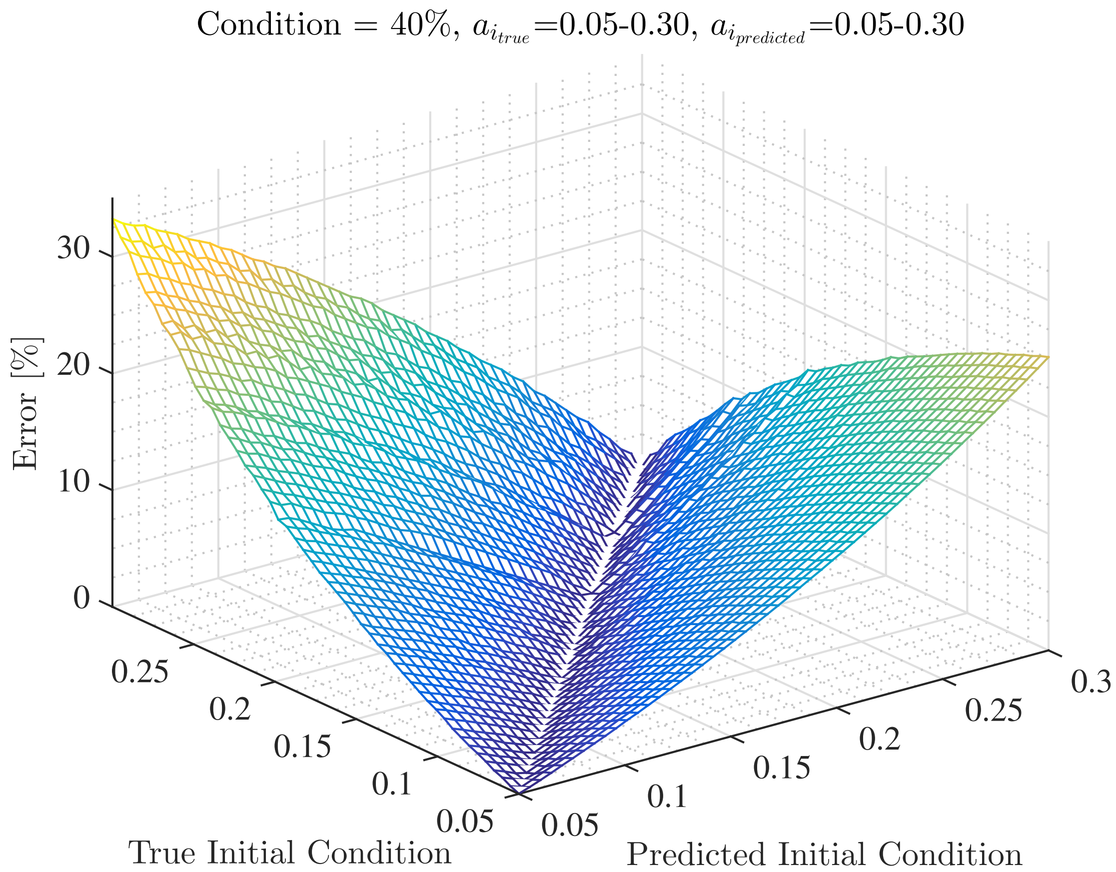

Figure B.3: Numerical Experiment Results: Error Surface at 40% Condition

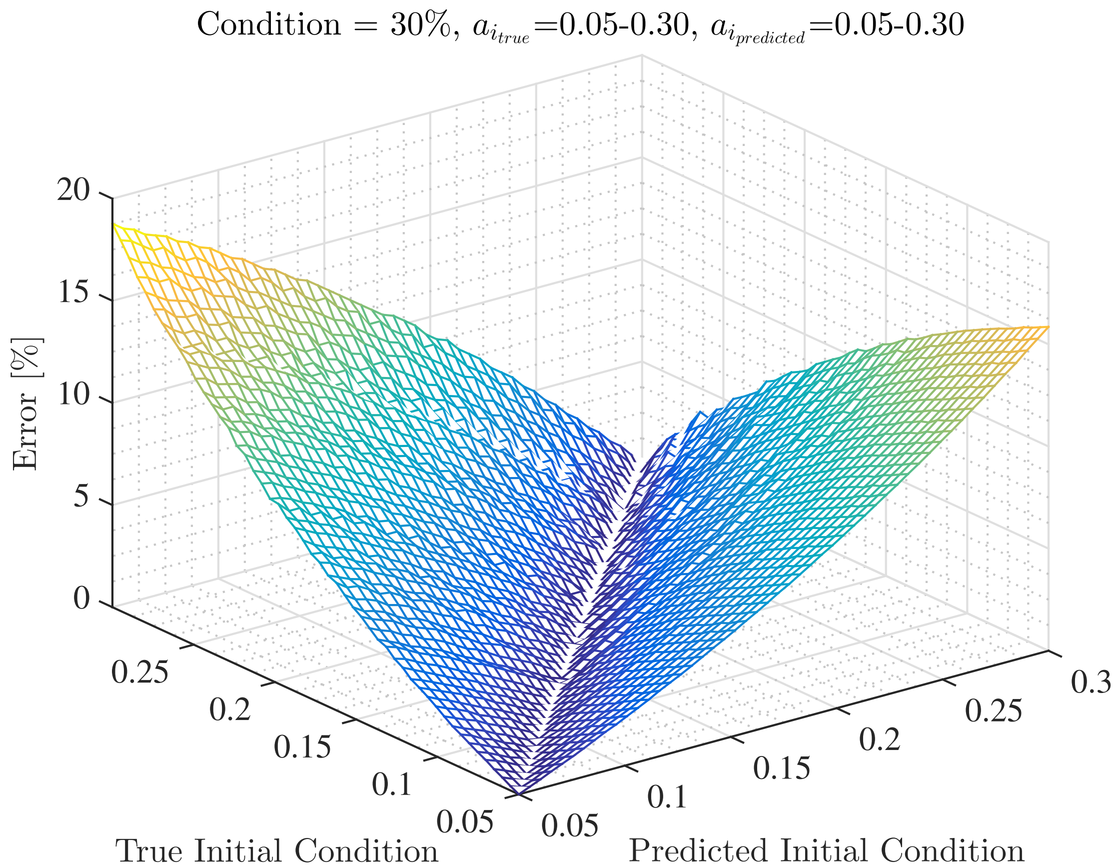

Figure B.4: Numerical Experiment Results: Error Surface at 30% Condition

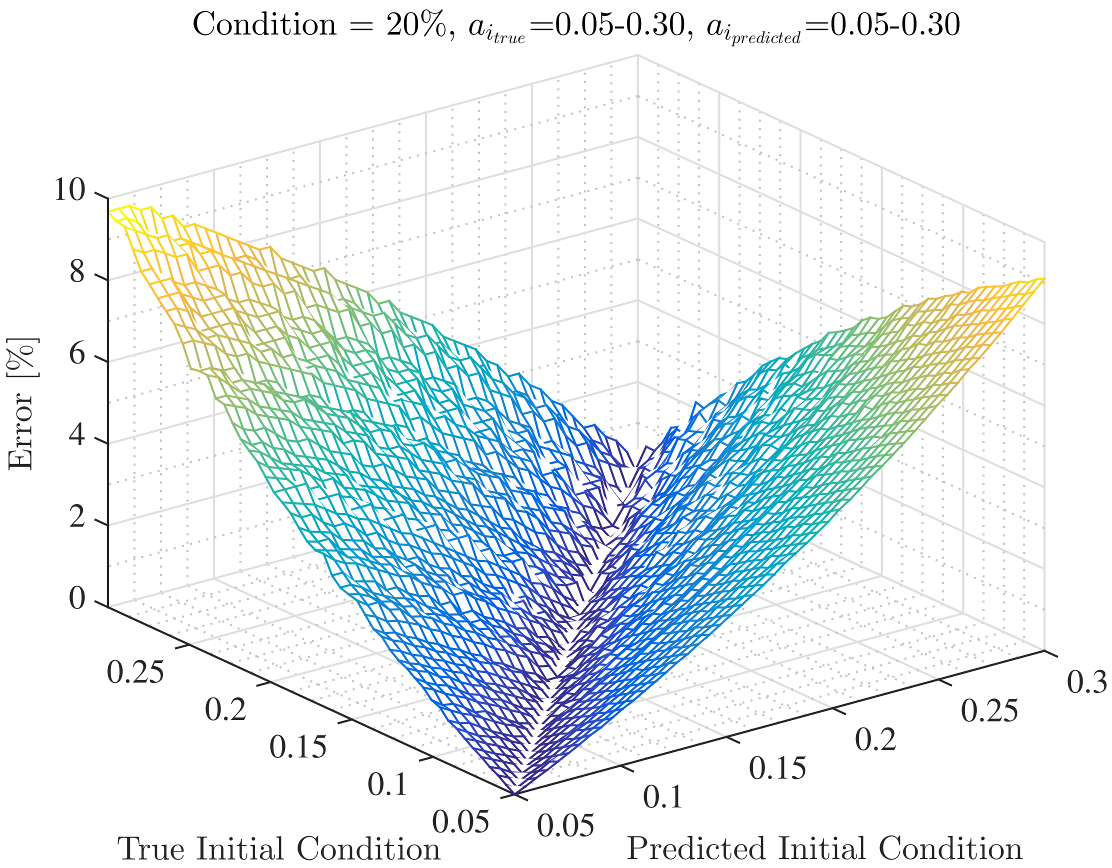

Figure B.5: Numerical Experiment Results: Error Surface at 20% Condition

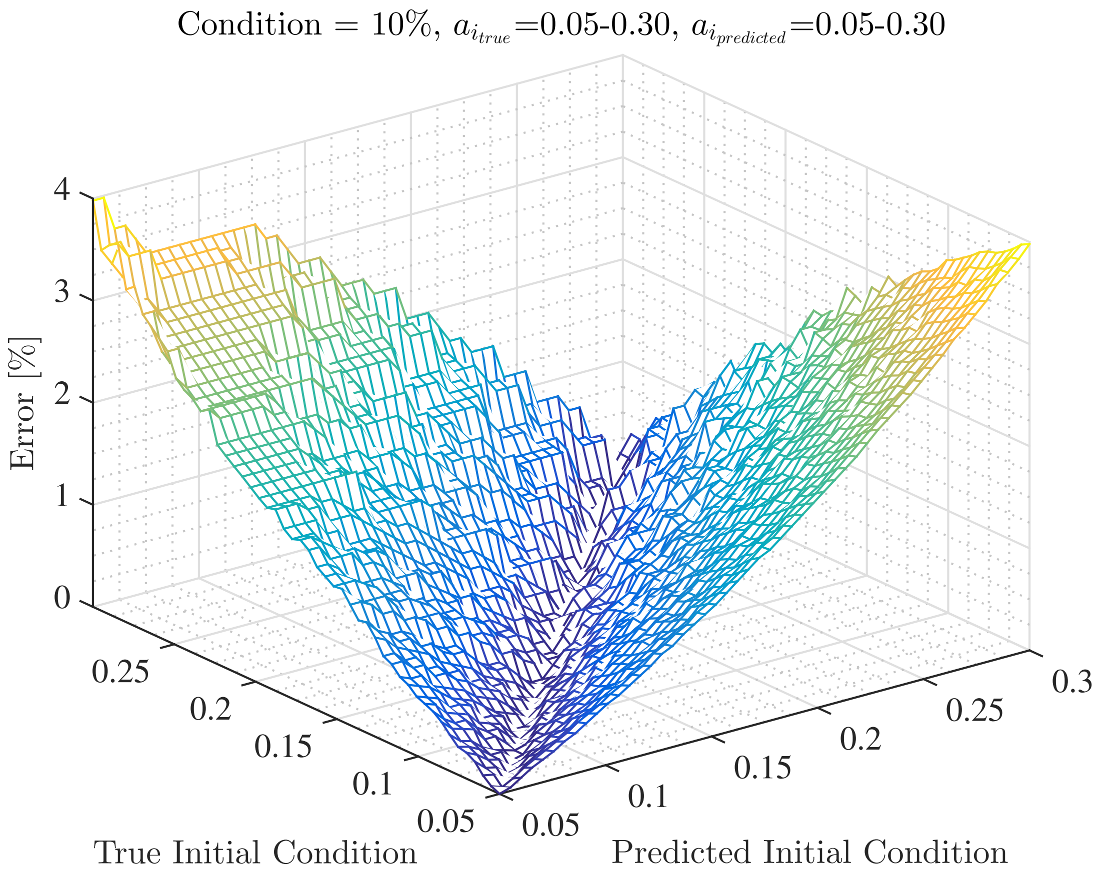

Figure B.6: Numerical Experiment Results: Error Surface at 10% Condition

Appendix C

Bayesian Update for Component Lifetime Distributions

C.1 Bayesian Update for Component Lifetime Distributions

The method used here is described section 1.2.1.4 that is proposed by Nederlof [Nederlof, 2010] and is more commonly known as the Bayesian update method. The results of this method is shown in table C.3 and a sample calculation for component type one is shown below. The same methodology is followed for the other component types. Firstly, the prior -, sample - and posterior distribution need to be developed from a process distribution in order to get to the predictive distribution. A mean of 50 and standard deviation of 30 is chosen for the process distribution.

$$\mu_{Process} = 50$$

$$\sigma_{Process} = 35$$

$$\sigma^2 = 35^2 = 1225$$

According to Nederlof, the prior mean is the same as the process mean and the variance is the process variance divided by the sample size, which is 13 in the case of the component 1 [Nederlof, 2010]:

$$\mu_{Prior} = \mu' = 50$$
$$\sigma^2_{Prior} = \sigma'^2 = \frac{1225}{13} = 94.2$$
$$\therefore \sigma_{Prior} = \sigma' = \sqrt{\sigma'^2} = \sqrt{94.2} = 9.7$$

The sample data is shown in table C.1 and the mean and standard deviation are calculated. The posterior mean and variance are calculated using equation 1.19 and 1.20,

$$\mu" = \frac{\sigma^2\mu' + n\sigma'^2\mu}{n\sigma'^2 + \sigma^2}$$

$$\sigma"^2 = \frac{\sigma^2\sigma'^2}{n\sigma'^2 + \sigma^2}$$

where μ' = prior mean, σ' = prior variance, μ = sample mean, σ = sample variance and n = sample size.

Table C.1: Sample Data

Failure	Time to Failure [Days]
1	0
2	0
3	1
4	2
5	4
6	4
7	11
8	14
9	54
10	61
11	90
12	101
13	189
Mean ($\mu_{Sample} = \mu$)	41
Variance ($\sigma^2_{Sample} = \sigma^2$)	3024.9
Standard Deviation ($\sigma_{Sample} = \sigma$)	54.99

The posterior properties can now be calculated.

$$\mu" = \frac{\sigma^2\mu' + n\sigma'^2\mu}{n\sigma'^2 + \sigma^2} = \frac{(3024.9)(50) + (13)(94.2)(41)}{(13)(94.2) + 3024.9} = 47.4$$

$$\sigma"^2 = \frac{\sigma^2\sigma'^2}{n\sigma'^2 + \sigma^2} = \frac{(3024.9)(94.2)}{(13)(94.2) + 3024.9} = 67.1$$

$$\therefore \sigma'' = \sqrt{67.1} = 8.2$$

The predictive distribution mean equals that of the posterior distribution and its variance equals the posterior distribution multiplied by the sample size [Nederlof, 2010]:

$$\mu_{Predictive} = 47.4$$

$$\sigma^2_{Predictive} = (67.1)(13) = 871.7$$

$$\therefore \sigma_{Predictive} = \sqrt{871.7} = 29.5$$

Table C.2 summarises the Bayesian update results for the component type one lifetime distribution.

Table C.2: Prior -, Sample - and Posterior Distribution for Component Type 1

Distribution	**Mean**	**Variance**	**Standard Deviation**
Process	50	1225	35
Prior	50	94.2	9.7
Sample	41	3024.9	54.99
Posterior	47.4	67.1	8.2
Predictive	47.4	871.7	29.5

The same process distribution was used for all four component types to replicate a scenario where no prior knowledge of the components' failure mechanisms are known. The results, following the same calculation process as shown above, for all four components are summarised in table C.3. The prior distributions differ for each component type due to the difference in sample sizes. The sample data and prior distributions are combined which yield the posterior distributions. Nederlof's [Nederlof, 2010] method takes a step further by developing a predictive distribution. The predictive distribution has the same mean as that of the posterior distribution, but the variance is modified by the sample size and hence the standard deviation is altered. The normal results in table C.3 are converted to log-normal parameters, as shown in table C.4 and are shown in figures C.1 to C.4.

Table C.3: Bayesian Update Results for Respective Component Types: Normal Distribution

	Process		**Prior**		**Sample Data**		**Posterior**		**Predictive**	
	μ	σ	μ	σ	μ	σ	μ	σ	μ	σ
Type 1	50	35	50	9.707	40.85	55	47.36	8.19	47.36	29.53
Type 2	50	35	50	7.638	27.1	29.52	36.62	4.924	36.62	22.57
Type 3	50	35	50	10.55	54.55	41.38	51.9	8.057	51.9	26.72
Type 4	50	35	50	12.37	79.25	70.96	55.72	11.1	55.72	31.39

Table C.4: Bayesian Update Results for Respective Component Types: Log-normal Distribution

	Process		**Prior**		**Sample Data**		**Posterior**		**Predictive**	
	μ	σ	μ	σ	μ	σ	μ	σ	μ	σ
Type 1	3.71	0.63	3.89	0.19	3.19	1.02	3.69	0.17	3.69	0.57
Type 2	3.71	0.63	3.90	0.15	2.91	0.88	3.44	0.13	3.44	0.57
Type 3	3.71	0.63	3.89	0.21	3.77	0.67	3.83	0.15	3.83	0.48
Type 4	3.71	0.63	3.88	0.24	4.08	0.77	3.88	0.20	3.88	0.52

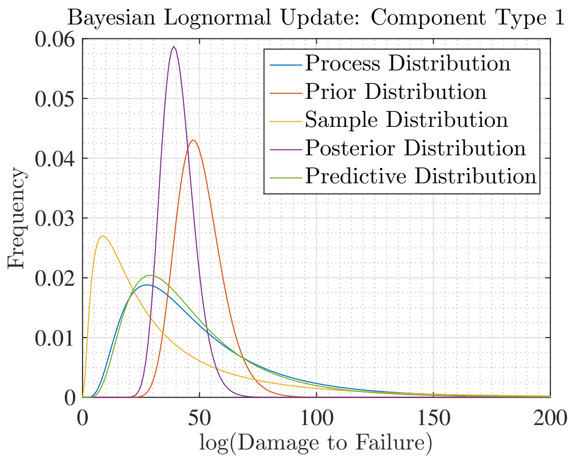

Figure C.1: Component Type 1

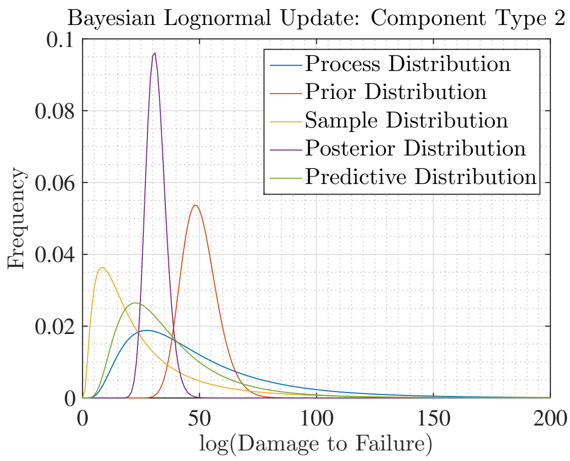

Figure C.2: Component Type 2

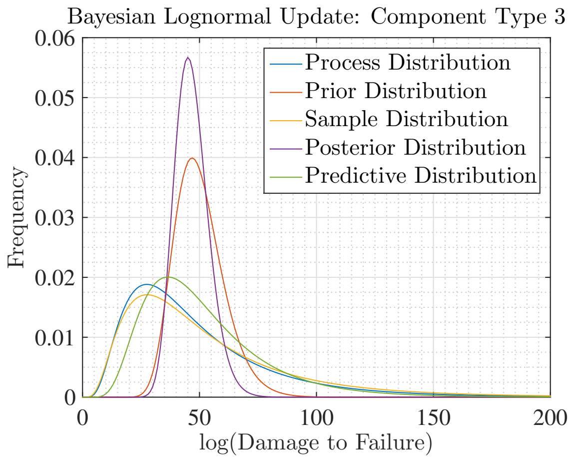

Figure C.3: Component Type 3

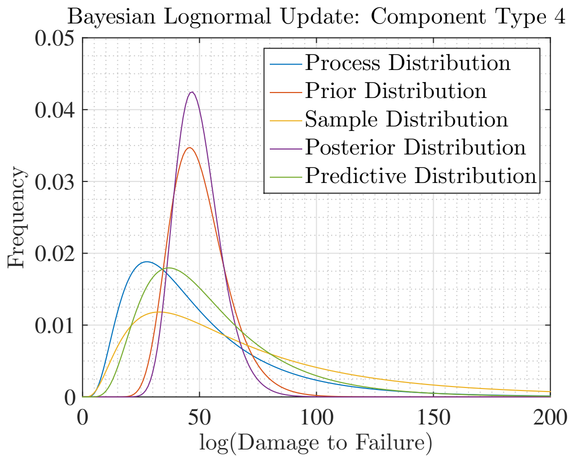

Figure C.4: Component Type 4

It can be seen in each case that the prior distribution influences the sample data greatly to develop the posterior distribution. The predictive distribution takes the sample size into account and distributes the data more evenly than the prior distribution does. It is clear that the predictive distribution is narrower than the sample data, which will yield more dense data when generated from the distribution.